Dear editor,

Thank you very much for the editorial handling of this manuscript. According to the comments of the three referees, we have made a substantial revision to the manuscript. Some of the paragraphs have been rewritten. The important changes are:

1. The Introduction has been completely rewritten. Cloud electrification is now introduced in more detail, as suggested by referee #3. The physical mechanism and the effects of electrostatic induction are now written in a more organized way. The novelty of this manuscript is also emphasized, as suggested by referee #1.

2. In Section 2, the kernel in the stochastic collection equation for uncharged droplets and charged droplets are now explained in more detail.

3. In section 3.2, the formulas of stream functions and flow fields have been corrected, as suggested by referee #2. The explanations of them have been rewritten. In the previous version, same symbols in section 3.2 and 3.3 are used to represent different variables. This is now corrected. We now introduce $\tilde{R} = R/r$, $\theta_0 = \theta - \varphi$ to make sure different variables are represented by different symbols in Section 3.2 and 3.3.

4. In Section 3.3, a new figure (Fig. 2) is added to show the forces acting on each droplet, the velocity of each droplet, and the induced flow velocity, as suggested by referee #3. Detailed discussion is also added to the manuscript.

5. Section 4 has been divided into 3 subsections. The explanations of model settings and initial droplet size distributions have been revised, and they are much more understandable now. The initial setting of droplet charge distribution now uses a more appropriate model, as response to referee #2's comment.

6. In section 5.1, new figures (Fig. 7b and Fig. 8) are added to show collision efficiencies for various collector sizes, including collectors with sizes typical of cloud droplets, as suggested by referee #3.

7. In Section 5.2, we have added new figures (Figs. 10, 12, and 15) to show the temporal changes of droplet total number concentration and total charge concentration during the collision-coalescence process, as suggested by referee #3.

8. In Section 6, the axis of the Fig. 16 has been changed to explicitly show the change of the terminal velocity, as response to referee #1's comment.

Furthermore, the grammatical errors and inappropriate expressions have been corrected. We have checked the languages of the revised manuscript. Attached are the responses to the comments of the three referees, and a marked-up version of the revised manuscript. In the responses to referees' comments, the sentences in blue are responses to the referee, and the sentences in red are revised texts of the manuscript. In the marked-up version of the revised manuscript, words and sentences in blue are contents added in the revision of our manuscript, and those in red with strikethrough are contents which have been deleted.

Thank you very much and we look forward to your reply.

Sincerely,
Shian Guo, Huiwen Xue

Response to Referee #1

General comments:

This manuscript investigated the effect of electric charges and atmospheric electric fields on the size distribution of cloud droplets numerically. The authors concluded that electric charges and fields enhance the collision efficiency of small droplets. My main concern of the manuscript is the novelty. As far as I understand, the manuscript does not specify clearly how different the study is from the one of Khain et al, 2004. The novelty should be stated clearly in the abstract and conclusion as well as in the introduction. Especially, the introduction needs to be improved substantially. This manuscript can be improved if the authors can summarize the open questions in previous studies and address them in their study. By such a treatment, the authors can place their contribution in a more general context. Overall, this manuscript does not satisfy the novelty requirement of the ACP journal. Major revision is needed before it can be considered for publication.

Response:

We thank the reviewer for pointing out that the novelty of this study should be more addressed in the manuscript. The Introduction of the manuscript is now completely rewritten. Now the Introduction summarizes the previous work on cloud electrification, the physical mechanism of the electrostatic induction, the effect of electrostatic induction on droplet collision efficiency, and the subsequent effect on precipitation formation. Now the rewritten Introduction is shown below in red fonts. Abstract and Conclusion have also been substantially revised, but not shown here. The novelty has been emphasized in all these sections.

This study is motivated as the aerosol-cloud interaction study regarding climate change has been widely carried out. It has been confirmed by both observational studies and modeling studies that increased aerosols can result in more numerous but smaller droplets, hence slower collision-coalescence process, and suppressed warm-rain precipitation process. Since cloud electrification has been found for both thunderstorms and warm clouds, and electrification can increase the possibility of collision-coalescence, as described in the revised Introduction of this manuscript, it is worthy of investigating whether the electrostatic effects can mitigate the aerosol effects. This kind of study has not been performed. Previous studies of electrostatic effect such as Khain et al. (2004) focuses on weather modification, including rain enhancement and fog elimination. Here we are interested in finding out to what extent the electrostatic effect can mitigate the aerosol effect.

To investigate the electrostatic effect vs. aerosol effect on droplet collision-coalescence, we purposely choose an initial droplet size distribution function based on Bott (1998), i.e., Equation 13 in the original manuscript. This distribution function has two parameters: liquid water content and averaged size of droplets. We set the liquid water content as constant (1 g m^{-3}) and vary the averaged size of droplets in the initial size distribution ($\bar{r}$ = 15, 9, and 6.5 μm) to represent the effect of aerosols on cloud microphysics. These settings give an initial droplet number concentration of 70, 325, and 850 cm^{-3}, respectively. As suggested by Reviewer #3, description of droplet number concentration is added to the manuscript. The electrostatic effect is then investigated for the three cases.

Here is a simple example to compare the electrostatic effect vs. the aerosol effect: When there is no

electric charge and field, the case with initial $\bar{r}$ = 15 μm can develop a significant second peak in the size distribution through collision-coalescence in less than 30 min, while it takes about 60 min for the $\bar{r}$ = 9 μm case to develop a similar second peak. This represents an aerosol effect. When considering the electric charge and field effects, it only takes about 45 min for the $\bar{r}$ = 9 μm case to develop a similar second peak (as can be seen in Figs. 7 and 8 in the original manuscript). The aerosol-induced precipitation suppression effect is mitigated by the electrostatic effects. We emphasize on this issue in various places in the revised manuscript.

The Introduction now reads as:

1. Introduction

Clouds are usually electrified (Pruppacher and Klett 1997). For thunderstorms, several theories of electrification have been proposed in the past decades. The proposed theories assume that the electrification involves the collision of graupel or hailstones with ice crystals or supercooled cloud droplets, based on radar observational result that the onset of strong electrification follows the formation of graupel or hailstones within the cloud (Wallace and Hobbs, 2006). However, the exact conditions and mechanisms are still under debate. One charging process could be due to the thermoelectric effect between the relatively warm, rimed graupel or hailstones and the relatively cold ice crystals or supercooled cloud droplets. Another charging process could be due to the polarization of particles by the downward atmospheric electric field. The thunderstorm electrification can increase the electric fields to several thousand V cm^{-1}, while the magnitude of electric fields in fair weather air is only about 1 V cm^{-1} (Pruppacher and Klett 1997). Droplet charges can reach $|q| \approx 42r^2$ in unit of elementary charge in thunderstorms, with the droplet radius r in unit of μm according to observations (Takahashi, 1973). For cumuli clouds, previous studies show smaller charge amount.

Liquid stratified clouds do not have such strong charge generation as in the thunderstorms. But charging of droplets can indeed occur at the upper and lower cloud boundaries as the fair weather current passes through the clouds (Harrison et al. 2015, Baumgaertner et al. 2014). The global fair weather current and the electric field are in the downward direction. Given the electric potential of 250 kV for the ionosphere, the exact value of fair weather current density over a location depends on the electric resistance of the atmospheric column, but its typical value is about 2×10^{-12} A m^{-2} (Baumgaertner et al. 2014). The fair weather electric field is typically about 1 V cm^{-1} in the cloud-free air, but is usually much stronger inside stratus clouds, because the cloudy air has a lower electrical conductivity than the cloud-free air. There is a conductivity transition at cloud boundaries. Therefore, the cloud top is positively charged and the cloud base is negatively charged. Based on the in situ measurements of charge density in liquid stratified cloud, and assuming that the cloud has a droplet number concentration on the order of 100 cm^{-3}, it is estimated that the mean charge per droplet is +5e (ranging from +1e to +8e) at cloud top, and -6e (ranging from -1e to -16e) at cloud base (Harroson et al. 2015). According to Tsutomu Takahashi (1973) and Khain (1997), the mean absolute charge of droplets in warm clouds is around $|q| \approx 6.6\, r^{1.3}$ (e, μm). For a droplet with radii of 10 μm, it is about 131 e.

In general, charging of droplets can lead to the following effects on warm cloud microphysics. Firstly, for charged haze droplets, the charges can lower the saturation vapor pressure over the droplets and enhance the cloud droplet activation (Harrison and Carslaw, 2003, Harrison et al. 2015). Secondly, the

electrostatic induction effect between charged droplets can lead to strong attraction at very small distance (Davis, 1964) and higher collision-coalescence efficiencies (Beard et al. 2002). But Harrison et al. (2015) showed that charging is more likely to affect collision processes than activation, for small droplets.

The electrostatic induction effect can be explained by regarding the charged cloud droplets as spherical conductors. The electrostatic force between two conductors is different from the well-known Coulomb force between two point charges. When the distance between a pair of charged droplets approaches infinity, the electrostatic force converges to Coulomb force between two point charges. But when the distance of surfaces of two droplets is small (e.g. much smaller than their radii), their interaction shows extremely strong attraction. Even when the pair of droplets carry the same sign of charges, the electrostatic force can still change from repulsion to attraction at small distance. Although there is no explicit analytical expression such as Coulomb force for the electrostatic interaction between two charged droplets, a model with high accuracy has been developed (Davis 1964) for the interaction of charged droplets in a uniform electric field. Many different approximate methods are also proposed for the convenience of computation in cloud physics (e.g. Khain et al., 2004).

Based on this induction concept, electrostatic effects on droplet collision-coalescence process have been studied in the past decades. A few experiments show that electric charges and fields can enhance coalescence between droplets. Beard et. al. (2002) conducted experiments in cloud chambers and showed that even minimal electric charge can significantly increase the probability of coalescence when the two droplets collide. Eow et. al., (2001) examined several different electrostatic effects in water-in-oil emulsion, indicating that electric field can enhance coalescence by several mechanisms such as film drainage.

More numerical researches indicate that charges and fields can increase droplet collision efficiencies because of the electrostatic forces. Schlamp et al. (1976) used the model of Davis (1964) to study the effect of electric charges and atmospheric electric fields on collision efficiencies. They demonstrated that the collision efficiencies between small droplets (about 1~10 μm) are enhanced by an order of magnitude in thunderstorm condition, while collision between large droplets is hardly affected. Harrison et al. (2015) investigate the electrostatic effects in weakly electrified liquid clouds rather than thunderstorms. They calculated collision efficiencies between droplets with radii less than 20 μm and charge less than 50 e, by the equations of motion in Klimin (1994). Their results indicate that electric charges at the upper and lower boundaries of warm stratified clouds are sufficient to enhance collisions, and the enhancement is especially significant for small droplets. Moreover, they proposed that solar influences may change the fair weather current and droplet collision process, a possible pathway for affecting the climate system. Tinsley (2006) and Zhou (2009) also studied the collision efficiencies between charged droplets and aerosol particles in weakly electrified clouds, by treating the particles as conducting spheres. They considered many aerosol effects such as thermophoretic forces, diffusophoretic forces and Brownian diffusion.

As for the electrostatic effect on the evolution of droplet size distributon and the cloud system, few researches have been conducted. Focusing on weather modification, Khain et al. (2004) showed that a small fraction of highly charged particles could trigger the collision process, and thus accelerate raindrop formation in warm clouds or lead to fog elimination significantly. In their study, the electrostatic force between the droplet pair is represented by an approximate formula. The charge limit is set to the air-breakdown limit. The Stokes Flow is adopted to represent the hydrodynamic interaction, for deriving the trajectories of a pair of droplets. Harrison et. al. (2015) calculated droplet collision efficiencies affected by electric charges in warm clouds. When simulating the evolution of droplet size distribution in their study, the enhanced collision efficiencies are not used. Instead, the collection cross

sections are multiplied by a factor of no more than 120% to approximately represent the electric enhancement of collision efficiency. The roles of electric charges and fields on precipitation acceleration still needs to be studied.

The increased aerosol loading by anthropogenic activities can lead to an increase in cloud droplet number concentration, a reduction in droplet size, and therefore an increase in cloud albedo (Twomey 1974). This imposes a cooling effect on climate. It is further recognized that the aerosol-induced reduction in droplet size can slow down droplet collision-coalescence and cause precipitation suppression. This leads to increased cloud fraction and liquid water amount, and imposes an additional cooling effect on climate (Albrecht 1989). As the charging of cloud droplets can enhance droplet collision-coalescence, especially for small droplets, it is worth studying to what extent the electrostatic effect can mitigate the aerosol effect on the evolution of droplet size distribution and precipitation formation.

This study investigates the effect of electric charges and fields on droplet collision efficiency and the evolution of the droplet size distribution. The amount of charges is set as the condition in warm clouds, and the electric fields are set as the early stage of thunderstorms. The more accurate method for calculating the electric forces is adopted (Davis, 1964). Correction of flow field for large Reynolds numbers are also considered. Section 2 describes the theory of droplet collision-coalescence and the stochastic collection equation. Section 3 presents the equations of motion for charged droplets in an electric field. The method for obtaining the terminal velocities and collision efficiencies for charged droplets are also presented. Section 4 describes the model setup for solving the stochastic collection equation. Different initial droplet size distributions and different electric conditions are considered. Section 5 shows the numerical results of electrostatic effects on collision efficiency, and on the evolution of droplet size distribution. We intend to find out to what extent the electric charges and fields as in the observed atmospheric conditions can accelerate warm rain process, and how sensitive these electrostatic effects are to aerosol-induced changes of droplet sizes.

New references:

Eow, J.S., Ghadiri, M., Sharif, A. O., Williams, TJ.: Electrostatic enhancement of coalescence of water droplets in oil: a review of the current understanding, Chem. Eng. J., 84, 173–192, doi:10.1016/S1385-8947(00)00386-7, 2001.

Tsutomu Takahashi: Measurement of electric charge of cloud droplets, drizzle, and raindrops, Reviews of Geophysics and Space Physics,11, 903-924, 1973.

Harrison, R. G., Nicoll, K. A., Ambaum, M. H. P.: On the microphysical effects of observed cloud edge charging, Q. J. R. Meteorol. Soc., 141, 2690–2699, doi:10.1002/qj.2554, 2015.

Beard, K. V., Durkee, R. I., Ochs, H. T.: Coalescence efficiency measurements for minimally charged cloud drops, J. Atmos. Sci., 59, 233–243., doi: 10.1175/1520-0469(2002)059<0233:CEMFMC>2.0.CO;2, 2002.

Baumgaertner, A. J. G., Lucas, G. M., Thayer, J. P., Mallios, S. A.: On the role of clouds in the fair weather part of the global electric circuit, Atmos. Chem. Phys., 14, 8599–8610, doi:10.5194/acp-14-8599-2014, 2014.

Harrison, R. G., Carslaw, K. S.: Ion-Aerosol-Cloud Processes in the Lower Atmosphere, Rev. Geophys., 41(3), doi:10.1029/2002RG000114, 2003.

Wallace, J. M., Hobbs, P. V.: Atmospheric Science, Second Edition, Academic Press, 2006.

Tinsley, B. A., Zhou, L., Plemmons, A.: Changes in scavenging of particles by droplets due to weak electrification in clouds, Atmos. Res., 79, 266 – 295, doi:10.1016/j.atmosres.2005.06.004, 2006.

Zhou, L., Tinsley, B. A., Plemmons, A.: Scavenging in weakly electrified saturated and subsaturated

clouds, treating aerosol particles and droplets as conducting spheres, J. Geophys. Res., 114, D18201, doi:10.1029/2008JD011527, 2009.

Klimin, N. N., Rivkind, V. Ya., Pachin, V. A.: Collision efficiency calculation model as a software tool for microphysics of electrified clouds, Meteorol. Atmos. Phys, 53, 111-120, doi:10.1007/BF01031908, 1994.

Twomey, S.: Pollution and the planetary albedo, Atmos. Environ., 8, 1251-1256. doi:10.1016/0004-6981(74)90004-3, 1974.

Main Comments

1. The authors concluded that electric charges and fields enhance the collision efficiency of small droplets. Is this new in the cloud physics field? If so, how different this study is compared with the one of Khain et al, 2004? Which open question does this manuscript address? The third paragraph (starting from Line 35) of the introduction part summarized the work of Khain et al, 2004, but didn't bring up the open question in Khain et al, 2004.

Response:

Thanks to the reviewer for asking these questions. It is not new that the electric charges and fields enhance collision efficiency of small droplets. Studies of Khain et al. (2004) and Harrison et al. (2015) already had this finding. In our study, we intend to compare the precipitation suppression effect due to increased aerosols and the electrostatic enhancement effect. We have revised the manuscript to emphasize on this issue.

Regarding the difference between our study and Khain et al. (2004), the two studies are different in many aspects. Firstly, Khain et al. (2004) focuses on justifying cloudy seeding via artificial charging process, for use in weather modification, while our study investigates to what extent the electrostatic effect mitigates the aerosol effect on the evolution of droplet size distribution. Secondly, the amount of electric charges on cloud droplets are extremely large in their study, and natural clouds probably do not meet that condition. In our study, however, the amount of electric charges and fields used in our study represent conditions in natural clouds such as warm clouds or the early stage of thunderstorms. Thirdly, simplified models are used for the electric force between charged droplets and for describing droplet motion in Khain et al. (2004). Our study uses more accurate models for electric force and droplet motions. Our study finds that electric charges and fields can accelerate precipitation under conditions in the real atmosphere and that the aerosol-induced precipitation suppression can be mitigated.

Reference:

Harrison, R. G., Carslaw, K. S.: Ion-Aerosol-Cloud Processes in the Lower Atmosphere, Rev. Geophys., 41(3), doi:10.1029/2002RG000114, 2003

2. The main conclusion of the manuscript is that electric charges and electric fields enhance the collision efficiency of small droplets pairs. The evolution of droplet size distribution with different initial radius is shown in Fig.7, 8, 10. To compare the evolution for different initial radii, I would suggest the authors to plot the size distributions in one plot at a single snapshot, i.e., plot r/r_0 at x-axis and n(x, t=15 min) of different r_0 at y-axis in one plot. This can help clearly

demonstrate the conclusion.

Response:

We tried to plot droplet size distributions as suggested by the reviewer. The figures are shown below. The main problem is that collision-coalescence is significantly slowed down in the smaller r_0 cases. Therefore the time (t_0) required for a second peak to form in the size distribution is quite different for different r_0. For the three cases in this study, the time t_0 is about 30, 60 and 120 min, respectively. We use a normalized time, namely t/t_0, for 5 snapshots. Because both the radius and the time are normalized, information shown in the figures are not very straightforward. Therefore we prefer that Figures 7, 8 and 10 remain unchanged. (Now they are Figs. 9, 11, and 14 in the revised manuscript).

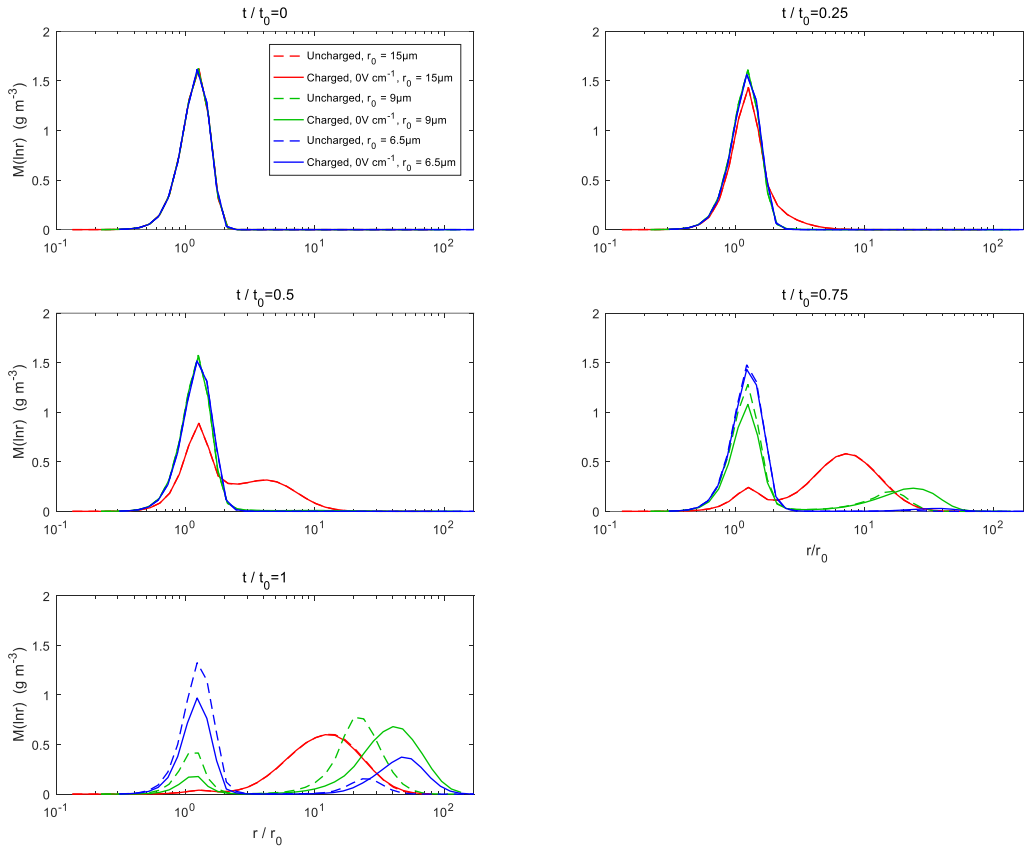

Figure 1. The evolution of normalized droplet size distributions. X-axis denotes the normalized droplet size r/r_0, where r_0=15, 9 and 6.5 μm separately. Different panels show different snapshots, i.e., at different normalized time t/t_0, where t_0=30, 60 and 120 min separately. Comparisons are made between uncharged droplets and charged droplets without electric fields.

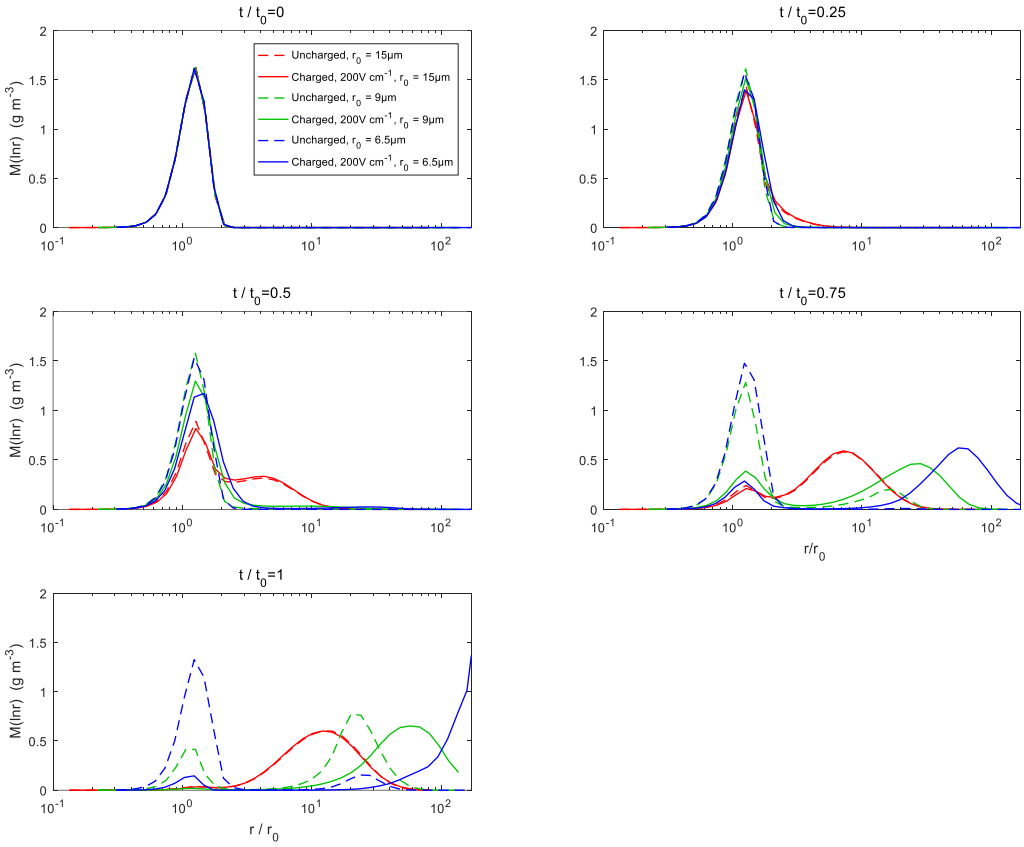

Figure 2. The evolution of normalized droplet size distributions. Comparisons are made between uncharged droplets and charged droplets with an electric field of 200 V cm^{-1}.

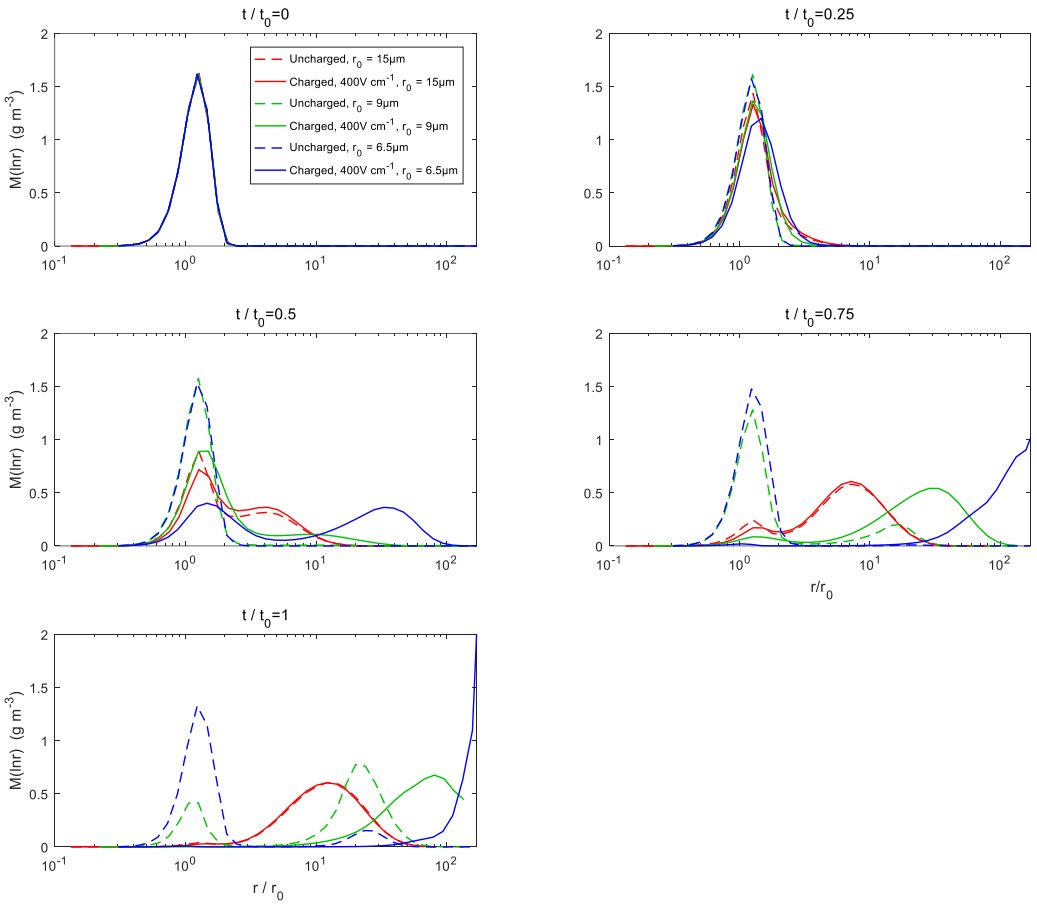

Figure 3. The evolution of normalized droplet size distributions. Comparisons are made between uncharged droplets and charged droplets with an electric field of 400 V cm^{-1}.

3. The authors mentioned the Navier-Stokes (NS) equation just above Eq.5. if you consider the backreaction from droplets to the flow, you can add the backreaction term to the NS equation. I don't see immediately why solving the N-S equation numerically with a low Reynolds number is difficult in this study.

Response:

We now realized that the sentence where N-S equation are mentioned is very misleading. In the revised manuscript, we have deleted this sentence in line 103 "Considering a sphere moving in a viscous fluid, the exact solution of the induced flow velocity field is to solve the Navier-Stokes equations. But the computation is too complicated in this study."

Solving the N-S equation is not difficult. However, the computation burden for the problem in this study would be heavy. With 37 size bins and 15 charge bins, the number of collision efficiency is on the order of 37×37×15×15. For each collision efficiency, about 10^4 steps are needed, including using the bisection method. It takes several days of computer time to derive all the collision efficiencies using the current method. Solving the N-S equation would be a much heavier computation burden.

4. How can I see from the terminal velocity curve in Fig.11 that the 5-um size droplet turns

upwards?

Response:

Thanks for pointing this out. In Fig.11 of the original manuscript, y-axis is in logarithmic scale and stands for the absolute value of terminal velocity. Negative terminal velocity means upward motion. However, minus is not compatible with the logarithmic coordinate. We therefore plotted the absolute value of terminal velocity in the figure (new Fig.16).

In the revised manuscript, we plot the negative terminal velocity in a separate panel, as shown below.

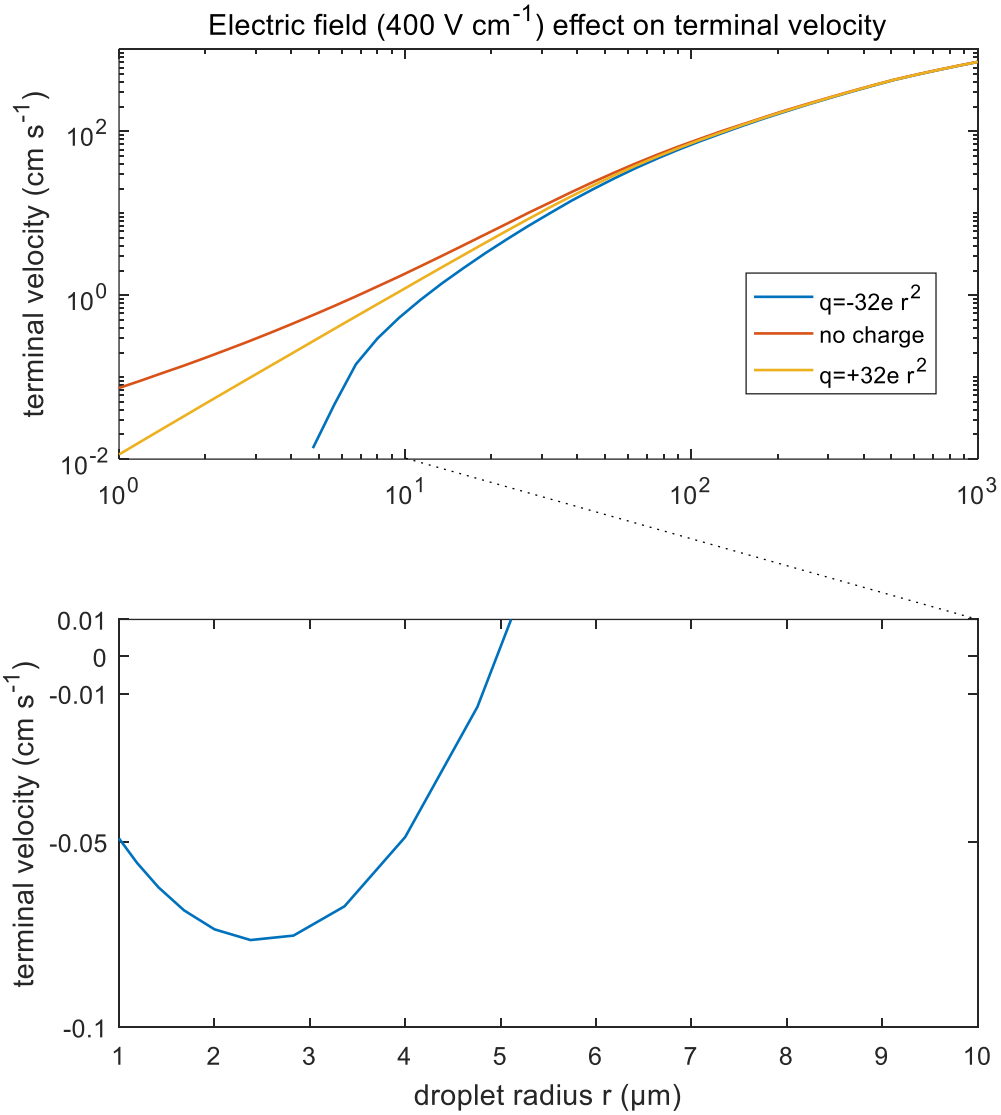

Figure 16. Terminal velocities of droplets in an external electric field 400 V cm^{-1}. Different lines denote different droplet charge conditions. It is seen that the terminal velocity of negatively-charged droplets smaller than 5 μm would turn upwards, which leads to the discontinuity of the lower curve in the figure.

Specific comments:

I would suggest the authors improve the English writing of this manuscript carefully across the paper. One way to improve the readability is to read the manuscript more carefully before submit it.

Response: Thank you very much for pointing this out. We have made substantial changes to the manuscript. The Introduction is completely rewritten. Most parts of Results and some descriptions of Methods are also rewritten. The writing of the paper is much more organized now.

1. Could it be an idea to use "droplet size distribution" instead of "droplet spectrum/spectra" so that readers from a different background (physics, astrophysics) can understand it? As you don't do any Fourier transform, right? What does the spectrum/spectra mean here?

Response: As the reviewer suggested, we have changed all the "spectrum/spectra" to "size distribution" in the manuscript, including text in figures. And it is true that we do not do any Fourier transform.

2. L10: a pair -> pairs. Changed.

3. L12: the cloud -> clouds. Please read through the paper and check if the same revision is needed. Changed and checked.

4. L22: in unit of um. We have corrected all of them.

5. L30: "this method" is unclear.

The sentence has been changed to "Schlamp et al. (1976) used the model of Davis (1964) to study the effect of …".

6. L36: used Stokes flow to represent. Changed.

7. L43: So -> Therefore. Changed.

8. L56: means -> represents. Changed.

9. L69: you already defined "/epsilon" just below Eq.2. So, the first sentence is a repetition and is misleading. You may also consider merge the two paragraphs, where E and /epsilon are discussed. Also, could you provide the expression of /epsilon?

Response:

Thanks for raising this question. Both E and ε are discussed in details now. We have revised line 59 "…and ε is the coalescence efficiency" to "Collision efficiency $E(m_1, m_2)$ and coalescence efficiency $\varepsilon(m_1, m_2)$ are introduced to the kernel because not all the droplets in this volume will have collision-coalesce with the collector." The first sentence of line 69 has been deleted, and the whole paragraph of lines 69-73 has been changed to:

Two droplets may not coalesce even when they collide with each other. Observations show that the droplet pair can rebound in some cases, because of an air film temporally trapped between the two surfaces. Especially for droplets with radii both larger than 100 μm, the coalescence efficiency is remarkably less than 1.0. Beard and Ochs (1984) provides a formula of coalescence efficiency for a certain range of droplet radii. Basically coalescence efficiency is a function of the sizes of the two droplets in their formula.

As for the expression of ε, it is just an empirical law (Beard and Ochs, 1984)

$$\varepsilon = (a-b)^{\frac{1}{3}} - (a+b)^{\frac{1}{3}} + 0.459$$

$$a = (b^2 + 0.00441)^{\frac{1}{2}}$$

$$b = 0.0946\beta - 0.319$$
$$\beta = \ln(r_2/\mu m) + 0.44\ln(r_1/200\mu m)$$

10. L73: used -> adopted. Corrected.

11. L85: What about "Momentum equation droplets"? Could you go through the paper and check "motion equation"? In physics, it is "the equation of motion".

Response: Thanks for pointing this out. We have gone through the paper and correct the following sentences.
Line 85: "Droplet motion equation" is changed to "Equations of motion for droplets"
Line 87: "In order to get the collision efficiency, the motion equation of droplets is integrated to get the trajectories of droplets" is changed to "In order to get the collision efficiency between a pair of droplets, the equations of motion are integrated to get the trajectories of the two droplets."
Line 89: "The motion equations for a pair of droplets…" is changed to "The equations of motion for a pair of droplets…"
Line 310: "The motion equation of droplets in the atmosphere is solved…" is changed to "The equations of motion for droplets in the atmosphere are solved…"

12. L88: the flow drag. Changed.

13. L92: velocity vector -> velocity. You may remove "relative to the earth". Changed.

14. L95: What does "The fluid property is treated as air" mean?
Response: We have changed "The fluid property is treated as air with temperature…" to
We set air temperature T = 283 K and pressure p = 900 hPa in this study for the calculation of air viscosity.

15. L100: I don't understand this paragraph. Do you mean that there are no droplet-droplet interactions? In English, it is very rare to put two nouns together in a sentence. You may read through the paper and try to rewrite those, which can help improve the readability of the manuscript.

Response: Thank the reviewer for raising these concerns. Actually, the "superposition method" is a term in many papers of cloud physics, including our references. We should make a detailed explanation. This paragraph is revised and is more comprehensible:

The flow drag force is described by the second term on the right side of Eq. (4), which assumes a simple hydrodynamic interaction of the two droplets. That is, each droplet moves in the flow field induced by the other one moving alone, and it is called "superposition method" in cloud physics. This method has been successfully used in many researches of the calculation of collision efficiencies (Pruppacher and Klett, 1997). To calculate the flow drag force, the induced flow field $\boldsymbol{u}$ is required. The method for obtaining the induced flow field $\boldsymbol{u}$ is discussed below.

16. L105: The nomenclature of the Reynolds number is unique here. It is "Re". How do you define your Reynolds number here? I know in some atmospheric books, "N_Re" was invented.

Response: Actually N_{Re} is widely used. We chose to use this instead of Re because Re can be misleading when it appears in an equation, especially in an equation like Eq. 6 in the manuscript. The two letters in Re can be mistakenly thought as distance R and elementary charge e.
The Reynolds number N_{Re} is defined as

$$N_{Re} = \frac{2rv\rho}{\mu}$$

in line 193 of the revised manuscript, when it appears for the first time.

17. **L115: a function.** Changed.
18. **L131: a complex mathematical problem in physics.** Changed.
19. **L146: the sign.** Changed.
20. **L147: it is obvious that.** Changed.
21. **L169: are not included.** Changed.
22. **L171: In thunderstorm conditions.** Changed.
23. **L173: approaches -> is close to.** Changed.
24. **L176: to the certain mass bins -> to mass bins.** Changed.
25. **L239: by a factor of about.** Changed.
26. **L249: evolution of the droplet size distribution.** Changed.
27. **L291: nearly not -> hardly.** Changed.
28. **L291: and difference -> and the one.** Changed.

29. **L294: to the observation. Can you add the reference as well?**

Response: As suggested, we have added "according to Tsutomu Takahashi (1973) and Pruppacher and Klett (1997)" after line 294 "…to the observation". The results of observation in several previous researches are shown in Chapter 17.4.2.1 of Pruppacher and Klett (1997) .

Reference:
Tsutomu Takahashi: Measurement of electric charge of cloud droplets, drizzle, and raindrops, Reviews of Geophysics and Space Physics,11, 903-924, 1973

30. **L326: Do you mean "the observed atmospheric conditions"? What does "real" mean here?**

Response: Yes. As suggested, we have changed line 326 "…represent the real conditions in the atmosphere" to "…represent the observed atmospheric conditions."

Response to Referee #2

General comments:

This manuscript studied the effect of electric charges and atmospheric electric fields on collision efficiency and the size distribution of cloud droplets numerically. The author concluded that electric charges and fields could accelerate large-drop formation in natural conditions, particularly for clouds with small droplet size. In my opinion, the manuscript is not acceptable for publication in its present form. Some major corrections should be done to make sure that the results can be more appropriate.

Main points:

1. There are some errors in Eq. (3). The second term of the right hands of Eq. (3) should be the loss of droplets of mass m, however, the collection kernel is about droplets of mass mx and mass m-mx.

Response: Thanks for the reviewer's careful reading. We have changed the following expression in the second term on the right hand of Eq. (3):

$$K(m_x, q_x; m-m_x, q-q_x)$$

To

$$K(m_x, q_x; m, q)$$

2. Equation (7) describes the induced flow field u, however, Eq. (7) does not satisfy no-slip boundary for two interacting droplets. Specifically, in the superimposed induced flow field according Eq. (7), the fluid velocity on the surface of the droplet is not equal to the velocity of the droplet. The detailed description paper of the theory was published in Journal of the Atmospheric Sciences in 2005 (https://journals.ametsoc.org/doi/full/10.1175/JAS3397.1).

Response: Thanks for the reviewer's comment. We have made the corrections. The error was made when we typed the equations.
Actually, the equations in our computer program are correct and satisfy no-slip boundary condition. We have made a thorough check for Section 3.2. We found that the dimensions of these stream functions are wrong in the original manuscript. We also used same symbols for different variables in Section 3.2 and 3.3 in the original manuscript. Now in the revised manuscript, we introduce $\tilde{R} = R/r$, $\theta_0 = \theta - \varphi$ to make sure different variables are represented by different symbols in Section 3.2 and 3.3. θ is replaced by θ_0 in section 3.2 because θ also appears in section 3.3 and represents a different variable. Their relation is $\theta_0 = \theta - \varphi$, where θ is the angle between the downward vector $\hat{\boldsymbol{e}}_{\boldsymbol{z}}$ and the line connecting the centres of two droplets, and φ is the angle between $\hat{\boldsymbol{e}}_{\boldsymbol{z}}$ and the droplet's velocity $\boldsymbol{v}$. The coefficient of Stokes flow has also been corrected in section 3.2.
Lines 103 to 114 in the original manuscript now reads as:

Considering a rigid sphere moving in a viscous fluid with a velocity U relative to the flow, the steam function depends on Reynolds number, $N_{Re} = \frac{2rv\rho}{\mu}$, where ρ is the density of the air, and μ is the dynamic viscosity of the air. It is known that when Reynolds number is small, the flow is considered as Stokes flow and the stream

function can be expressed as

$$\psi_s = U\left(\frac{1}{4\tilde{R}} - \frac{3\tilde{R}}{4}\right)\sin^2\theta_0 \tag{5}$$

where $\tilde{R} = R/r$ is the normalized distance (R is the distance from the sphere centre, and r is the droplet radius), θ_0 is the angle between the droplet velocity and vector $\boldsymbol{R}$ pointing from the sphere centre. U is droplet velocity relative to the flow, i.e., $U_1 = |\boldsymbol{v_1} - \boldsymbol{u_2}|$ for droplet 1, and $U_2 = |\boldsymbol{v_2} - \boldsymbol{u_1}|$ for droplet 2. However, this stream function for Stokes flow does not apply to the system with a large Reynolds number. Hamielec and Johnson (1962, 1963) gave the stream function ψ_h induced by a moving rigid sphere, which can be used for flows with large Reynolds numbers:

$$\psi_h = U\left(\frac{A_1}{\tilde{R}} + \frac{A_3}{\tilde{R}^2} + \frac{A_3}{\tilde{R}^3} + \frac{A_4}{\tilde{R}^4}\right)\sin^2\theta_0 - U\left(\frac{B_1}{\tilde{R}} + \frac{B_3}{\tilde{R}^2} + \frac{B_3}{\tilde{R}^3} + \frac{B_4}{\tilde{R}^4}\right)\sin^2\theta_0\cos\theta_0 \tag{6}$$

where $A_1, \ldots, B_4$ are functions only of Reynolds number N_{Re} for each droplet. The method is valid for $N_{Re} < 5000$. But the solution deviates from the Stokes flow solution when $N_{Re} \to 0$ for small droplets. Therefore, it is needed to construct a stream function that applies to a wide range of N_{Re}. This work adopts a stream function that is a linear combination of ψ_h and Stokes stream function ψ_s (Pinsky and Khain, 2000)

$$\psi = \frac{N_{Re}\psi_h + {N_{Re}}^{-1}\psi_s}{N_{Re} + {N_{Re}}^{-1}} \tag{7}$$

which converges to stokes flow when $N_{Re} \to 0$. Then the induced flow field $\boldsymbol{u}$ is derived,

$$\boldsymbol{u} = -\frac{1}{\tilde{R}^2\sin\theta_0}\frac{\partial\psi}{\partial\theta_0}\hat{\boldsymbol{e}}_{\boldsymbol{R}} + \frac{1}{\tilde{R}\sin\theta_0}\frac{\partial\psi}{\partial\tilde{R}}\hat{\boldsymbol{e}}_{\boldsymbol{\theta}} = u_R\hat{\boldsymbol{e}}_{\boldsymbol{R}} + u_\theta\hat{\boldsymbol{e}}_{\boldsymbol{\theta}} \tag{8}$$

where $\hat{\boldsymbol{e}}_{\boldsymbol{R}}$ and $\hat{\boldsymbol{e}}_{\boldsymbol{\theta}}$ are unit vectors in the polar coordinate (R, θ_0). It can also be expressed in the Cartesian coordinate (x, z)

$$\boldsymbol{u} = (u_R\cos\varphi - u_\theta\sin\varphi)\hat{\boldsymbol{e}}_{\boldsymbol{z}} + (u_R\sin\varphi + u_\theta\cos\varphi)\hat{\boldsymbol{e}}_{\boldsymbol{x}} \tag{9}$$

where the direction of $\hat{\boldsymbol{e}}_{\boldsymbol{z}}$ is vertically down, the same as gravitation. φ is the angle between $\hat{\boldsymbol{e}}_{\boldsymbol{z}}$ and the droplet velocity $\boldsymbol{v}$.

Both Stokes and Hamielec stream functions satisfy the no-slip boundary condition, i.e., the fluid velocity on the surface of the droplet is equal to the velocity of the droplet. Hamielec stream function is no-slip because those functions $A_1, \ldots, B_4$ in Eq. (6) satisfy $A_1 + 2A_2 + 3A_3 + 4A_4 = 1$ and $B_1 + 2B_2 + 3B_3 + 4B_4 = 0$, as long as the droplet is considered as a rigid sphere (Hamielec, 1963). These relations ensure that $u_\theta = -U\sin\theta_0$ at the surface of the droplet, which means the no-slip boundary condition. (Note that u_θ is the velocity of the fluid at droplet surface, and $U\sin\theta_0$ is the tangential velocity of the droplet surface.)

In our study, the adopted stream function is a linear combination of Stokes flow and Hamielec (1963) flow field, because the latter one works well for a wide range of Reynolds numbers up to 10^3. Both Hamielec and Stokes stream functions satisfy the no-slip boundary condition.

In addition, the superposition method used in our study does accord with Eq. (19) and (20) in Wang and Ayala's paper in 2005 (https://journals.ametsoc.org/doi/full/10.1175/JAS3397.1) based on the Stokes flow.

Reference:

Wang, L. P., Ayala, O., Grabowski, W. W.: Improved Formulations of the Superposition Method, J. Atmos. Sci, 62(4):1255-1266, doi: 10.1175/JAS3397.1, 2005

3. Fig. 4 gives the initial spectrum mass distribution in 2D grids of bin. For charged clouds, the initial charge is distributed symmetrically, as shown in Fig. 4b: 14% with charge +1r^2, 14% with charge -1r^2, 22% with charge +0.5r^2, 22% with charge -0.5r^2, and 28% with no charge. What is the principle determining the abovementioned charge ratio? Is there any observation data to prove the charge ratio?

Response: We thank the reviewer for raising these questions. The ratio in the original manuscript is an approximation of 2:3:4:3:2, but it is arbitrarily chosen. The basic idea was to let the droplets distribution over charge bins mimic a normal distribution, and also to satisfy electric neutrality $\bar{q} = 0$. In fact, there are some observations on mean charges of droplets, as can be seen in Figure 1 below (from Pruppacher and Klett, 1997). But there is no observational data for the kind of charge ratio that we used. Now we use a Gaussian distribution in the revised manuscript to describe the droplet distribution over the charge bins.

Lines 199-202 have been revised and it reads as follows in the revised manuscript:

To simulate an early stage of the warm-cloud precipitation, we need to distribute the droplets in each size bin to different charge bins, so that these droplets have different charges. Since there is little data on this, we assume a Gaussian distribution,

$$N(q) = \frac{N_0}{\sqrt{2\pi}\sigma} \exp\left(-\frac{q^2}{2\sigma^2}\right) \tag{19}$$

where N_0 is the number concentration in the size bin, and σ is the standard deviation of the Gaussian distribution in that size bin. $N(q)$ represents the number concentration of droplets with charge q. This distribution satisfies electric neutrality $\bar{q} = 0$. For different size bin, droplet number concentration N_0 is different. We purposely set the standard deviation σ to be different for different size bins. For a larger size, the charge amount is larger, based on $\overline{|q|}$ = 1.31 r^2 (q in unit of elementary charge and r in μm) as stated in the Introduction. Therefore, we set larger standard deviation σ for the larger size bins. With this setting of droplet charge, the total amount of charge in each case is shown in Table 1. The $\bar{r} =$ 15, 9, and 6.5 μm cases have an initial charge concentration of 9438, 15638, and 21634 e cm^{-3}, respectively, for both positive charge and negative charge.

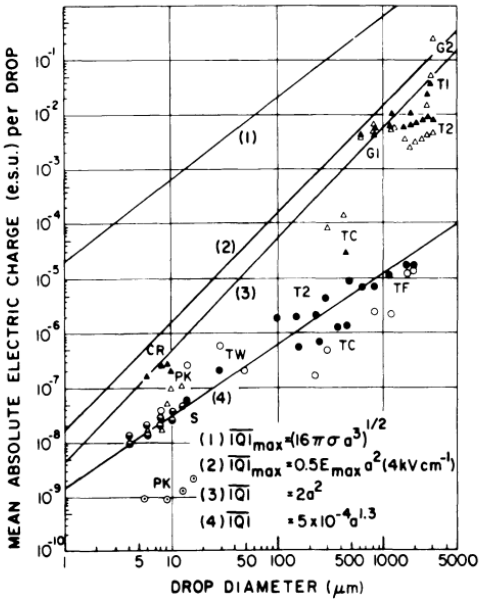

Fig. 17-2. Mean absolute electric charge on cloud and raindrops. Round symbols indicate warm cloud cases, triangular symbols indicate thunderstorm cases; solid symbols indicate negative charge, open symbols indicate positive charge. PK Phillips and Kinzer (1958), S Sergieva (1959), CR Colgate and Romero (1970), TW Twomey (1956), TC Takahashi and Craig (1973), T*1* Takahashi (1965), T*2* Takahashi (1972), TF Takahashi and Fullerton (1972), G*1* Gunn (1949), G*2* Gunn (1950). (Adapted with changes from Takahashi (1973).)

Appendix 1. Observational data for the relationship between droplet charge and radius (Pruppacher and Klett 1997). Our new setting $\overline{|q|} = 1.31\ r^2$ (q in unit of elementary charge and r in μm) approaches line (4) around $r \approx 10\mu m$, which is the weakly electrified warm cloud case.

New simulations using the Gaussian charge distribution have been performed. Figs. 4, 7-10 in the original manuscript are now replaced with the new simulations, and comparisons are shown below. But the changes in results are not significant.

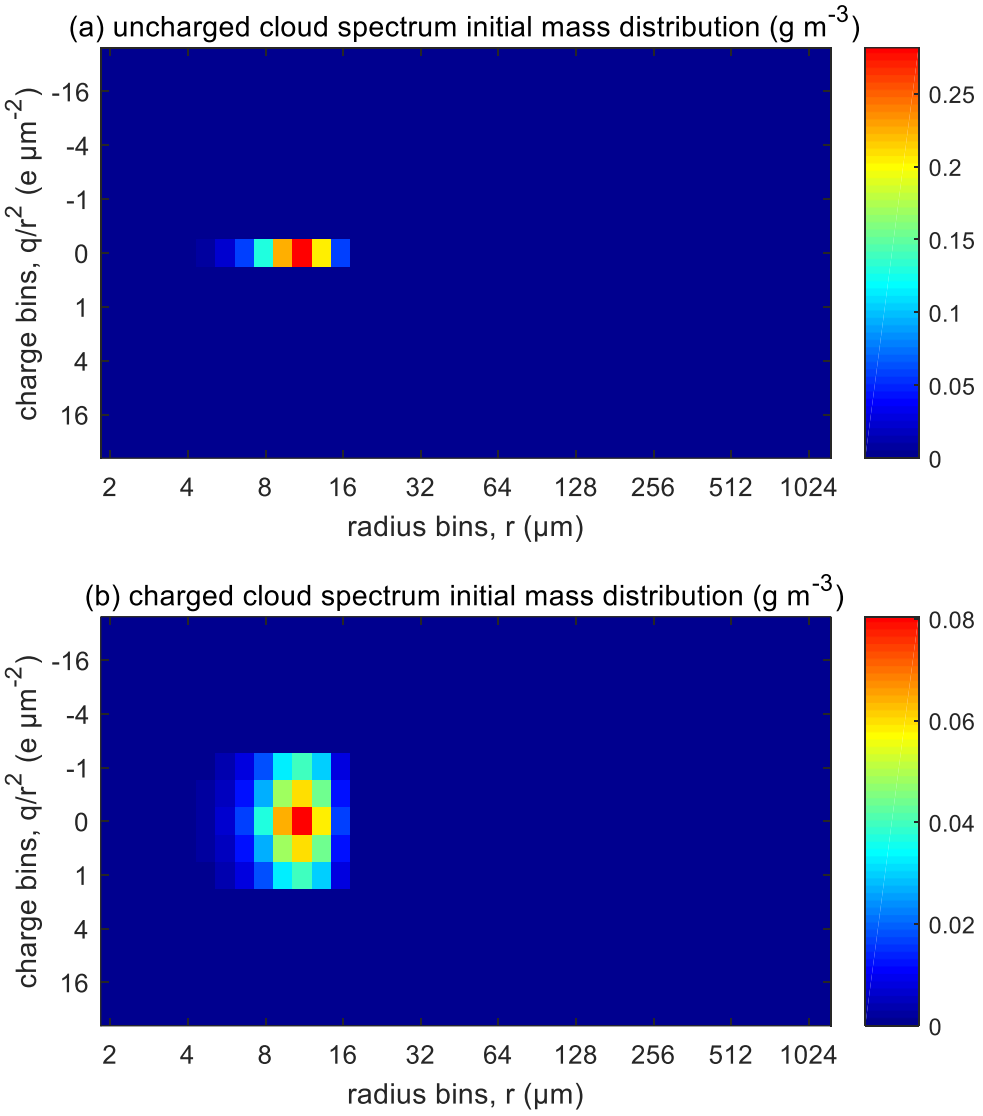

(Figure 4 in the original manuscript)

Figure 4. The initial droplet mass distributed over the size and charge bins. Colours stand for water mass content in the bins (in unit of g m^{-3}). (a) Uncharged droplets (b) charged droplets.

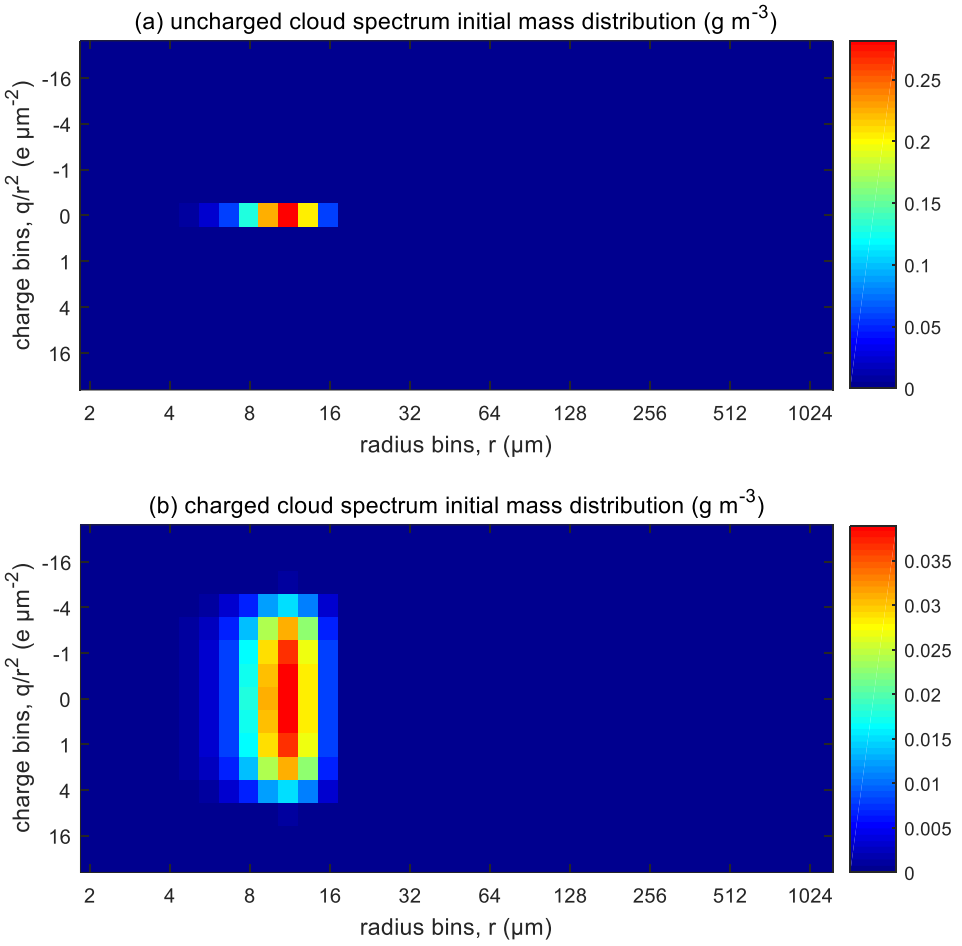

(Figure 4 in the revised manuscript)

Figure 4 (it is Figure 5 now). The initial droplet mass distributed over the size and charge bins. Colours stand for water mass content in the bins (in unit of g m^{-3}). (a) Uncharged droplets (b) charged droplets.

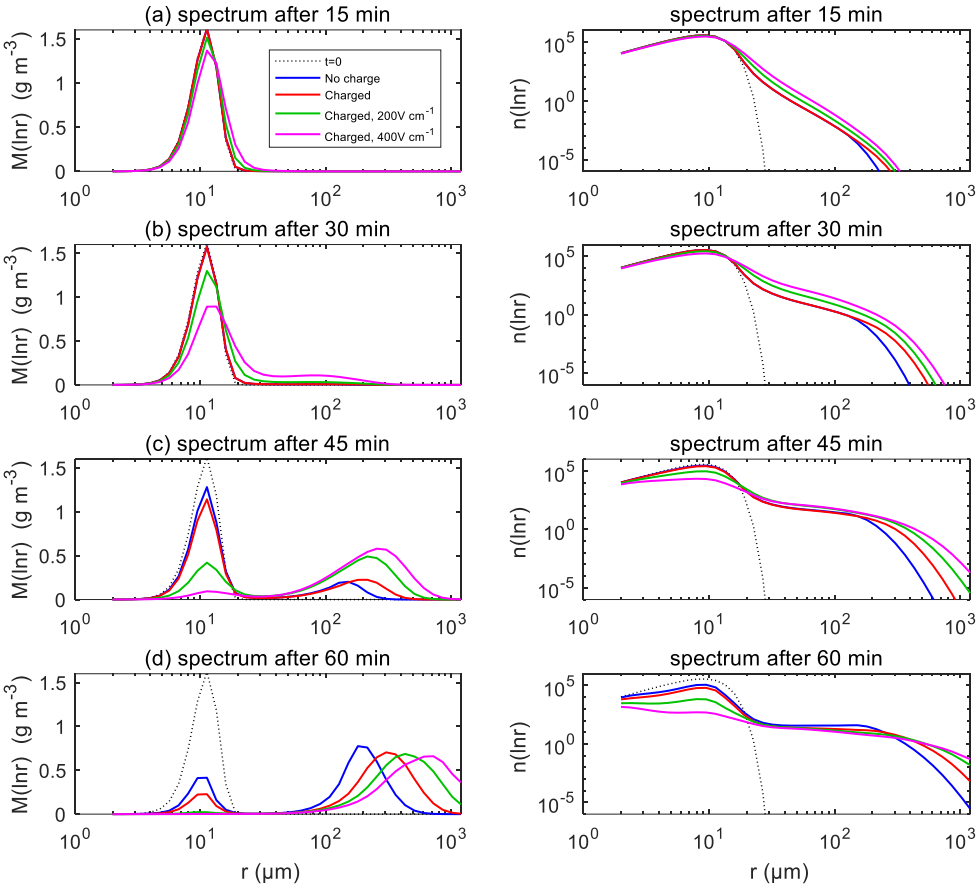

(Figure 8 in the original manuscript)

FIG. 8. (it is Figure 9 now.) The evolution of the droplet size distribution with initial $\bar{r}$ = 9 μm.

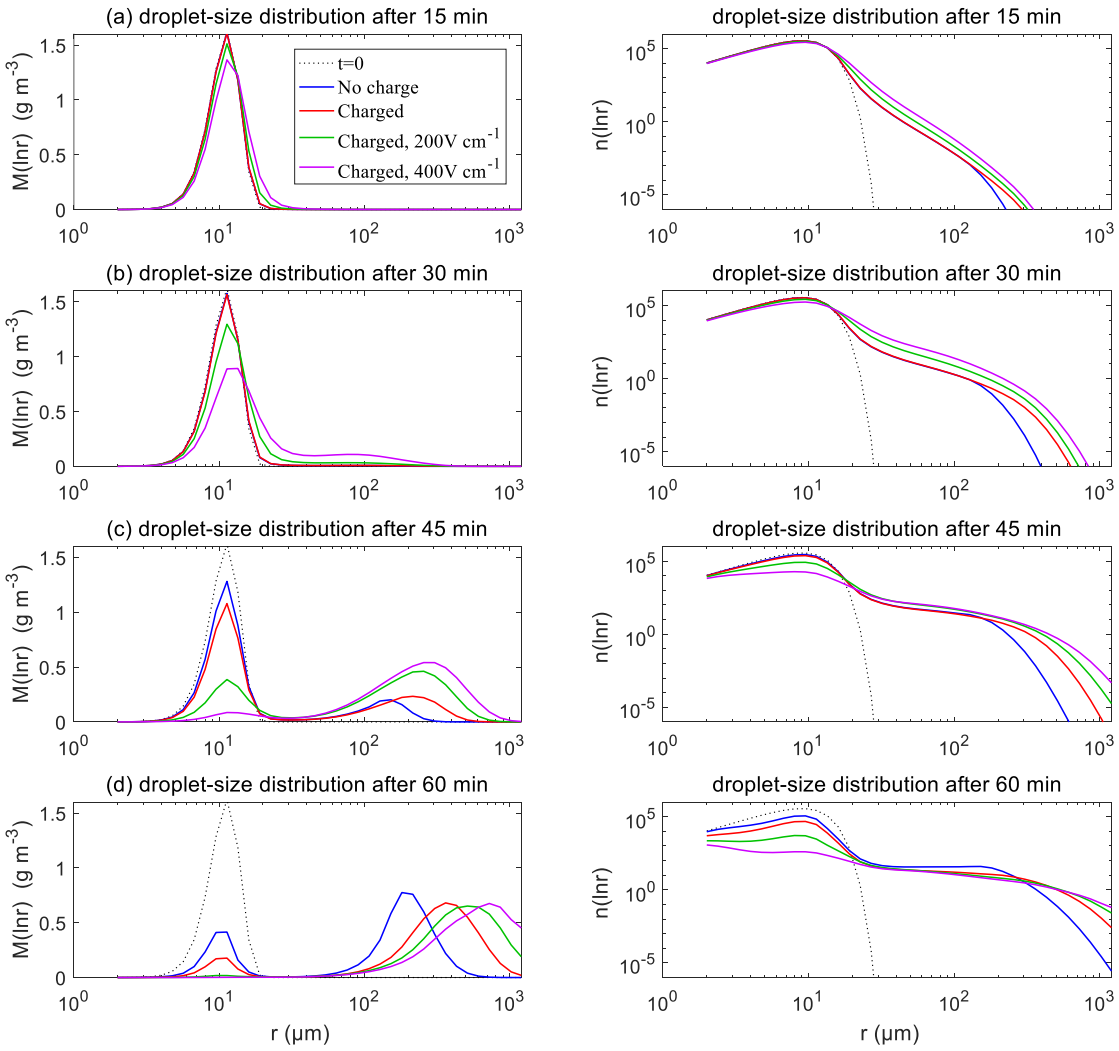

(Figure 8 in the new manuscript)

FIG. 8 (it is Figure 11 now). The evolution of the droplet size distribution with initial $\bar{r} = 9$ μm.

Response to Referee #3

The authors numerically investigate collisions of charged cloud droplets and rain drops, accounting for influence of atmospheric electric field. For this purpose, they first calculate collision efficiency table considering gravity force, drag forces and electrical forces acting on drops in course of their interaction. Corresponding drop motion equations are formulated using superposition method and are integrated using second order Runge-Kutta method. Then authors solve stochastic collection equation (SCE) for 2D drop size distribution (DSD), where the first independent variable is drop mass and the second the drop charge. SCE is solved for various initial DSDs, charges and electric field strengths. Authors conclude that "electric field could significantly enhance the collision process" in the case when the initial DSD is given in the range of small cloud droplets. I would like to note that theory and methods used by the authors in their research are not new (all the needed references are given in the study). Nevertheless, the results obtained in the study are of interest so I recommend the manuscript for publication in ACP after major revision.

1. The English language of the manuscript is of a very low quality. Please find a way to enhance it in order to render the text more readable and comprehensible.

Response: Thanks for the reviewer's comment on the writing of the paper. We have substantially revised the whole manuscript. The Introduction of the manuscript is completely rewritten. Most part of the Results, Abstract, and Conclusion are rewritten. Description of the methods are now improved in writing. The whole manuscript is now more organized and more readable. We have also checked the grammar throughout the manuscript. Grammar errors and unclear sentences are all changed. In the response to reviewer's 2nd comment, we show part of the rewritten Introduction to summarize the electrification process in clouds. In the response to reviewer's 12th comment, we show the rewritten section 5.1, where the electrostatic effects on collision efficiency is discussed.

2. It is worth explaining in the introduction how charges appear in cloudy drops.

Response: Yes, it is necessary to explain the charging process in clouds. At the beginning of the rewritten Introduction, we use two paragraphs to explain the electrification in thunderstorms and in warm clouds. These paragraphs now read as:

Clouds are usually electrified (Pruppacher and Klett 1997). For thunderstorms, several theories of electrification have been proposed in the past decades. The proposed theories assume that the electrification involves the collision of graupel or hailstones with ice crystals or supercooled cloud droplets, based on radar observational result that the onset of strong electrification follows the formation of graupel or hailstones within the cloud (Wallace and Hobbs, 2006). However, the exact conditions and mechanisms are still under debate. One charging process could be due to the thermoelectric effect between the relatively warm, rimed graupel or hailstones and the relatively cold ice crystals or supercooled cloud droplets. Another charging process could be due to the polarization of particles by the downward atmospheric electric field. The thunderstorm electrification can increase the electric fields to several thousand V cm^{-1}, while the magnitude of electric fields in fair weather air is only about 1 V cm^{-1} (Pruppacher and Klett 1997). Droplet charges can reach $|q| \approx 42r^2$ in unit

of elementary charge in thunderstorms, with the droplet radius r in unit of μm according to observations (Takahashi, 1973). For cumuli clouds, previous studies show smaller charge amount.

Liquid stratified clouds do not have such strong charge generation as in the thunderstorms. But charging of droplets can indeed occur at the upper and lower cloud boundaries as the fair weather current passes through the clouds (Harrison et al. 2015, Baumgaertner et al. 2014). The global fair weather current and the electric field are in the downward direction. Given the electric potential of 250 kV for the ionosphere, the exact value of fair weather current density over a location depends on the electric resistance of the atmospheric column, but its typical value is about 2×10^{-12} A m^{-2} (Baumgaertner et al. 2014). The fair weather electric field is typically about 1 V cm^{-1} in the cloud-free air, but is usually much stronger inside stratus clouds, because the cloudy air has a lower electrical conductivity than the cloud-free air. There is a conductivity transition at cloud boundaries. Therefore, the cloud top is positively charged and the cloud base is negatively charged. Based on the in situ measurements of charge density in liquid stratified cloud, and assuming that the cloud has a droplet number concentration on the order of 100 cm^{-3}, it is estimated that the mean charge per droplet is +5e (ranging from +1e to +8e) at cloud top, and -6e (ranging from -1e to -16e) at cloud base (Harroson et al. 2015). According to Tsutomu Takahashi (1973) and Khain (1997), the mean absolute charge of droplets in warm clouds is around $|q| \approx 6.6\, r^{1.3}$ (e, μm). For a droplet with radii of 10 μm, it is about 131 e.

New references:

Tsutomu Takahashi: Measurement of electric charge of cloud droplets, drizzle, and raindrops, Reviews of Geophysics and Space Physics,11, 903-924, 1973.

Harrison, R. G., Nicoll, K. A., Ambaum, M. H. P.: On the microphysical effects of observed cloud edge charging, Q. J. R. Meteorol. Soc., 141, 2690–2699, doi:10.1002/qj.2554, 2015.

Baumgaertner, A. J. G., Lucas, G. M., Thayer, J. P., Mallios, S. A.: On the role of clouds in the fair weather part of the global electric circuit, Atmos. Chem. Phys., 14, 8599–8610, doi:10.5194/acp-14-8599-2014, 2014.

Wallace, J. M., Hobbs, P. V.: Atmospheric Science, Second Edition, Academic Press, 2006.

3. Line 123: Suddenly, the concept of "no-slip boundary conditions" appear. To explain.

Response: Thanks for the reviewer to point this out. An explanation is added to the manuscript. Before line 115, the following paragraph is added. (In the revised manuscript, U is the droplet velocity relative to the fluid.)

Both Stokes and Hamielec stream functions satisfy the no-slip boundary condition, i.e., the fluid velocity on the surface of the droplet is equal to the velocity of the droplet. Hamielec stream function is no-slip because those functions $A_1, \ldots, B_4$ in Eq. (6) satisfy $A_1 + 2A_2 + 3A_3 + 4A_4 = 1$ and $B_1 + 2B_2 + 3B_3 + 4B_4 = 0$, as long as the droplet is considered as a rigid sphere (Hamielec, 1963). These relations ensure that $u_\theta = -U \sin\theta_0$ at the surface of the droplet, which means the no-slip boundary condition. (Note that u_θ is the velocity of the fluid at droplet surface, and $U \sin\theta_0$ is the tangential velocity of the droplet surface.)

4. To illustrate Eqs. (11) and (12) by a figure. To show directions of all the forces acting on drops and the velocities of the drops.

Response: Thanks for the reviewer's comment. Equation (11) (now it is Eq.13) represents the electrostatic force acting on droplet 2, due to the charge of droplet 1 and the external electric field. The new figure below shows all the forces acting on droplet 1 and droplet 2, and the velocities of the droplets. It has been added to the revised manuscript as Figure 2. These forces are terms on the right hand side of Eq. 4, including gravity force, flow drag force, and electrostatic force. We changed the presentation of Equation (13) in the revised manuscript so that the electric forces acting on droplet 2 can be understood more easily.
Lines 135-146 have been revised to:

$$\boldsymbol{F}_{e2} = E_0 q_2 \cos\theta \hat{\boldsymbol{e}}_{\boldsymbol{R}} + E_0 q_2 \sin\theta \hat{\boldsymbol{e}}_{\boldsymbol{\theta}} + \{r_2{}^2 E_0^2 (F_1 \cos^2\theta + F_2 \sin^2\theta) + E_0 \cos\theta (F_3 q_1 + F_4 q_2) + \frac{1}{r_2^2}(F_5 q_1{}^2 + F_6 q_1 q_2 + F_7 q_2{}^2)\}\hat{\boldsymbol{e}}_{\boldsymbol{R}} + \{r_2{}^2 E_0^2 F_8 \sin 2\theta + E_0 \sin\theta (F_9 q_1 + F_{10} q_2)\}\hat{\boldsymbol{e}}_{\boldsymbol{\theta}} \quad (13)$$

where $\hat{\boldsymbol{e}}_{\boldsymbol{R}}$ is the radial unit vector, and $\hat{\boldsymbol{e}}_{\boldsymbol{\theta}}$ is tangential unit vector, $\boldsymbol{E_0}$ is the eternal electric field, q_1 and q_2 are the charges of droplet 1 and droplet 2 respectively, and parameters F_1 to F_{10} are a series of complicated functions of geometric parameters (r_1, r_2, R; Davis 1964).

The electric force directly from the external field is shown as the two terms in the first line of Eq. (13), and can be simply written as $\boldsymbol{E_0} q_2$ if combining the two terms. Line 2 and line 3 in Eq. (13) represent the interactive force from droplet 1 in the radial direction and tangential direction, respectively. Note that the third term in line 2 represent the interactive force from droplet 1 if there is no external electric field. Except for this term, all the other terms in lines 2 and 3 are the interactive forces from droplet 1 due the induction from the external field.

Similarly, the resultant electric force $\boldsymbol{F}_{e1}$ acting on droplet 1 includes both the force directly from the external field and the interactive force from droplet 2. The sum of the electric forces on the two droplets, $\boldsymbol{F}_{e1} + \boldsymbol{F}_{e2}$, must equal to the external electric force acting on the system, which can be expressed as $\boldsymbol{E_0}(q_1 + q_2)$, because the two droplets can be considered as a system. Then, the electric force acting on droplet 1 could be derived immediately as

$$\boldsymbol{F}_{e1} = \boldsymbol{E_0}(q_1 + q_2) - \boldsymbol{F}_{e2} \quad (14)$$

Figure 2 is a schematic diagram showing the forces acting on each droplet in a pair. Also shown in Fig. 2 are the velocity of each droplet relative to the flow if there is no other droplets present ($\boldsymbol{v}$), and the flow velocity induced by the other droplet ($\boldsymbol{u}$). Droplet velocity relative to the flow is $\boldsymbol{v} - \boldsymbol{u}$. The electric field $\boldsymbol{E_0}$ is in the downward direction, the same as gravity. Droplet 1 has positive charge and droplet 2 has negative charge in this example. The forces acting on each droplet include gravity, flow drag force, and the electrostatic force, as seen on the right side of Eq. (4). For droplet 1, the electric force directly from the external field is in the downward direction, and is shown as $\boldsymbol{E_0} q_1$ in the figure. The interactive electric force from droplet 2, shown as $\boldsymbol{F}_{\text{inter}}$ in the figure, has a radial component and a tangential component, so that it is in a direction that does not necessarily align with the line connecting the two droplets. Because of the interactive electric force from droplet 2, the velocity $\boldsymbol{v}$ of droplet 1 is not in the vertical direction. The electrostatic force between charged droplets tend to make the droplets attract each other. This force is particularly strong when droplets are close to each other, thus to enhance collisions. The flow drag force on droplet 1 is in the opposite

direction with $\boldsymbol{v}-\boldsymbol{u}$.

If there is no external electric field but only with charge effect, Eq. (13) is reduced to

$$\boldsymbol{F}_{e2}=\frac{1}{r_2^2}(F_5{q_1}^2+F_6q_1q_2+F_7{q_2}^2)\hat{\boldsymbol{e}}_{\boldsymbol{R}} \tag{15}$$

To illustrate it, the comparison between the electrostatic forces derived by the inverse-square law and conductor model without electric field (i.e., Eq. 15) are shown in Fig. 3, where the electric force between droplets with opposite-sign charges (dashed lines) and with same-sign charges (solid lines) varies with distance. When $R \gg r_1, r_2$,we have $F_5, F_7 \to 0$, $F_6 \to r_2^2/R^2$, and it is also shown that two models are basically identical in remote distance. But when the spheres approach closely, the conductor interaction (blue lines) changes to strong attraction, because of electrostatic induction. The interaction is always attraction at small distance, regardless of the sign of charges.

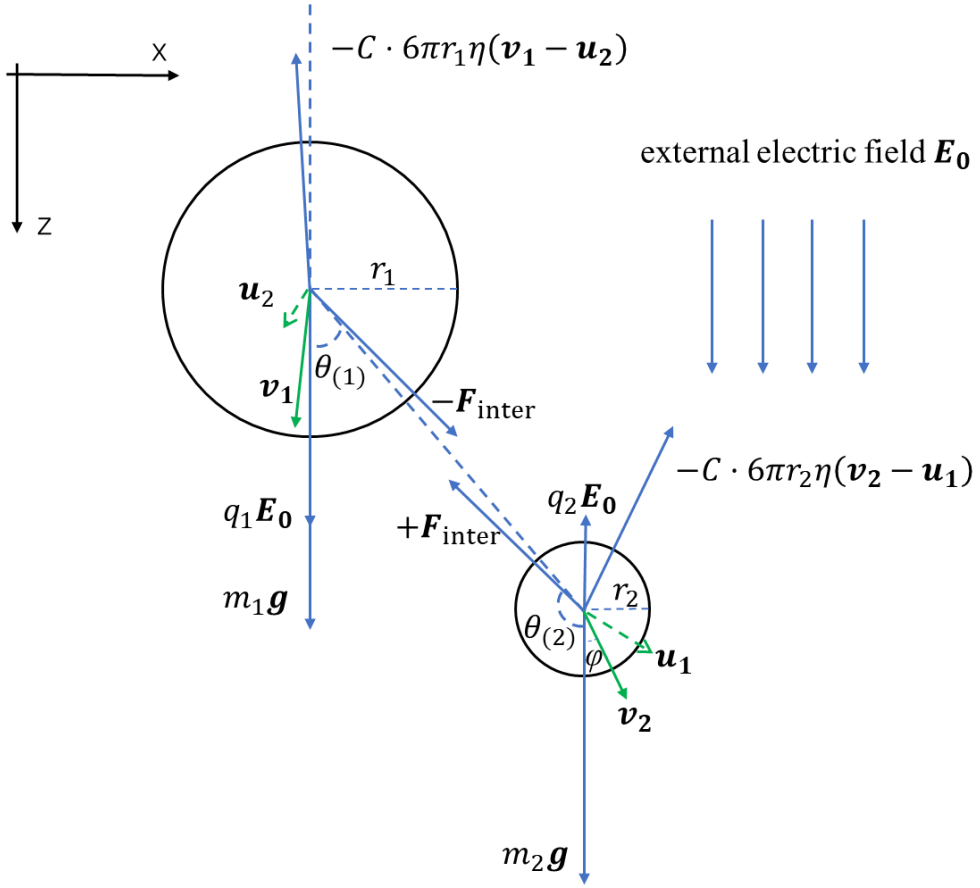

FIG. 2. A schematic diagram of all the forces acting on the two droplets, as well as the velocities of the droplets. The electric field $\boldsymbol{E_0}$ is vertically downward, and electric charges $q_1>0$, $q_2<0$. Note that the electrostatic force $\boldsymbol{F}_{e1}$, $\boldsymbol{F}_{e2}$ include two parts: the electric force from the other droplet ($\boldsymbol{F_{inter}}$ in the figure), and the force from the external electric field (shown as $q_1\boldsymbol{E_0}$ **and** $q_2\boldsymbol{E_0}$In the figure).

5. Is it right that appear in the Eq. (12)?

Response: Yes it is right. We should have emphasized that $\boldsymbol{F}_{e1}$ and $\boldsymbol{F}_{e2}$ consist not only the electric force from the other droplet, but also the force from the external electric field. As mentioned in the response to reviewer's 4th comment, the order of two terms in Equation (11) is changed, so that it is easier to identify the force due to the external electric field and the force due to the charge in the other droplet. Because the two droplets can be considered as a system, the sum of the forces they experience independently ($\boldsymbol{F}_{e1}+\boldsymbol{F}_{e2}$) must be equal to the external electric force acting on the system

$E_0(q_1 + q_2)\hat{\boldsymbol{e}}_{\boldsymbol{z}}$. This relation is expressed in equation (12). If we have already known F_{e2}, then F_{e1} is derived immediately from Eq. (12). In line 140 of the original manuscript, we have made some changes in the writing of the manuscript to explain this.

6. Line 153: actually, you integrate the system of 12 (or 8) equations

Response: Thanks for the reviewer's careful reading. We have added this information to the manuscript based on reviewer's comment.

7. Line 187: Eq. (13) is the exponential distribution and not the gamma distribution.

Response: Yes Eq. (13) (which is Eq. 16 in the revised manuscript) is the exponential distribution. Thanks to the reviewer for pointing this out. We have made the correction in the manuscript. We should mention that Eq. (14) and (15) are gamma distributions. Please refer to the response to the 8th comment for detailed discussions on how to obtain Eq. (15).

8. How did you obtain Eq. (15) from Eq. (14)?

Response:

Thanks for this question. We now have added more information to this part, so that it is easier to understand the equations for size distribution. Basically, definitions of the size distribution is used for the derivation. Recall that $n(m)$ is the droplet number concentration per unit mass interval, and $M(m)$ is the mass concentration per unit mass interval.

The distribution of droplet number concentration $n(m)$ can also be written as $n(r)$, or $n(\ln r)$. We know that the definition of $n(m)$ is: $n(m) = \mathrm{d}N/\mathrm{d}m$, where $\mathrm{d}m$ is the mass interval, and $\mathrm{d}N$ is the droplet number concentration in that mass interval. $n(r) = \mathrm{d}N/\mathrm{d}r$ represents the droplet number concentration per unit size interval. $n(\ln r) = \mathrm{d}N/\mathrm{d}\ln r$ represents droplet number concentration per unit interval of logarithmic size. Similarly, the distribution of droplet mass concentration $M(m)$ can be written as $M(r)$, and $M(\ln r)$. These functions are related together.
$M(\ln r)$ and $M(r)$ are related through:

$$M(\ln r) = \mathrm{d}M/\mathrm{d}\ln r = r \cdot \mathrm{d}M/\mathrm{d}r = r \cdot M(r)$$

While $M(r)$ can be related with $M(m)$ through:

$$M(m) = \frac{\mathrm{d}M}{\mathrm{d}m} = \frac{1}{4\pi r^2}\frac{\mathrm{d}M}{\mathrm{d}r} = \frac{M(r)}{4\pi r^2}$$

With $m = 4\pi r^3\rho/3$, and assuming that $\bar{m} = 4\pi\bar{r}^3\rho/3$, where $\bar{r}$ is the mean radius, we can obtain $M(\ln r)$ from $M(m)$,

$$M(\ln r) = 3L\frac{r^6}{\bar{r}^6}exp\left(-\frac{r^3}{\bar{r}^3}\right)$$

In the revised manuscript, we added a new equation for $n(\ln r)$, because $n(\ln r)$ is also plotted and discussed in the Results section.

$$n(\ln r) = L\frac{9r^3}{4\pi\bar{r}^6}exp\left(-\frac{r^3}{\bar{r}^3}\right)$$

We feel that the derivations above is not very concise and does not look very straightforward. Therefore, in the revised manuscript, we choose a different way to present the initial size distribution function. Lines 187-194 in the original manuscript are now replaced by the following paragraph:

The initial droplet size distribution used in this study is derived based on an exponential function in Bott (1998),

$$n(m) = \frac{L}{\bar{m}^2}\exp\left(-\frac{m}{\bar{m}}\right) \quad (16)$$

where $n(m)$ is the distribution of droplet number concentration over droplet mass, L is the liquid water content, and $\bar{m}$ is the mean mass of droplets. This function is used to derive $n(lnr)$, which is the distribution of droplet number concentration over droplet radius. With the definitions of $n(m)$ and $n(lnr)$, and $m = 4\pi r^3\rho/3$, where ρ is droplet density, we can derive $n(lnr)$ as

$$n(\ln r) = \frac{dN}{d\ln r} = r\frac{dN}{dr} = r\frac{dN}{dm}4\pi\rho r^2 = 4\pi\rho r^3 n(m) \quad (17)$$

By substituting Eq. (16) into Eq. (17), and assuming that $\bar{m} = 4\pi\bar{r}^3\rho/3$, where $\bar{r}$ is the mean radius, we have

$$n(\ln r) = L\frac{9r^3}{4\pi\bar{r}^6}exp\left(-\frac{r^3}{\bar{r}^3}\right) \quad (18)$$

9. The authors should check the correctness of equations (13-15).

Response: Thanks for the suggestion. We have checked the equations to make sure they are correct. Please also refer to the response to the 8th comment for information on the initial size distribution.

10. Lines 195-200. To add information about number concentration, liquid water content and charge content for all initial drop spectra.

Response: The initial liquid water content is set to be L=1 g m^{-3}, for all simulations. This is a typical value in warm clouds. The initial averaged droplet radius $\bar{r}$ is set to be 15 μm, 9 μm and 6.5 μm, where $\bar{r}$ = 15 μm case represents the clean conditions (less aerosol), and 6.5 μm represents polluted conditions (more aerosol). These settings give an initial droplet number concentration of 70, 325, and 850 cm^{-3}, respectively. The charge content is set as in the following table. The number concentration and charge content for all initial drop size distribution are shown in table 2 in the revised manuscript.

Table 2. Total number concentration, charge content for the initial droplet size distribution

mean radius $\bar{r}$ (μm)	total number concentration (cm^{-3})	total positive charge concentration Q^+ (e cm^{-3})	total negative charge concentration Q^- (e cm^{-3})
15	70.6	+9384	-9384
9	324.8	+15638	-15638
6.5	850.5	+21634	-21634

Note that the initial droplet number concentration is distributed into different size bins and different charge bins. The size distribution is based on functions described in Equations (13)-(15). The charge distribution is now based on a Gaussian distribution in the revised manuscript, instead of the method described in lines 200-202 in the original manuscript. Ratios shown in lines 200-202 in the original manuscript is an approximation of 2:3:4:3:2, but it is arbitrarily chosen to mimic a normal distribution, and also to satisfy electric neutrality $\bar{q} = 0$. In the revised manuscript, we use a Gaussian distribution to describe droplet distribution over the charge bins.

Lines 199-202 have been revised and it reads as follows in the revised manuscript:

To simulate an early stage of the warm-cloud precipitation, we need to distribute the droplets in each size bin to different charge bins, so that these droplets have different charges. Since there is little data on this, we assume a Gaussian distribution,

$$N(q) = \frac{N_0}{\sqrt{2\pi}\sigma} \exp\left(-\frac{q^2}{2\sigma^2}\right) \tag{19}$$

where N_0 is the number concentration in the size bin, and σ is the standard deviation of the Gaussian distribution in that size bin. $N(q)$ represents the number concentration of droplets with charge q. This distribution satisfies electric neutrality $\bar{q} = 0$. For different size bin, droplet number concentration N_0 is different. We purposely set the standard deviation σ to be different for different size bins. For a larger size, the charge amount is larger, based on $\overline{|q|}$ = 1.31 r^2 (q in unit of elementary charge and r in μm) as stated in the Introduction. Therefore, we set larger standard deviation σ for the larger size bins. With this setting of droplet charge, the total amount of charge in each case is shown in Table 1. The $\bar{r}$ = 15, 9, and 6.5 μm cases have an initial charge concentration of 9438, 15638, and 21634 e cm^{-3}, respectively, for both positive charge and negative charge.

11. Line 216: Please add the figure showing collision efficiency between cloud droplets (1-20 μm in radii), the same as in fig. 5. It is all the more important because you obtained the maximal effect for cloud droplets.

Response: As suggested, we plot a new figure below, to show the collision efficiencies for smaller collectors (r_1 = 5, 10, 15, 20 and 25 μm) when the droplet pairs have no charge. X-axis denotes the ratio of radius r_2/r_1. As will be seen in the response to reviewer's 12th comment, the 10 μm and 20 μm lines will be shown together with the results for charged droplets (new Fig. 6). Therefore, we think this figure is not necessary in the manuscript.

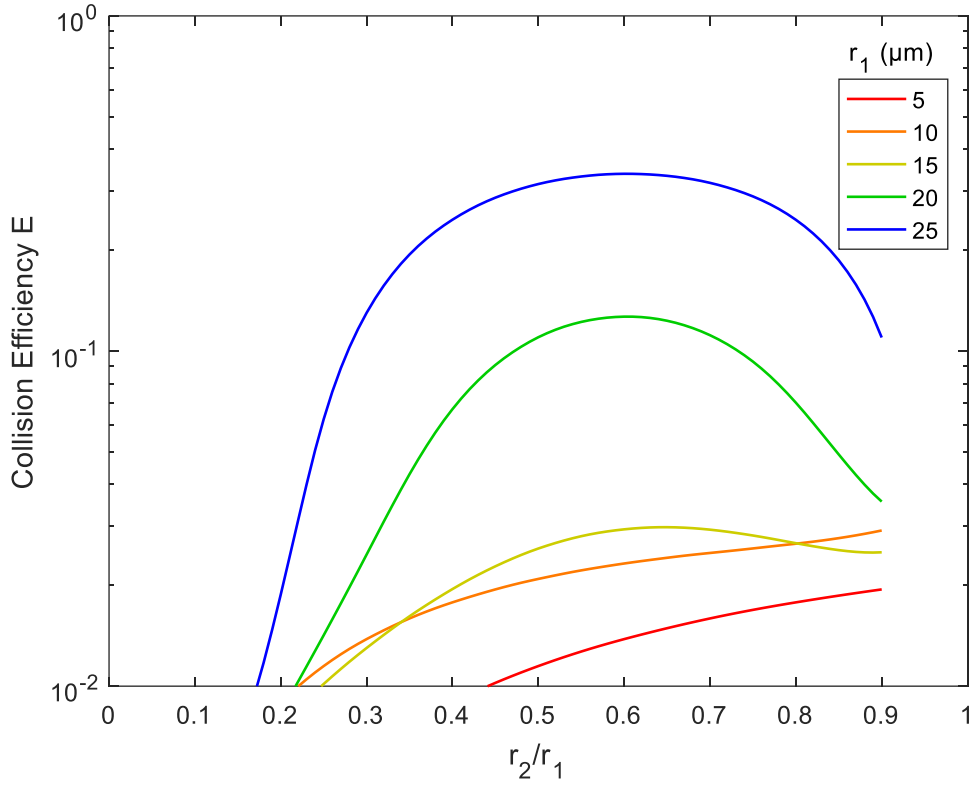

12. Figure 6: Please, add illustrations for different collectors (say 15 ïA¸ m, and 10 ïA¸ m in radii) and comment them.

Response: Thank you very much for the suggestion. As suggested, we have shown the different collectors r_1= 10, 20, 30 and 40 μm in the new figure below. Fig. 7 now describes the collision efficiency for the 30 and 40 μm collectors (precipitating droples). Fig. 8 now describes the collision efficiency for the 10 and 20 μm collectors (cloud droplets). Therefore, section 5.1 has been substantially revised. Most part of it has been rewritten. It is clear that electrostatic effects are significant for small droplets. We show the rewritten section 5.1 here:

5.1 Collision efficiency

Here we present collision efficiencies for typical droplet pairs to illustrate the electrostatic effects. During the evolution of droplet size distribution, the radius and charge amount of colliding droplets have large variability. In addition, the charge sign of the colliding droplets may be the same or the opposite. Therefore, only some examples are shown.

The collision efficiencies for droplet pairs with no electric charge and field are presented in Fig. 6 as a reference. Collector droplets with radii larger than 30 μm are shown here to represent the precipitating droplets. The calculated collision efficiencies from this study are also compared with the measurements from previous studies. It is seen that results from this study are generally consistent with the measurements. Collision efficiencies increase as r_2 changes from 2 to 14 μm, and also increase as r_1 changes from 30 to 305 μm. For two droplets that are both large enough, collision efficiency could be close to 1.

Figure 7 shows the collision efficiencies for droplet pairs with electric charge and field. The detailed

characteristics of the droplet pairs are shown in Table 1. Basically, droplet pairs that have no charge, with same-sign charges, and with opposite-sign charges are selected here, and under the 0 and 400 V m^{-1} electric fields. Results for the collector droplet with a radius of 30 μm (Fig. 7a) and 40 μm (Fig. 7b) are shown. When comparing Fig. 7a and 7b, it can be seen that electrostatic effects are less significant for a larger collector. The electrostatic effects are even weaker for collector radius larger than 40 μm (figures not shown). Therefore, we use the 30 μm collector as an example to explain the electrostatic effects on collision efficiencies below.

For the collector droplet with a radius of 30 μm (Fig. 7a), noticeable, and sometimes significant electrostatic effect can be seen. Compared to the droplet pair with no charge (line 1), the positively-charged pair under no electric field (line 2) has a slightly smaller collision efficiency, due to the repulsive force. As can be seen in Fig. 3, when the charged droplets move together, they first experience repulsive force, then attractive force at small distance. The integrated effect is that the droplets have smaller collision efficiency. The results for negatively-charged pair under no electric field are identical to line 2 and therefore are not shown. When a downward electric field of 400 V m^{-1} is added, the positively-charged pair (line 3) has a collision efficiency very close to the pair with no charge. This implies that the enhancement of collision efficiency by the electric field offsets the repulsive force effect. For a negatively-charged pair in a downward electric field (line 4), the collision efficiency with small r_2 is significantly enhanced. This could be easily explained by electrostatic induction: the strong downward electric field induces positive charge on the lower part of the collector droplet (even though it is overall negatively-charged), so the negative-charged collected droplet below experiences attractive force.

As for a pair with opposite-sign charges, line 5 in Fig. 7a shows that the collision efficiency is enhanced by the electrostatic effect even when there is no electric field. The collision efficiency is nearly an order of magnitude higher with $r_2 < 5$ μm. Line 6 in Fig. 7a shows that, with an electric field of 400 V cm^{-1}, the electrostatic effect for the pairs with opposite-sign charges is even stronger. There is also an interesting feature in Fig. 7a: as the collector and collected droplets have similar sizes, collision efficiency is high for the pairs with opposite-sign charges. This is quite different from the other four lines, where collision efficiencies are very low for droplet pairs with similar sizes.

Figure 8 shows the collision efficiencies for droplet pairs with charge and field, with smaller collectors. The collector droplet has a radius of 10 μm (Fig. 8a) and 20 μm (Fig. 8b) here, and can be used to represent cloud droplets. Collision efficiencies for these smaller collectors are much smaller than 1 when there is no charge (line 1 in Figs. 8a and 8b), which is already well known in cloud physics community. However, the electrostatic effects are so strong that the collision efficiencies could be significantly changed for these collectors. For the collector droplet with a radius of 10 μm (Fig. 8a), the positively-charged pair has a very small collision efficiency that is out of the scale in the figure, due to the dominating effect of the repulsive force as discussed above. For the positively-charged pair under a downward electric field, the collision efficiencies is on the similar order of magnitude as the pair with no charge. For the negatively-charged pair under the downward electric field, and for the pairs with opposite-sign charges, the electrostatic effects is very strong. The negatively-charged pair even has the collision efficiency increased by two orders of magnitude. Similarly, for the collector droplet with a radius of 20 μm (Fig. 8b), the electrostatic effect can lead to an order of magnitude increase in collision efficiencies.

It is evident that droplet charge and field can significantly affect collision efficiency, especially for smaller collectors. This means that the electrostatic effects depend on the radius of collector droplets, and mainly affects small droplets. The section below provides a detailed description on how these electrostatic effects can influence droplet size distributions.

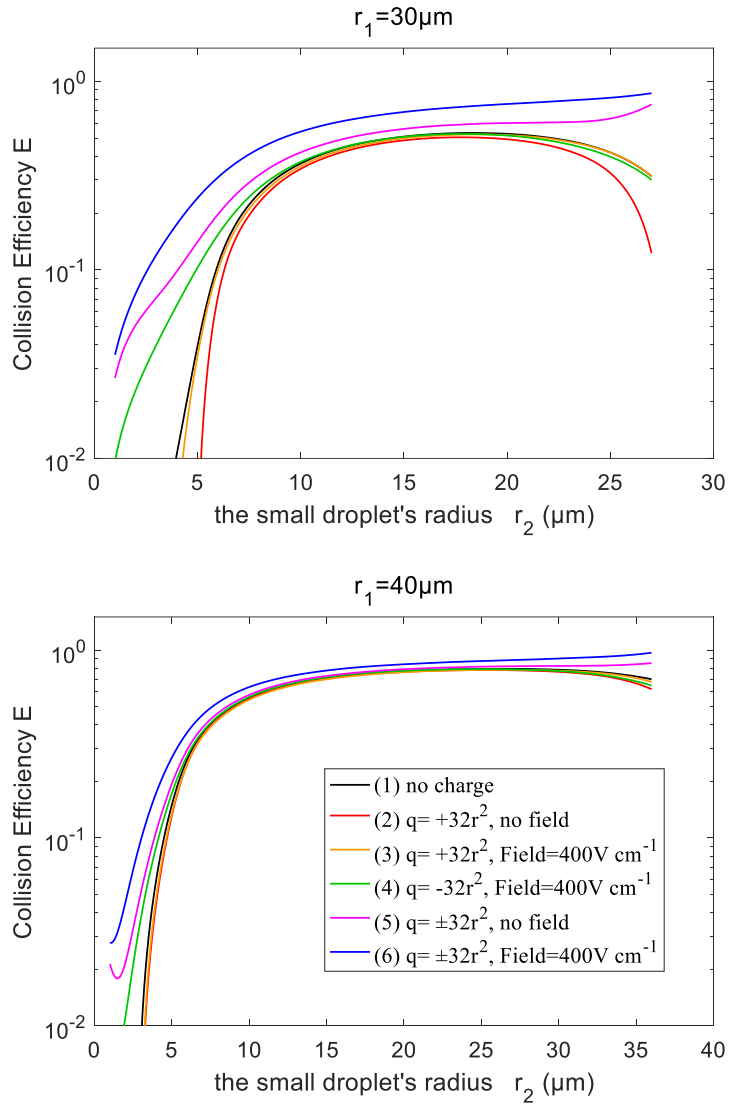

FIG. 7. Collision efficiency for droplets with electric charge and field. The radius of the collector droplet r_1 is: (a) 30.0 μm, (b) 40.0 μm . X-axis denotes the collected droplet raidus r_2. The two droplets carry electric charges proportional to r^2. The lines for droplet pairs with no charge (line 1 in Fig. 6a and 6b) are the same as the 30 μm and 40 μm lines in Fig. 5.

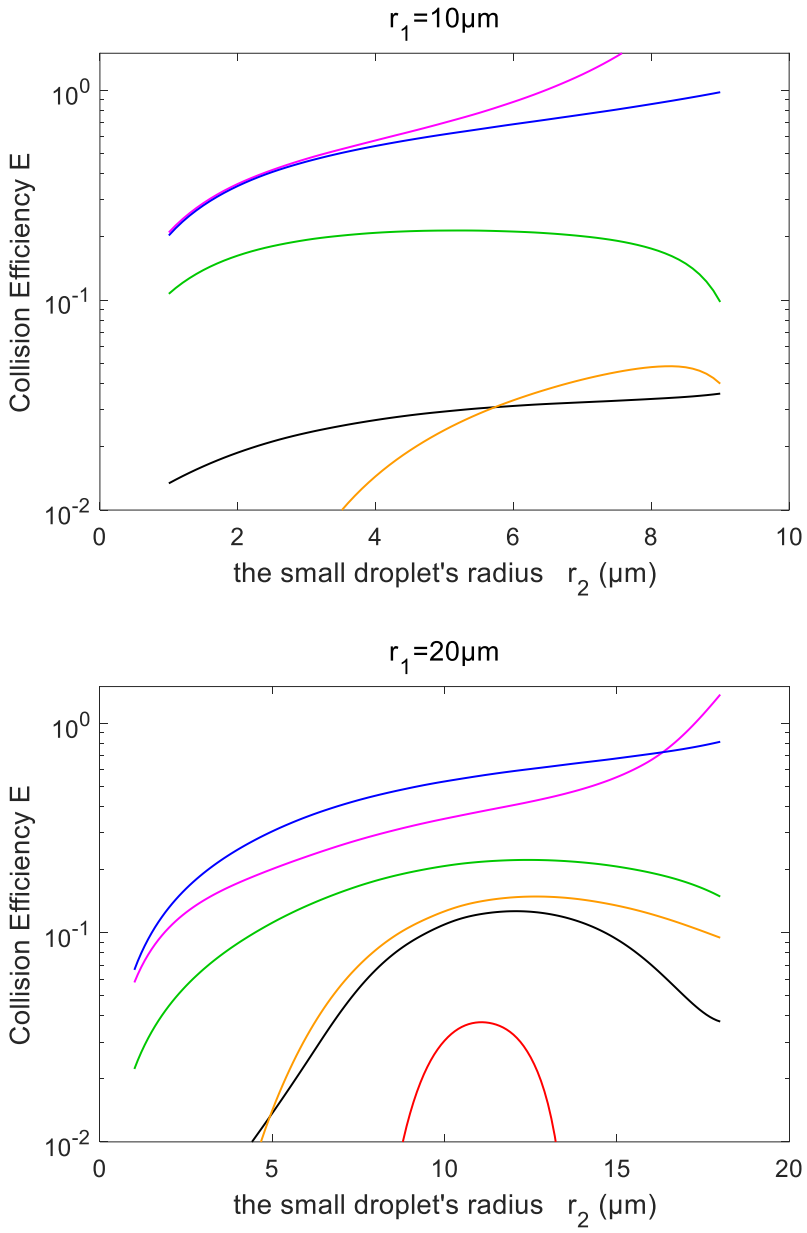

FIG. 8. Collision efficiency for droplets with electric charge and field. The radius of the collector droplet r_1 is: (a) 10.0 μm, (b) 20.0 μm. The other characteristics of the droplet pairs are similar to those in Fig. 6.

13. Section 5.2: Please show temporal changes of drop concentration and charge content and comment on them. How fast the charges of opposite signs compensate each other?

Response: Thanks for the reviewer's suggestion. The evolution of droplet concentration and charge content are shown in the below. These figures are also added to the manuscript as new Fig. 10, 12, and 15.

From Fig. 10 ($\bar{r}$ =15 μm), it is evident that droplet concentrations in the 4 different electric conditions decrease from about 70 cm^{-3} to less than 5 cm^{-3}, and the evolution is nearly not affected by the electric conditions. The electrostatic effect is therefore negligible in this case.

From Fig. 12 ($\bar{r}$ =9 μm), we can see the evolution is distinctly affected by the 4 different electric conditions. Electric charges and fields play an important role in converting smaller droplets to larger droplets, and decreasing the droplet number concentration.

From Figure 15 ($\bar{r}$ =6.5 μm), droplet concentration is strongly affected by the 4 different electric conditions. Results show that the electric field would remarkably trigger the collision-coalescence process for the small droplets.

Comparing the upper and lower panels of each figure, it is evident that the charges of opposite signs compensate each other as fast as the decrease of number concentration (except for the uncharged case). The phases of charge neutralizations are the same as changes of drop concentration. In all the three figures, more than 90% charges of opposite signs are neutralized during the evolution.

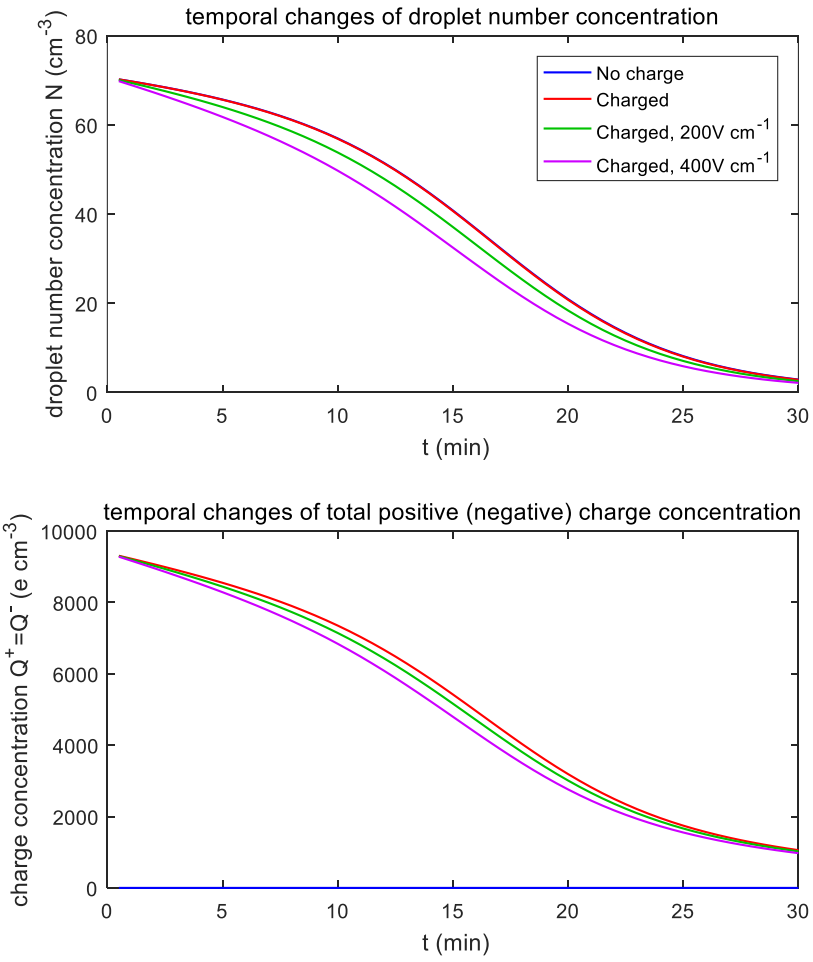

FIG. 10. Temporal changes of droplet total number concentration and total charge content for $\bar{r}$ =15 μm.

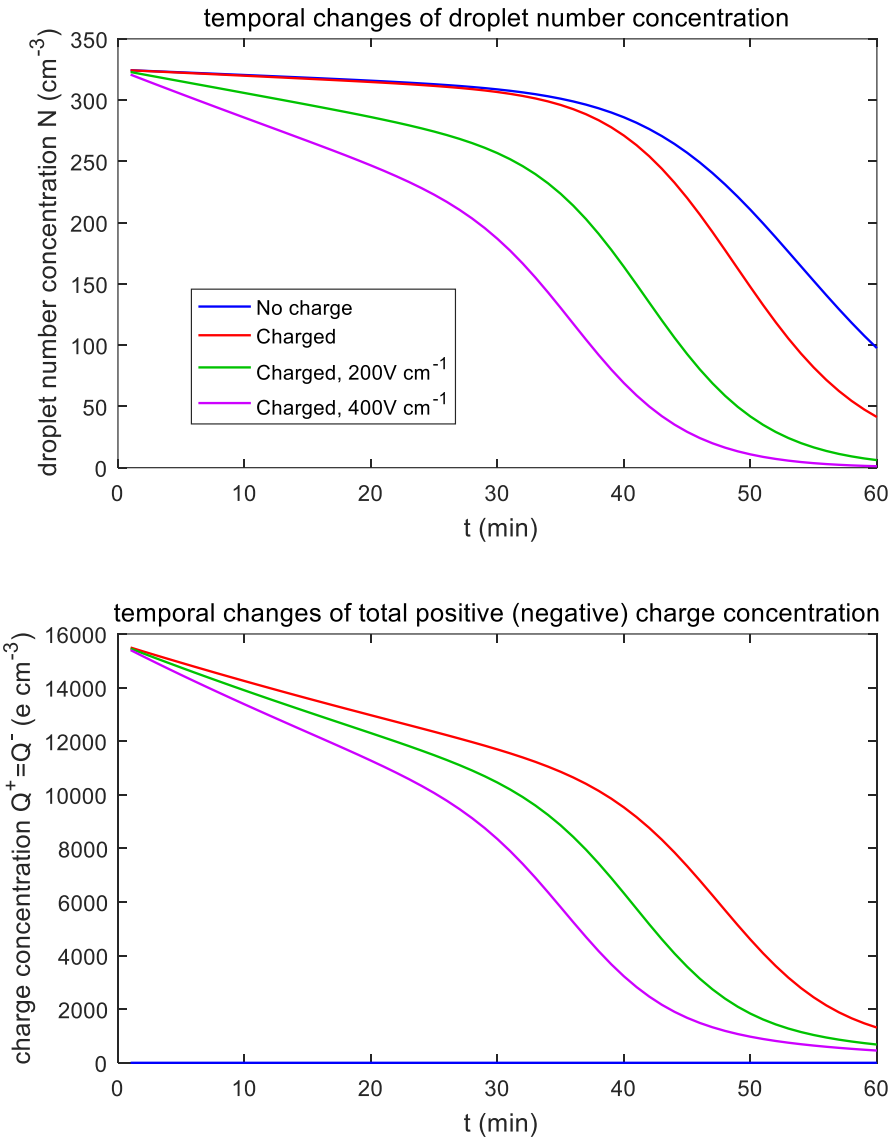

FIG. 12. Temporal changes of droplet total number concentration and total charge content for $\bar{r}$ =9 μm

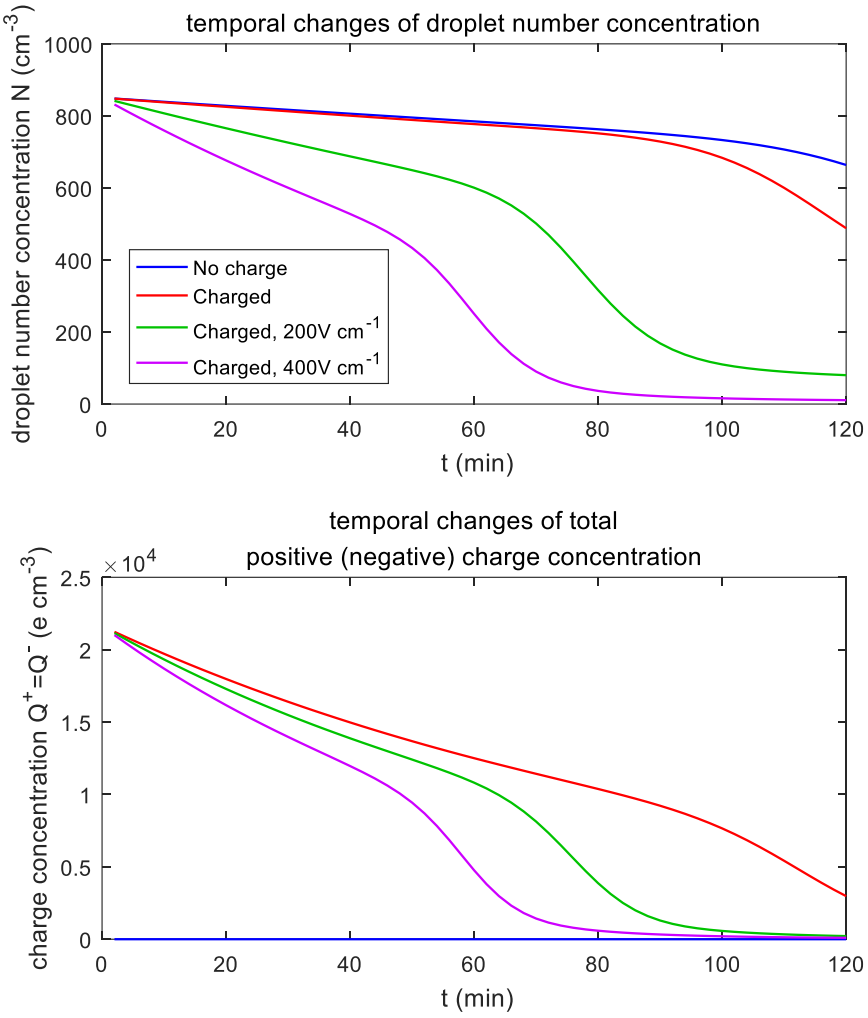

FIG. 15. Temporal changes of droplet total number concentration and total charge content for $\bar{r}$ =6.5 μm.

14. Line 288: "The relative terminal velocity term also contributes to the collection kernel, and the electric field can affect terminal velocity of small charged droplets significantly." – Please, cover this issue in more detail in the article.

Response: Thanks for the reviewer's suggestion. We have improved the writing of this part
Lines 287-295 "The electric enhancement of…" have been revised to:

The relative terminal velocity term also contributes to the collection kernel *K*. As mentioned in Section 3.4, terminal velocities $\boldsymbol{V_1}$ or $\boldsymbol{V_2}$ are derived by simulating just single one charged droplet in air with a certain electric field, and letting it fall until its velocity converges to the terminal velocity. Therefore, the electric field can affect terminal velocities of charged droplets, thus to affect the collection kernels. Terminal velocities of droplets in an external electric field is illustrated in Fig. 16. In a downward electric field of 400 V cm^{-1}, the terminal velocity of a large droplet is hardly affected. The difference of velocity caused by the electric field for $r =$ 1000 μm does not exceed 1%, and the one for 100 μm

does not exceed 5%. On the contrary, electric fields strongly affect the terminal velocities of charged small droplets. For $r < 5$ μm, the terminal velocity of a negatively-charged droplet even turns "upwards". Electric fields mainly affect terminal velocities of small charged droplets because droplet mass $m \propto r^3$, while droplet charge $q \propto r^2$ according to observation. Therefore, $q \propto m^{2/3}$ means that the acceleration contributed by the electric force decreases with increasing droplet mass.

In Fig.11 of the original manuscript, y-axis is in logarithmic scale and stands for the absolute value of terminal velocity, which is ambiguous. In the revised manuscript, we plot the negative terminal velocity in a separate panel, as shown below. (The whole manuscript has been revised substantially, so it becomes Fig. 16 now)

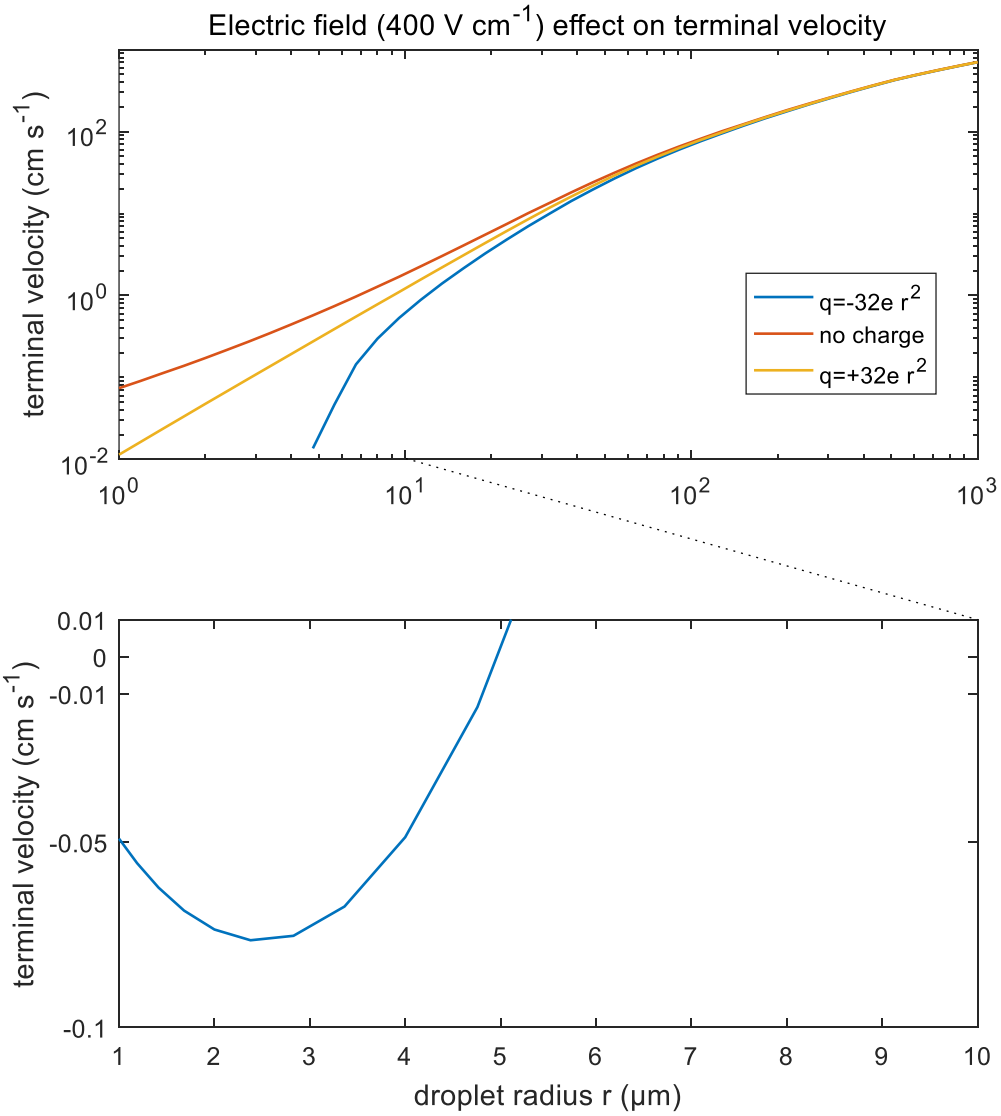

Figure 16. Terminal velocities of droplets in an external electric field 400 V cm^{-1}. Different lines denote different droplet charge conditions. It is seen that the terminal velocity of negatively-charged droplets smaller than 5 μm would turn upwards, which leads to the discontinuity of the lower curve in the figure.

The enhancement of droplet collision by electric charges and atmospheric electric fields

Shian Guo, Huiwen Xue

School of Physics, Peking University, Beijing, China

Correspondence to: Huiwen Xue (hxue@pku.edu.cn)

Abstract.

The effects of electric charges and ~~atmospheric electric~~ fields on droplet ~~spectrum evolution~~ collision-coalescence and the evolution of cloud droplet size distribution are studied numerically. Collision efficiencies for droplet pairs with radii from 2 to 1024 μm and charges from -32 r^2 to +32 r^2 (in unit of elementary charge, droplet radius r in unit of μm) in different strengths of downward electric fields (0, 200 and 400 V cm^{-1}) are computed by solving the equations of motion for the droplets. It is seen that collision efficiency is increased by electric charges and fields, especially for pairs of small droplets. These can be considered as electrostatic effects.

The evolution of cloud droplet ~~spectrum~~ size distribution with ~~different initial sizes~~ the electrostatic effects is simulated using the stochastic collection equation. Results show that the ~~electric~~ electrostatic effect is not notable for clouds with the initial mean droplet radius $\bar{r}$ =15 μm or larger. For clouds with the initial $\bar{r}$ = 9 μm, the electric charge without field could evidently accelerate ~~large drop~~ raindrop formation compared to the uncharged condition, and the existence of electric fields further accelerates it. For clouds with the initial $\bar{r}$ = 6.5 μm, it is difficult for gravitational collision to occur, and the electric field could significantly enhance the collision process. Results of this study indicate that ~~electric charges and fields could~~ electrostatic effects can accelerate ~~large drop~~ raindrop formation in natural conditions, particularly for ~~clouds with small droplet size~~ polluted clouds. It is seen that the aerosol effect on the suppression of raindrop formation is significant in polluted clouds, when comparing the three cases with $\bar{r}$ = 15, 9, and 6.5 μm. However, the electrostatic effects can accelerate raindrop formation in polluted clouds and mitigate the aerosol effect to some extent.

1 Introduction

~~Observations show that cloud droplets and aerosols carry net electric charge. Droplet charge can reach $|q| \approx 42r^2$ in the unit of elementary charge, with the droplet radius in the unit of μm (after unit conversion from Pruppacher and Klett, 1997). Vertical electric field always exists in atmosphere. Especially in convective clouds, the electric field can reach the magnitude of 10^2~10^3 V cm^{-1}. Cloud droplets (whether with or without net charge) could be regarded as spherical conductor approximately (Davis, 1964). It is significant that, as conductors, droplet pairs have electrostatic induction effect. This can lead to strong attraction at very small distance, regardless of the sign of charge. Charged droplets can thus be attracted strongly at small distances.~~

Clouds are usually electrified (Pruppacher and Klett 1997). For thunderstorms, several theories of electrification have been proposed in the past decades. The proposed theories assume that the electrification involves the collision of graupel or hailstones with ice crystals or supercooled cloud droplets, based on radar observational result that the onset of strong

electrification follows the formation of graupel or hailstones within the cloud (Wallace and Hobbs, 2006). However, the exact conditions and mechanisms are still under debate. One charging process could be due to the thermoelectric effect between the relatively warm, rimed graupel or hailstones and the relatively cold ice crystals or supercooled cloud droplets. Another charging process could be due to the polarization of particles by the downward atmospheric electric field. The thunderstorm electrification can increase the electric fields to several thousand V cm^{-1}, while the magnitude of electric fields in fair weather air is only about 1 V cm^{-1} (Pruppacher and Klett 1997). Droplet charges can reach $|q| \approx 42r^2$ in unit of elementary charge in thunderstorms, with the droplet radius r in unit of μm according to observations (Takahashi, 1973). For cumuli clouds, previous studies show smaller charge amount.

Liquid stratified clouds do not have such strong charge generation as in the thunderstorms. But charging of droplets can indeed occur at the upper and lower cloud boundaries as the fair weather current passes through the clouds (Harrison et al. 2015, Baumgaertner et al. 2014). The global fair weather current and the electric field are in the downward direction. Given the electric potential of 250 kV for the ionosphere, the exact value of fair weather current density over a location depends on the electric resistance of the atmospheric column, but its typical value is about 2×10^{-12} A m^{-2} (Baumgaertner et al. 2014). The fair weather electric field is typically about 1 V cm^{-1} in the cloud-free air, but is usually much stronger inside stratus clouds, because the cloudy air has a lower electrical conductivity than the cloud-free air. There is a conductivity transition at cloud boundaries. Therefore, the cloud top is positively charged and the cloud base is negatively charged. Based on the in situ measurements of charge density in liquid stratified cloud, and assuming that the cloud has a droplet number concentration on the order of 100 cm^{-3}, it is estimated that the mean charge per droplet is +5e (ranging from +1e to +8e) at cloud top, and -6e (ranging from -1e to -16e) at cloud base (Harroson et al. 2015). According to Tsutomu Takahashi (1973) and Khain (1997), the mean absolute charge of droplets in warm clouds is around $|q| \approx 6.6\, r^{1.3}$ (e, μm). For a droplet with radii of 10 μm, it is about 131 e.

~~According to Davis (1964), the force between two charged droplets in uniform electric field is well approximated as two spherical electric conductors. Though there is no explicit analytical expression for the interaction, a set of computational method is given. Schlamp et al. (1976) used this method to show the effect of electric charge and atmospheric electric field on collision efficiency, which demonstrated that the collision efficiencies between small droplets (about 1~10 μm) are enhanced by an order of magnitude in thunderstorm condition, while collision between large droplets is hardly affected. Note that Schlamp et al. (1976) didn't simulate the spectrum evolution process.~~

In general, charging of droplets can lead to the following effects on warm cloud microphysics. Firstly, for charged haze droplets, the charges can lower the saturation vapor pressure over the droplets and enhance the cloud droplet activation (Harrison and Carslaw, 2003, Harrison et al. 2015). Secondly, the electrostatic induction effect between charged droplets

can lead to strong attraction at very small distance (Davis, 1964) and higher collision-coalescence efficiencies (Beard et al. 2002). But Harrison et al. (2015) showed that charging is more likely to affect collision processes than activation, for small droplets.

The electrostatic induction effect can be explained by regarding the charged cloud droplets as spherical conductors. The electrostatic force between two conductors is different from the well-known Coulomb force between two point charges. When the distance between a pair of charged droplets approaches infinity, the electrostatic force converges to Coulomb force between two point charges. But when the distance of surfaces of two droplets is small (e.g. much smaller than their radii), their interaction shows extremely strong attraction. Even when the pair of droplets carry the same sign of charges, the electrostatic force can still change from repulsion to attraction at small distance. Although there is no explicit analytical expression such as Coulomb force for the electrostatic interaction between two charged droplets, a model with high accuracy has been developed (Davis 1964) for the interaction of charged droplets in a uniform electric field. Many different approximate methods are also proposed for the convenience of computation in cloud physics (e.g. Khain et al., 2004).

Based on this induction concept, electrostatic effects on droplet collision-coalescence process have been studied in the past decades. A few experiments show that electric charges and fields can enhance coalescence between droplets. Beard et. al. (2002) conducted experiments in cloud chambers and showed that even minimal electric charge can significantly increase the probability of coalescence when the two droplets collide. Eow et. al., (2001) examined several different electrostatic effects in water-in-oil emulsion, indicating that electric field can enhance coalescence by several mechanisms such as film drainage.

More numerical researches indicate that charges and fields can increase droplet collision efficiencies because of the electrostatic forces. Schlamp et al. (1976) used the model of Davis (1964) to study the effect of electric charges and atmospheric electric fields on collision efficiencies. They demonstrated that the collision efficiencies between small droplets (about 1~10 μm) are enhanced by an order of magnitude in thunderstorm condition, while collision between large droplets is hardly affected. Harrison et al. (2015) investigate the electrostatic effects in weakly electrified liquid clouds rather than thunderstorms. They calculated collision efficiencies between droplets with radii less than 20 μm and charge less than 50 e, by the equations of motion in Klimin (1994). Their results indicate that electric charges at the upper and lower boundaries of warm stratified clouds are sufficient to enhance collisions, and the enhancement is especially significant for small droplets. Moreover, they proposed that solar influences may change the fair weather current and droplet collision process, a possible pathway for affecting the climate system. Tinsley (2006) and Zhou (2009) also studied the collision efficiencies between charged droplets and aerosol particles in weakly electrified clouds, by treating the

particles as conducting spheres. They considered many aerosol effects such as thermophoretic forces, diffusophoretic forces and Brownian diffusion.

~~As for the electric effect on droplet spectrum evolution, few researches have been conducted. Khain et al. (2004), focused on weather modification, showed that droplet electric charge could enhance precipitation. They considered interaction of droplet pair by image charge, and use Stokes Flow to calculate hydrodynamic interaction. The charge limit is set up to the air-breakdown limit. It is found that a small fraction of extremely charged particles could trigger the collision process, and thus accelerate raindrop formation or fog elimination significantly.~~

As for the electrostatic effect on the evolution of droplet size distributon and the cloud system, few researches have been conducted. Focusing on weather modification, Khain et al. (2004) showed that a small fraction of highly charged particles could trigger the collision process, and thus accelerate raindrop formation in warm clouds or lead to fog elimination significantly. In their study, the electrostatic force between the droplet pair is represented by an approximate formula. The charge limit is set to the air-breakdown limit. The Stokes Flow is adopted to represent the hydrodynamic interaction, for deriving the trajectories of a pair of droplets. Harrison et. al. (2015) calculated droplet collision efficiencies affected by electric charges in warm clouds. When simulating the evolution of droplet size distribution in their study, the enhanced collision efficiencies are not used. Instead, the collection cross sections are multiplied by a factor of no more than 120% to approximately represent the electric enhancement of collision efficiency. The roles of electric charges and fields on precipitation acceleration still needs to be studied.

~~Previous studies about Albrecht (1989) effect show that increase of aerosol number decreases cloud droplet size, and thus extending cloud lifetime and suppress precipitation. But with the existence of electric charge, the Albrecht effect might be partially weakened. As mentioned above, Schlamp et al. (1976) had already shown that smaller droplets are more sensitive to electric effect. So, the coupling of electric effect and Albrecht effect needs to be considered.~~

The increased aerosol loading by anthropogenic activities can lead to an increase in cloud droplet number concentration, a reduction in droplet size, and therefore an increase in cloud albedo (Twomey 1974). This imposes a cooling effect on climate. It is further recognized that the aerosol-induced reduction in droplet size can slow down droplet collision-coalescence and cause precipitation suppression. This leads to increased cloud fraction and liquid water amount, and imposes an additional cooling effect on climate (Albrecht 1989). As the charging of cloud droplets can enhance droplet collision-coalescence, especially for small droplets, it is worth studying to what extent the electrostatic effect can mitigate the aerosol effect on the evolution of droplet size distribution and precipitation formation.

This study investigates the effect of electric charges and fields on droplet collision efficiency and the evolution of ~~droplet spectrum.~~ the droplet size distribution. The amount of charges is set as the condition in warm clouds, and the electric fields are set as the early stage of thunderstorms. The more accurate method for calculating the electric forces is adopted (Davis, 1964). Correction of flow field for large Reynolds numbers are also considered. Section 2 describes the theory of

droplet collision-coalescence and stochastic collection equation. ~~Section 3 and 4 present these numerical methods.~~ ~~S~~ection 3 presents the equations of motion for charged droplets in an electric field. The method for obtaining the terminal velocities and collision efficiencies for charged droplets are also presented. Section 4 describes the model setup for solving the stochastic collection equation. Different initial droplet size ~~spectra~~ distributions and different electric conditions are considered. Section 5 shows the numerical results of electrostatic effects on collision efficiency, and on ~~cloud spectrum evolution.~~ the evolution of droplet size distribution. We intend to find out to what extent the electric charges and fields as in the observed atmospheric conditions can accelerate warm rain process, and how sensitive these electrostatic effects are to aerosol-induced changes of droplet sizes.

2 Stochastic Collection Equation

The evolution of droplet size ~~spectrum~~ distribution due to collision-coalescence is described by the stochastic collection equation (SCE), which was first proposed by Telford (1955), and is shown as (Lamb and Verlinde, 2011, p.442)

$$\frac{\partial n(m,t)}{\partial t} = \int_0^{m/2} K(m_x, m-m_x)\cdot n(m_x)n(m-m_x)\mathrm{d}m_x - n(m)\int_0^{\infty} K(m_x,m)\cdot n(m_x)\mathrm{d}m_x \quad (1)$$

where $n(m,t)$ is the ~~spectrum density of droplets~~ distribution of droplet number concentration over droplet mass at time t, and K is the collection kernel between the two classes of droplets. For example, the collection kernel $K(m_x, m-m_x)$ describes the rate that droplets of mass m_x collected by $m-m_x$ and form new droplets of mass m. ~~In~~ The first term on the right side of Eq. (1), the first term describes formation of droplets of mass m through the collision of smaller droplets, and the second term means the loss of droplets of mass m through collision with other droplets. ~~In order to solve SCE, it is necessary to get the collection kernel K. The collection kernel between droplets with mass m_1 and m_2 is~~

The collection kernel between droplets with mass m_1 and mass m_2 can be written as

$$K(m_1,m_2) = |V_1 - V_2|\cdot\pi(r_1+r_2)^2\cdot E(m_1,m_2)\cdot\varepsilon(m_1,m_2) \quad (2)$$

~~where V_1 and V_2 are the terminal velocity of each droplet, r_1 and r_2 are droplet radius, E is the collision efficiency, and ε is the coalescence efficiency. Obviously, $|V_1 - V_2|\cdot\pi(r_1+r_2)^2$ means the geometric volume swept in unit time, but not all the small droplets in this volume could collide with large droplet. Because the flow induced by the larger droplet may drive some smaller droplets to flow past it. Thus, collision efficiency E is introduced as a proportion factor for true collision and it is much smaller than 1.0 when the droplet sizes are significantly different.~~

where subscripts 1 and 2 denote droplet 1 and droplet 2, respectively, V is the terminal velocity of the droplet, and r is droplet radius. Terminal velocity is the steady-state velocity of the droplet relative to the flow, when no other droplets are present and therefore there is no interaction from other droplets. Suppose droplet 1 is the collector and droplet 2 is the collected droplet, the term $|V_1 - V_2|\cdot\pi(r_1+r_2)^2$ represents the geometric volume swept by droplet 1 in unit time. Collision efficiency $E(m_1,m_2)$ and coalescence efficiency $\varepsilon(m_1,m_2)$ are introduced to the kernel because not all the droplets in this volume will have collision-coalesce with the collector.

~~The physical meaning of E is shown in Fig. 1. The smaller droplet has smaller terminal velocity, so it moves upwards relative to the larger droplet. Collision happens only when initial horizontal distance is smaller than threshold horizontal~~

~~distance r_c, or else the pair move apart. So, collision cross section is $S_c = \pi r_c^2$. Then collision efficiency is defined as $E = r_c^2/(r_1 + r_2)^2$. There are lots of previous researches on collision efficiency E, by both numerical simulations and chamber experiments.~~

For a pair of droplets, each of them induces a flow field that interacts with the other. As the collector falls and sweeps the air volume, the droplets in the volume tend to follow the streamlines of the flow field induced by the collector. Droplets collide with the collector only when they have enough inertia and cross the streamlines. Collision efficiency is then defined as the ratio of the actual collisions over all possible collisions in the swept volume. It can be much smaller than 1.0 when the sizes of the two droplets are significantly different. The physical meaning of collision efficiency is shown in Fig. 1 for a droplet pair. The collector droplet falls faster and induces a flow field to interact with the small droplet. The small droplet follows a grazing trajectory (as shown in the figure) when the centers of the two droplets have an initial horizontal distance r_c, which can be regarded as the threshold horizontal distance. Collision occurs only when the two droplets have an initial horizontal distance smaller than r_c. For any droplet pair, r_c depends on the sizes of the two droplets. Then the collision cross section is $S_c = \pi r_c^2$, and collision efficiency is $E = r_c{}^2/(r_1 + r_2)^2$. There are many previous studies on collision efficiency, by both numerical simulations and chamber experiments (Pruppacher and Klett 1997)

~~And ε is the coalescence efficiency, namely the coalescence probability when two droplets collide. In fact, two droplets do not always~~ Two droplets may not coalesce even when they collide with each other. ~~Instead,~~ Observations show that the droplet pair can ~~possibly~~ rebound in some cases, because of an air film temporally trapped between the two surfaces. Especially for droplets with radii both larger than 100 μm, the coalescence efficiency is remarkably less than 1.0. ~~The formula of coalescence efficiency ε is used from Beard and Ochs (1984).~~ Beard and Ochs (1984) provides a formula of coalescence efficiency for a certain range of droplet radii. Basically, coalescence efficiency is a function of the sizes of the two droplets in their formula.

In this study, electric charge and external electric field are taken into consideration for droplet collision-coalescence process. ~~Cloud spectrum~~ Droplet distribution function has two ~~parameters~~ variables—droplets mass m (or radius r) and electric charge q. ~~So, SCE with the two parameters (m, q) is~~ The SCE can be expressed as

$$\frac{\partial n(m,q,t)}{\partial t} = \int_0^{m/2} \left[\int_{-\infty}^{+\infty} K(m_x, q_x; m - m_x, q - q_x) \cdot n(m_x, q_x) n(m - m_x, q - q_x)\, \mathrm{d}q_x \right] \mathrm{d}m_x - n(m,q) \int_0^{\infty} \left[\int_{-\infty}^{+\infty} K(m_x, q_x; m - m_x, q - q_x) \cdot n(m_x, q_x) \mathrm{d}q_x \right] \mathrm{d}m_x \quad (3)$$

~~Bott (2000) proposed a method to solve SCE on two-parameter spectrum, which took droplet mass and also interior aerosol mass into consideration. In this work, however, the problem is more complicated, since the electric charge could affect the collection kernel, just like Khain et al. (2004).~~

where $n(m, q, t)$ is the distribution of droplet number concentration over mass and charge, and K is the collection kernel of the two classes of droplets. The collection kernel $K(m_x, q_x; m - m_x, q - q_x)$ represents the rate that droplets of

mass m_x and charge q_x collide with droplets of mass $m - m_x$ and charge $q - q_x$ to form new droplets of mass m and charge q.

The collection kernel for charged droplets in an external electric field has the same form as Eq. (2). However, terminal velocity, collision efficiency, and coalescence efficiency in the kernel my all be affected by the electric charge and field. We consider these as electrostatic effects. In a vertical electric field, the terminal velocity of a charged droplet may be increased or decreased, depending on the charge sign and the direction of the field. The threshold horizontal distance r_c, the collision cross section, and the collision efficiency of a droplet pair may be changed because the electric charge and field can make the droplets to cross the streamlines more easily under some circumstances. Therefore, terminal velocity, collision efficiency, and coalescence efficiency not only depend on the sizes of the two droplets, but may also depend on the electric charge and the external electric field.

As will be seen in this study, the electrostatic effects on collision efficiency is much stronger than on terminal velocity. Therefore, the electrostatic effect on terminal velocity is presented in Section 6 as discussion, and we focus on the electrostatic effects on collision efficiency in this paper. The method for obtaining droplet terminal velocity and collision efficiency with the electrostatic effects will be presented in section 3. The electrostatic effect on coalescence efficiency is not considered here. The coalescence efficiency used in this study is the same as that for uncharged droplets, based on the results of Beard and Ochs (1984). In their study, coalescence efficiency is a function of r_1 and r_2, and is valid for 1 < r_2 < 30 μm and 50 < r_1 < 500 μm. In this study, however, the range of r_1 and r_2 is much wider, from 2 to 1024 μm. The formula of coalescence efficiency in Beard and Ochs (1984) is extrapolated for the droplet size range here. Coalescence efficiency is set to be 1 if the extrapolated value is higher than 1, and set to be 0.3 if the extrapolated value is smaller than 0.3.

3 Method for calculating terminal velocity and collision efficiency ~~of charged droplets~~ with electrostatic effects

3.1 ~~Droplet motion equation~~ Equations of motion for charged droplets

In order to get the terminal velocity and collision efficiency, ~~the motion equation of droplets is integrated to get the trajectories of droplets~~ the equations of motion need to be used. Droplet motion ~~not only depends on gravity and flow drag, but also depends on the electric force between droplets.~~ depends on the following three forces: gravity force, the flow drag force, and the electrostatic force due to droplet charge and the external electric field. The ~~motion~~ equations of motion for a pair of droplets are shown below,

$$\frac{\mathrm{d}\boldsymbol{v_1}}{\mathrm{d}t} = \boldsymbol{g} - C\frac{6\pi r_1 \eta}{m_1}(\boldsymbol{v_1} - \boldsymbol{u_2}) + \frac{\boldsymbol{F_{e1}}}{m_1} \tag{4a}$$

$$\frac{\mathrm{d}\boldsymbol{v_2}}{\mathrm{d}t} = \boldsymbol{g} - C\frac{6\pi r_2 \eta}{m_2}(\boldsymbol{v_2} - \boldsymbol{u_1}) + \frac{\boldsymbol{F_{e2}}}{m_2} \tag{4b}$$

where subscripts 1 and 2 denotes droplet 1 and droplet 2, respectively, $\boldsymbol{g}$ is the gravitational acceleration, $\boldsymbol{v}$ is the velocity ~~vector~~ of ~~each~~ the droplet relative to the ~~earth~~ flow if there are no other droplets present, $\boldsymbol{u}$ is the flow

velocity field induced ~~by each droplet (also relative to earth)~~ by the droplet, η is the ~~fluid~~ viscosity of air, and C is the drag coefficient, which is a function of Reynolds number, r is droplet radius, m is droplet mass, with ~~Droplet mass~~ $m = 4\pi r^3\rho/3$, and $\boldsymbol{F_e}$ is the electrostatic force ~~caused by droplet electric charge and external vertical electric field. The fluid property is treated as air with temperature T = 283 K and pressure p = 900 hPa. The three terms on the rhs is gravity, flow drag force, and electric force respectively.~~ We set air temperature T = 283 K and pressure p = 900 hPa in this study for the calculation of air viscosity.

3.2 The drag force term

The flow drag force is described by the second term on the right side of Eq. (4), which assumes a simple hydrodynamic interaction of the two droplets. That is, each droplet moves in the flow field induced by the other one moving alone, and it is called "superposition method" in cloud physics. ~~The superposition method is used to solve the motion equation of droplets in a hydrodynamic flow, assuming that each droplet moves in the flow field induced by the other one moving alone~~. This method has been successfully used in many researches of collision efficiency calculation (Pruppacher and Klett, 1997). The superposition method can also ensure that the stream function satisfies the no-slip boundary condition (i.e., Wang et al. 2005) To calculate the flow drag force, the induced flow field $\boldsymbol{u}$ is required. The method for obtaining the induced flow field $\boldsymbol{u}$ is discussed below.

Considering a rigid sphere moving in a viscous fluid with a velocity U relative to the flow, the steam function depends on Reynolds number, $N_{Re} = \frac{2rv\rho}{\mu}$, where ρ is the density of the air, and μ is the dynamic viscosity of the air. It is known that when Reynolds number is small, the flow is considered as Stokes flow and the stream function can be expressed as

$$\psi_s = U\left(\frac{1}{4\tilde{R}} - \frac{3\tilde{R}}{4}\right)\sin^2\theta_0 \tag{5}$$

where $\tilde{R} = R/r$ is the normalized distance (R is the distance from the sphere centre, and r is the droplet radius), θ_0 is the angle between the droplet velocity and vector $\boldsymbol{R}$ pointing from the sphere centre. U is droplet velocity relative to the flow, i.e., $U_1 = |\boldsymbol{v_1} - \boldsymbol{u_2}|$ for droplet 1, and $U_2 = |\boldsymbol{v_2} - \boldsymbol{u_1}|$ for droplet 2. However, this stream function for Stokes flow does not apply to the system with a large Reynolds number. Hamielec and Johnson (1962, 1963) gave the stream function ψ_h induced by a moving rigid sphere, which can be used for flows with large Reynolds numbers:

~~$$\psi_h = \left(\frac{A_1}{R} + \frac{A_3}{R^2} + \frac{A_3}{R^3} + \frac{A_4}{R^4}\right)\sin^2\theta - \left(\frac{B_1}{R} + \frac{B_3}{R^2} + \frac{B_3}{R^3} + \frac{B_4}{R^4}\right)\sin^2\theta\cos\theta \tag{5}$$~~

$$\psi_h = U\left(\frac{A_1}{\tilde{R}} + \frac{A_3}{\tilde{R}^2} + \frac{A_3}{\tilde{R}^3} + \frac{A_4}{\tilde{R}^4}\right)\sin^2\theta_0 - U\left(\frac{B_1}{\tilde{R}} + \frac{B_3}{\tilde{R}^2} + \frac{B_3}{\tilde{R}^3} + \frac{B_4}{\tilde{R}^4}\right)\sin^2\theta_0\cos\theta_0 \tag{6}$$

~~where R is the distance from the sphere centre, θ is the angle between the vertical direction and vector $\boldsymbol{R}$ pointing from the sphere centre, and $A_1, \ldots, B_4$ are functions of instant Reynolds number $N_{Re} = \frac{2rv\rho}{\mu}$ for each droplet.~~ where $A_1, \ldots, B_4$ are functions only of Reynolds number N_{Re} for each droplet. The method is valid for $N_{Re} < 5000$. But the solution deviates from the Stokes flow solution when $N_{Re} \to 0$ for small droplets. ~~Therefore, this work adopts a smooth combination of ψ_h and Stokes stream function $\psi_s = v\left(\frac{R^2}{2r} - \frac{3rR}{2}\right)\sin^2\theta$, (Pinsky and Khain, 2000)~~ Therefore, it is needed to construct a stream function that applies to a wide range of N_{Re}. This work adopts a stream function that is a linear combination of ψ_h and Stokes stream function ψ_s (Pinsky and Khain, 2000)

$$\psi = \frac{N_{Re}\psi_h + {N_{Re}}^{-1}\psi_s}{N_{Re} + {N_{Re}}^{-1}} \tag{7}$$

which converges to stokes flow when $N_{Re} \to 0$. Then the induced flow field $\boldsymbol{u}$ is derived,

~~$\boldsymbol{u} = \frac{1}{R^2 \sin\theta}\frac{\partial\psi}{\partial\theta}\boldsymbol{e_r} + \frac{1}{R\sin\theta}\frac{\partial\psi}{\partial R}\boldsymbol{e_\theta}$~~ ~~(7)~~

$$\boldsymbol{u} = -\frac{1}{\tilde{R}^2 \sin\theta_0}\frac{\partial\psi}{\partial\theta_0}\hat{\boldsymbol{e}}_{\boldsymbol{R}} + \frac{1}{\tilde{R}\sin\theta_0}\frac{\partial\psi}{\partial\tilde{R}}\hat{\boldsymbol{e}}_{\boldsymbol{\theta}} = u_R\hat{\boldsymbol{e}}_{\boldsymbol{R}} + u_\theta\hat{\boldsymbol{e}}_{\boldsymbol{\theta}} \quad (7)(8)$$

where $\hat{\boldsymbol{e}}_{\boldsymbol{R}}$ and $\hat{\boldsymbol{e}}_{\boldsymbol{\theta}}$ are unit vectors in the polar coordinate (R, θ_0). It can also be expressed in the Cartesian coordinate (x, z)

$$\boldsymbol{u} = (u_R\cos\varphi - u_\theta\sin\varphi)\hat{\boldsymbol{e}}_{\boldsymbol{z}} + (u_R\sin\varphi + u_\theta\cos\varphi)\hat{\boldsymbol{e}}_{\boldsymbol{x}} \quad (9)$$

where the direction of $\hat{\boldsymbol{e}}_{\boldsymbol{z}}$ is vertically down, the same as gravitation. φ is the angle between $\hat{\boldsymbol{e}}_{\boldsymbol{z}}$ and the droplet velocity $\boldsymbol{v}$.

Both Stokes and Hamielec stream functions satisfy the no-slip boundary condition, i.e., the fluid velocity on the surface of the droplet is equal to the velocity of the droplet. Hamielec stream function is no-slip because those functions $A_1, \ldots, B_4$ in Eq. (6) satisfy $A_1 + 2A_2 + 3A_3 + 4A_4 = 1$ and $B_1 + 2B_2 + 3B_3 + 4B_4 = 0$, as long as the droplet is considered as a rigid sphere (Hamielec, 1963). These relations ensure that $u_\theta = -U\sin\theta_0$ at the surface of the droplet, which means the no-slip boundary condition. (Note that u_θ is the velocity of the fluid at droplet surface, and $U\sin\theta_0$ is the tangential velocity of the droplet surface.)

The drag coefficient C in Eq. (4) is function of N_{Re},

$$C = 1 + \exp(a_0 + a_1X + a_2X^2) \quad (8)(10)$$

where $X = \ln(N_{Re})$, and fitting constants a_0, a_1, a_2 are from table 2 of Beard (1976). The drag coefficient increases with Reynolds number. For example, the terminal velocity of a droplet of 16 μm in radius is 3.12 cm s^{-1}, with N_{Re} =0.47 and C =1.07; the terminal velocity of a droplet of 1024 μm in radius is 7.15m s^{-1}, with N_{Re} =777 and C =21.3. For $N_{Re} \to 0$, the drag coefficient C is 1.

For droplets with $r < 10\,\mu m$, the assumption of no-slip boundary condition is no longer valid. The flow slips on the droplet surface. ~~So,~~ Therefore, the drag coefficient should multiply another coefficient (Lamb and Verlinde 2011, p386)

$$C' = C \cdot \left(1 + 1.26\frac{\lambda}{r}\right)^{-1} \quad (9)(11)$$

where λ is the free path of air molecules, and r is the droplet radius.

3.3 The electric force term

The electric force is described by the third term on the right side of Eq. (4). The electric force includes the interactive force between the two charged droplets, and also an external electric force if there is an external electric field. It is well known that the interaction between two point charges can be expressed as

~~$F_e = -\frac{q_1 q_2}{R^2}$~~ ~~(10)~~

$$\boldsymbol{F_e} = -\frac{1}{4\pi\varepsilon_0}\frac{q_1q_2}{R^2}\hat{\boldsymbol{e}}_{\boldsymbol{R}} \quad (12)$$

where F_e is the interactive force between point charges q_1 and q_2, and R is the distance between the two point charges. However, this inverse-square law does not apply to uneven charge distribution, such as the case of charged cloud droplets.

The interaction between charged conductors is a complex mathematical ~~physics~~ problem in physics. Davis (1964) demonstrated an appropriate computational method for electric force between two spherical conductors in ~~an external uniform~~ a uniform external field~~, which~~. The electric force depends on droplet radius (r_1, r_2), charge (q_1, q_2), centre distance R, electric field E_0, and the angle θ between the electric field and the line connecting the centres of two droplets (note that $\theta = \theta_0 + \varphi$). ~~The electric force on droplet 2 with radius r_2 and charge q_2 is~~ The resultant electric force acting on droplet 2 is expressed as

~~$$\boldsymbol{F}_{e2} = \{r_2^2 E_0^2 (F_1 \cos^2\theta + F_2 \sin^2\theta) + E_0 \cos\theta (F_3 q_1 + F_4 q_2) + \frac{1}{r_2^2}(F_5 q_1^2 + F_6 q_1 q_2 + F_7 q_2^2) + E_0 q_2 \cos\theta\}\hat{\boldsymbol{e}}_{\boldsymbol{R}} +$$

$$\{r_2^2 E_0^2 F_8 \sin 2\theta + E_0 \sin\theta (F_9 q_1 + F_{10} q_2) + E_0 q_2 \sin\theta\}\hat{\boldsymbol{e}}_{\boldsymbol{\theta}}$$~~

$$\boldsymbol{F}_{e2} = E_0 q_2 \cos\theta \hat{\boldsymbol{e}}_{\boldsymbol{R}} + E_0 q_2 \sin\theta \hat{\boldsymbol{e}}_{\boldsymbol{\theta}} +$$

$$\{r_2^2 E_0^2 (F_1 \cos^2\theta + F_2 \sin^2\theta) + E_0 \cos\theta (F_3 q_1 + F_4 q_2) + \frac{1}{r_2^2}(F_5 q_1^2 + F_6 q_1 q_2 + F_7 q_2^2)\}\hat{\boldsymbol{e}}_{\boldsymbol{R}}$$

$$+ \{r_2^2 E_0^2 F_8 \sin 2\theta + E_0 \sin\theta (F_9 q_1 + F_{10} q_2)\}\hat{\boldsymbol{e}}_{\boldsymbol{\theta}} \quad (13)$$

where $\hat{\boldsymbol{e}}_{\boldsymbol{R}}$ is the radial unit vector, and $\hat{\boldsymbol{e}}_{\boldsymbol{\theta}}$ is tangential unit vector, $\boldsymbol{E_0}$ is the eternal electric field, q_1 and q_2 are the charges of droplet 1 and droplet 2 respectively, ~~and parameters F_1 to F_{10}~~ . $F_1 \ldots F_{10}$ are a series of complicated functions of geometric parameters $(r_1, r_2, R$; Davis 1964).

The electric force directly from the external field is shown as the two terms in the first line of Eq. (13), and can be simply written as $\boldsymbol{E_0} q_2$ if combining the two terms. Line 2 and line 3 in Eq. (13) represent the interactive force from droplet 1 in the radial direction and tangential direction, respectively. Note that the third term in line 2 represent the interactive force from droplet 1 if there is no external electric field. Except for this term, all the other terms in lines 2 and 3 are the interactive forces from droplet 1 due the induction from the external field.

Similarly, the resultant electric force $\boldsymbol{F}_{e1}$ acting on droplet 1 includes both the force directly from the external field and the interactive force from droplet 2. The sum of the electric forces on the two droplets, $\boldsymbol{F}_{e1} + \boldsymbol{F}_{e2}$, must equal to the external electric force acting on the system, which can be expressed as $\boldsymbol{E_0}(q_1 + q_2)$, because the two droplets can be considered as a system. Then, the electric force on droplet 1 could be derived immediately ~~by~~ as

$$\boldsymbol{F}_{e1} = E_0(q_1 + q_2)\hat{\boldsymbol{e}}_{\boldsymbol{z}} - \boldsymbol{F}_{e2} \quad (14)$$

Figure 2 is a schematic diagram showing the forces acting on each droplet in a pair. Also shown in Fig. 2 are the velocity of each droplet relative to the flow if there is no other droplets present ($\boldsymbol{v}$), and the flow velocity induced by the other droplet ($\boldsymbol{u}$). Droplet velocity relative to the flow is $\boldsymbol{v} - \boldsymbol{u}$. The electric field $\boldsymbol{E_0}$ is in the downward direction, the same as gravity. Droplet 1 has positive charge and droplet 2 has negative charge in this example. The forces acting on each droplet include gravity, flow drag force, and the electrostatic force, as seen on the right side of Eq. (4). For droplet 1, the electric force directly from the external field is in the downward direction, and is shown as $\boldsymbol{E_0} q_1$ in the figure. The interactive electric force from droplet 2, shown as $\boldsymbol{F}_{\text{inter}}$ in the figure, has a radial component and a tangential component, so that it is in a direction that does not necessarily align with the line connecting the two droplets. Because of the interactive electric force from droplet 2, the velocity $\boldsymbol{v}$ of droplet 1 is not in the vertical direction. The electrostatic force

between charged droplets tend to make the droplets attract each other. This force is particularly strong when droplets are close to each other, thus to enhance collisions. The flow drag force on droplet 1 is in the opposite direction with $\boldsymbol{v}-\boldsymbol{u}$.

If there is no external electric field but only with charge effect, Eq. (13) is reduced to

$$\boldsymbol{F}_{e2}=\frac{1}{r_2^2}(F_5{q_1}^2+F_6q_1q_2+F_7{q_2}^2)\hat{\boldsymbol{e}}_{\boldsymbol{R}} \tag{15}$$

To illustrate it, the comparison between the electrostatic forces derived by the inverse-square law and conductor model without electric field (i.e., Eq. 15) are shown in ~~Fig. 2~~ Fig. 3, where the electric force between droplets with ~~of~~ opposite-sign charges (dashed lines) and with ~~of~~ same-sign charges (solid lines) varies with distance. When $R\gg r_1,r_2$,we have $F_5,F_7\to 0,\ F_6\to r_2^2/R^2$, and it is also shown that two models are basically identical in remote distance~~, two models are basically identical.~~. But when the spheres approach closely, the conductor interaction (blue lines) ~~turns into~~ changes to strong attraction, because of electrostatic induction. ~~It is significant that interaction must turn to attraction as long as the distance is small enough,~~ The interaction is always attraction at small distance, regardless of the sign of charges. If there is only inverse-square law without electrostatic induction, it is obvious ~~to say~~ that same-sign charges must decrease collision efficiency. However, after taking electrostatic induction into account, the effects of same-sign and opposite-sign charges need to be reconsidered.

3.4 ~~Droplet trajectory and the effective cross section~~ Terminal velocity and collision efficiency

The equations of motion (Eq. 4), along with the other equations in this section, are used to calculate the terminal velocities of charged droplets first. Note that the terminal velocity refers to the steady state velocity of a droplet relative to the flow when there is no other droplets present, as we mentioned earlier. Therefore, by setting the induced flow $\boldsymbol{u}$ to be 0, Eq. (4) can be integrated to obtain the terminal velocity of the droplets with electric charge and field.

Eq. (4), along with other equations, is also integrated to get the trajectories for the two droplets in any possible droplet pair $(r_1,q_1$ and $r_2,q_2)$ in various strengths of downward electric fields (0, 200 and 400 V cm^{-1}). The 2-order Runge-Kutta method is used for the integration. ~~Following their trajectories, the two droplets can either collide or not. In order to get the collision cross section $S_c=\pi r_c^2$ (or say the collision efficiency E),~~ The initial settings of droplet positions and velocities, and the flow velocities are required. For convenience of computation, initial vertical distance is set to be $30(r_1+r_2)$, as an approximation of infinity. Initial flow velocity field $\boldsymbol{u_1}$ and $\boldsymbol{u_2}$ are set to be zero. Initial velocities of the two droplets are set to be the terminal velocities $\boldsymbol{V_1}$ and $\boldsymbol{V_2}$. Following their trajectories, the two droplets can either collide or not depending on the initial horizontal distance. We vary the initial horizontal distance between the two droplets using the bisection method, until we find a threshold distance r_c that makes the two droplets follow the grazing trajectories and just exactly collide. The threshold distance is found with a precision of 0.1%. The collision cross section $S_c=\pi r_c^2$ and collision efficiency E are than calculated,

After computing the collision efficiency E ~~is derived~~ for droplet pair with (r_1,q_1) and (r_2,q_2), the collection kernel $K(r_1,q_1,r_2,q_2)$ is derived then~~, where the coalescence efficiency ε is restricted in the range from 0.3 to 1.0, using the formula of Beard and Ochs (1984).~~ With the collection kernel $K(r_1,q_1,r_2,q_2)$, the effect of electric charges and fields on droplet collision is determined by solving the SCE.

4 Model setup for solving the stochastic collection equation

4.1 Setting of the bins for droplet radius and charge

~~The evolution of the droplet spectrum is described by the 2-parameter SCE, i.e. Eq. (1). To solve the equation numerically,~~

To solve the stochastic collection equation (Eq. 3) numerically, droplet radius and charge are both divided into discrete bins that are logarithmically equidistant ~~bins~~. Droplet radius ranging from 2 to 1024 μm is divided into 37 bins, with the radius increased by a factor of $2^{1/4}$ from one bin to the next. Droplets with radii larger than 1024 μm are assumed to precipitate out and not included in the size distribution. ~~The radius is increased by a factor of $2^{1/4}$ from one bin to the next. For droplet radius $r > 1024$ μm, they are assumed to precipitate out and not included in droplet spectrum.~~

~~Droplet charge is set to be proportional to the square of droplet radius, based on observations. Droplet charge ranging from $-32r^2$ to $+32r^2$ is divided into 15 bins, that is, $q = r^2 \times \{-32, -16, \ldots, -0.5, 0, +0.5, +1, +2, \ldots, +16, +32\}$ (Here the unit of q is elementary charge and r in μm). Under thunderstorm conditions, the amount of droplet charge is about $42r^2$ (in elementary charge, and r in μm) (Pruppacher and Klett 1997). Therefore, the upper limit $32r^2$ in this work approaches the thunderstorm condition.~~

In each radius bin, droplets may have different amount and different sign of charges. For the bin of radius r, droplet charge ranges from -$32r^2$ to +$32r^2$ (in unit of elementary charge, and r in μm). This means that smaller droplets have a smaller range of charge. The setting here is based on the observations that the charge amount is proportional to the square of droplet radius, as discussed in Introduction. The upper limit charge bin of $32r^2$, is close to the thunderstorm condition of $42r^2$. The charge range is then divided into 15 bins, with the center bin having zero charge, 7 bins to the right having positive charges, and 7 bins to the left having negative charges. For the positive charge bins, the one next to the center bin has charge of +$0.5r^2$. The charge amount is increased by a factor of 2 from this bin to the next, until the upper limit of $32r^2$. The setting for the negative charge bins is completely symmetric to the positive charge bins. For the size bins and charge bins described above, a large matrix of kernel $K(r_1, q_1, r_2, q_2)$ is computed in advance as a lookup table for use in solving the SCE.

4.2 Redistribution of droplets into radius and charge bins after collision-coalescence

~~Usually the droplet mass and charge~~ Droplet size and charge after collision-coalescence usually do not fall in any existing bins. A simple method is to linearly redistribute the droplets to the two neighbouring bins (Khain et al, 2004). We first redistribute droplets to ~~the certain mass bins~~ the size bins. The ratio of redistribution is based on total-mass conservation and droplet-number conservation simultaneously. For example, to redistribute droplets with mass m ($m_i < m < m_{i+1}$) and number Δn, a proportion of $\Delta n_i = \frac{m_{i+1} - \mathrm{m}}{m_{i+1} - m_i} \Delta n$ is added to the ith bin, and $\Delta n_{i+1} = \frac{\mathrm{m} - m_i}{m_{i+1} - m_i} \Delta n$ is added to the (i+1)th bin. ~~After mass redistribution to the ith and (i+1)th mass bins, the charge is redistributed within each of the mass bins,~~ These droplets are then redistributed to the charge bins within each size bin, satisfying total-charge conservation and droplet-number conservation. For example, to redistribute droplets with charge q ($q_{i,j} < q < q_{i,j+1}$) within the ith size bin, a proportion of $\Delta n_{i,j} = \frac{q_{i,j+1} - \mathrm{q}}{q_{i,j+1} - q_{i,j}} \Delta n_i$ is added to the bin of (i, j), and a proportion of $\Delta n_{i,j+1} = \frac{\mathrm{q} - q_{i,j}}{q_{i,j+1} - q_{i,j}} \Delta n_i$ is added to the bin of (i, j+1).

As shown in ~~Fig. 3~~ Fig. 4, the collision-coalescence between bin (r_1, q_1) and bin (r_2, q_2), shown with black dots, generates ~~a~~ droplets shown with the red dot. ~~This newly generated droplet is~~ These newly generated droplets are then redistributed into ~~4 bins shown with blue dots.~~ 2 size bins, and further redistributed into 2 charge bins within each of the size bins, shown with blue dots. Note that the numbers ~~of~~ close to each of the blue dots in ~~Fig. 3~~ Fig. 4 are the percentages ~~in the redistribution of droplets to the bins~~ of droplets that are redistributed into that bin. In fact, this method only reaches the first-order accuracy. Although Bott (1998) compared several methods to redistribute droplets with high-order correction, the two-parameter ~~spectrum~~ distribution is too complicated to do the high-order correction in this study.

4.3 The initial droplet size and charge distributions

~~The initial droplet number density spectrum is assumed to be gamma distribution and adopted from Bott (1998),~~

The initial droplet size distribution used in this study is derived based on an exponential function in Bott (1998),

$$n(m) = \frac{L}{\bar{m}^2} \exp\left(-\frac{m}{\bar{m}}\right) \tag{16}$$

~~where L=1 g m^{-3} is liquid water content, and $\bar{m}$ is the mean droplet mass. The number density spectrum $n(m)$ can also multiply droplet mass, thus producing the mass spectrum,~~

~~$$M(m) = m \cdot n(m) = \frac{mL}{\bar{m}^2} \exp\left(\frac{m}{\bar{m}}\right) \tag{14}$$~~

~~and can also be written as:~~

~~$$M(\ln r) = r^6 \frac{3L}{\bar{r}^6} \exp\left(\frac{r^3}{\bar{r}^3}\right) \tag{15}$$~~

~~where $\bar{r}$ is mean droplet radius (with $\bar{m} = 4\pi\bar{r}^3\rho/3$), which is an important variant to describe the cloud droplet size.~~

where $n(m)$ is the distribution of droplet number concentration over droplet mass, L is the liquid water content, and $\bar{m}$ is the mean mass of droplets. This function is used to derive $n(lnr)$, which is the distribution of droplet number concentration over droplet radius. With the definitions of $n(m)$ and $n(lnr)$, and $m = 4\pi r^3\rho/3$, where ρ is droplet density, we can derive $n(lnr)$ as

$$n(\ln r) = \frac{dN}{d\ln r} = r\frac{dN}{dr} = r\frac{dN}{dm}4\pi\rho r^2 = 4\pi\rho r^3 n(m) \tag{17}$$

By substituting Eq. (16) into Eq. (17), and assuming that $\bar{m} = 4\pi\bar{r}^3\rho/3$, where $\bar{r}$ is the mean radius, we have

$$n(\ln r) = L\frac{9r^3}{4\pi\bar{r}^6} exp\left(-\frac{r^3}{\bar{r}^3}\right) \tag{18}$$

Eq. (18) is used as the initial droplet size distribution for the calculations of collision-coalescence in this study. It has two parameters, L and $\bar{r}$, and can be considered as a gamma distribution. Using parameters L and $\bar{r}$ in the initial size distribution has an advantage in representing the aerosol effect. The parameter L can be set as a constant. Using different mean radius can represent different aerosol condition and different number concentration of cloud droplets.

12 cases with different initial conditions are considered to study the ~~spectrum~~ evolution of droplet distribution. The mean droplet radius $\bar{r}$ is set ~~by~~ with three different sizes: 15 μm, 9 μm and 6.5 μm, where $\bar{r}$ = 15 μm case represents clean conditions, and 6.5 μm represents polluted conditions. The liquid water content in our study is set to

be L=1 g m^{-3}, which is a typical value in warm clouds according to observations (Warner, 1955, Miles et al. 2000). With the fixed liquid water content, a smaller mean radius corresponds to a larger number concentration. As shown in table 1, $\bar{r} =$ 15 , 9, and 6.5 μm give an initial droplet number concentration of 71, 325, and 851 cm^{-3}, respectively.

For each $\bar{r}$, comparisons are made among four different electric conditions: ~~including the uncharged cloud, charged cloud, charged cloud with a field of 200 V cm−1, and charged cloud with a field of 400 V cm−1 (This study considers the downward electric field as positive)~~ (a) droplets are uncharged; (b) droplets are charged but with no external electric field, (c) droplets are charged and also with an external downward electric field of 200 V cm^{-1}, (d) droplets are charged and also with an external downward electric field of 400 V cm^{-1}. For the uncharged cloud, the initial distribution is shown in ~~Fig. 4a~~ Fig. 5a, where all droplets are put in the bins with no charge. For the charged clouds, ~~the initial charge is distributed symmetrically, as shown in Fig. 4b: 14% with charge $+1r^2$, 14% with charge $-1r^2$, 22% with charge $+0.5r^2$, 22% with charge $-0.5r^2$, and 28% with no charge (charge in unit of elementary charge, and r in μm).~~ an initial charge distribution shown in Fig. 5b is made as follows.

To simulate an early stage of the warm-cloud precipitation, we need to distribute the droplets in each size bin to different charge bins, so that these droplets have different charges. Since there is little data on this, we assume a Gaussian distribution,

$$N(q) = \frac{N_0}{\sqrt{2\pi}\sigma} \exp\left(-\frac{q^2}{2\sigma^2}\right) \tag{19}$$

where N_0 is the number concentration in the size bin, and σ is the standard deviation of the Gaussian distribution in that size bin. $N(q)$ represents the number concentration of droplets with charge q. This distribution satisfies electric neutrality $\bar{q} = 0$. For different size bin, droplet number concentration N_0 is different. We purposely set the standard deviation σ to be different for different size bins. For a larger size, the charge amount is larger, based on $\overline{|q|}$ = 1.31 r^2 (q in unit of elementary charge and r in μm) as stated in the Introduction. Therefore, we set larger standard deviation σ for the larger size bins. With this setting of droplet charge, the total amount of charge in each case is shown in Table 1. The $\bar{r} =$ 15 , 9, and 6.5 μm cases have an initial charge concentration of 9438, 15638, and 21634 e cm^{-3}, respectively, for both positive charge and negative charge.

~~During the computation of spectrum evolution, each bin could coalesce with any other bins in each step time Δt, which require the collection kernel between the two bins. Thus, a large matrix of kernel $K(r_1, r_2, q_1, q_2)$ is computed in advance.~~ The initial electric charges, and electric field strength are set according to the conditions in warm clouds or the early stage of thunderstorms. In fact, in some extreme thunderstorm cases, both the electric charge and field could be one order of magnitude larger (Takahashi, 1973) than the values used in this study. Furthermore, in natural clouds, the electric charge on a droplet~~s~~ leaks away gradually. In this study, the charge leakage is assumed as a process of exponential decay (Pruppacher and Klett, 1997), and the relaxation time is set to τ =120 min. Namely, all the bins lose $\frac{\Delta t}{\tau}$ of electric charge in each step of time $\Delta t = 1s$.

5 Results

5.1 Collision efficiency

Here we present collision efficiencies for typical droplet pairs to illustrate the electrostatic effects. During the evolution of droplet size distribution, the radius and charge amount of colliding droplets have large variability. In addition, the charge sign of the colliding droplets may be the same or the opposite. Therefore, only some examples are shown.

The collision efficiencies for droplet pairs ~~without~~ with no electric charge and field are ~~shown~~ presented in Fig. 6 as a reference. Collector droplets with radii larger than 30 μm are shown here to represent the precipitating droplets. The calculated collision efficiencies from this study are also compared with the measurements from previous studies. ~~The radius of the larger droplet r_1 ranges from 30 to 305 μm. The coloured lines are computation results in this study, and the dots are from previous experiment results. It is clear that our results are basically consistent with those from previous studies.~~ It is seen that results from this study are generally consistent with the measurements. Collision efficiencies increase ~~with~~ as r_2 changes from 2 to 14 μm, and also increase ~~with~~ as r_1 changes from 30 to 305 μm. For ~~droplet pair~~ two droplets that are both large enough, collision efficiency could be close to 1.

~~With the collision efficiencies of droplets with different radii and charges in different strength of electric field all computed, it is found that the electric effect is sensitive to droplet radii. Results are only discussed for $r_1 = 30$ μm and shown in Fig. 6. Totally 6 combinations of electric conditions are selected to be shown here, and the details are summarized in table 1. The droplet pair is set to have no charge, same-sign charge, or opposite charge. The electric field is set to be 0 or 400 V m^{-1}. Compared to the no-charge pair (curve 1), the same-sign charge without electric field (curve 2) slightly decreases collision efficiency, because of the repulsive force. The results of both positively charged pair and negatively charged pair are identical, since there is no electric field. In a downward electric field, the collision efficiency of the two situations is changed. For a positively charged pair (curve 3), the collision efficiency is very close to the no-charge pair, which implies that enhancement of electric field offset the repulsive effect. For a negatively charged pair in a downward field (curve 4), the collision efficiency with small r_2 is significantly enhanced. This could be easily explained by electrostatic induction: strong downward electric field induces positive charge on the lower part of the larger droplet (even though it is overall negatively-charged), so the smaller negative-charged droplet below feels attraction.~~

Figure 7 shows the collision efficiencies for droplet pairs with electric charge and field. The detailed characteristics of the droplet pairs are shown in Table 1. Basically, droplet pairs that have no charge, with same-sign charges, and with opposite-sign charges are selected here, and under the 0 and 400 V m^{-1} electric fields. Results for the collector droplet with a radius of 30 μm (Fig. 7a) and 40 μm (Fig. 7b) are shown. When comparing Fig. 7a and 7b, it can be seen that electrostatic effects are less significant for a larger collector. The electrostatic effects are even weaker for collector radius larger than 40 μm (figures not shown). Therefore, we use the 30 μm collector as an example to explain the electrostatic effects on collision efficiencies below.

For the collector droplet with a radius of 30 μm (Fig. 7a), noticeable, and sometimes significant electrostatic effect can be seen. Compared to the droplet pair with no charge (line 1), the positively-charged pair under no electric field (line 2) has a slightly smaller collision efficiency, due to the repulsive force. As can be seen in Fig. 3, when the charged droplets

move together, they first experience repulsive force, then attractive force at small distance. The integrated effect is that the droplets have smaller collision efficiency. The results for negatively-charged pair under no electric field are identical to line 2 and therefore are not shown. When a downward electric field of 400 V m^{-1} is added, the positively-charged pair (line 3) has a collision efficiency very close to the pair with no charge. This implies that the enhancement of collision efficiency by the electric field offsets the repulsive force effect. For a negatively-charged pair in a downward electric field (line 4), the collision efficiency with small r_2 is significantly enhanced. This could be easily explained by electrostatic induction: the strong downward electric field induces positive charge on the lower part of the collector droplet (even though it is overall negatively-charged), so the negative-charged collected droplet below experiences attractive force.

As for a pair with opposite-sign charges, line 5 in Fig. 7a shows that the collision efficiency is enhanced by the electrostatic effect even when there is no electric field. The collision efficiency is nearly an order of magnitude higher with r_2 < 5 μm. Line 6 in Fig. 7a shows that, with an electric field of 400 V cm^{-1}, the electrostatic effect for the pairs with opposite-sign charges is even stronger. There is also an interesting feature in Fig. 7a: as the collector and collected droplets have similar sizes, collision efficiency is high for the pairs with opposite-sign charges. This is quite different from the other four lines, where collision efficiencies are very low for droplet pairs with similar sizes.

Figure 8 shows the collision efficiencies for droplet pairs with charge and field, with smaller collectors. The collector droplet has a radius of 10 μm (Fig. 8a) and 20 μm (Fig. 8b) here, and can be used to represent cloud droplets. Collision efficiencies for these smaller collectors are much smaller than 1 when there is no charge (line 1 in Figs. 8a and 8b), which is already well known in cloud physics community. However, the electrostatic effects are so strong that the collision efficiencies could be significantly changed for these collectors. For the collector droplet with a radius of 10 μm (Fig. 8a), the positively-charged pair has a very small collision efficiency that is out of the scale in the figure, due to the dominating effect of the repulsive force as discussed above. For the positively-charged pair under a downward electric field, the collision efficiencies is on the similar order of magnitude as the pair with no charge. For the negatively-charged pair under the downward electric field, and for the pairs with opposite-sign charges, the electrostatic effects is very strong. The negatively-charged pair even has the collision efficiency increased by two orders of magnitude. Similarly, for the collector droplet with a radius of 20 μm (Fig. 8b), the electrostatic effect can lead to an order of magnitude increase in collision efficiencies.

It is evident that droplet charge and field can significantly affect collision efficiency, especially for smaller collectors. This means that the electrostatic effects depend on the radius of collector droplets, and mainly affects small droplets. The section below provides a detailed description on how these electrostatic effects can influence droplet size distributions.

~~As for a pair with opposite charge, curve 5 shows that the collision efficiency is higher than the pair with no charge. For r_2 < 5 μm, the collision efficiency is nearly an order of magnitude higher; which for larger droplet the increase is not so strong. This means that the electric effect is sensitive to the radius of droplets, and mainly affects small droplets. Curve 6 shows that with an electric field of 400 V cm^{-1}, the electric effect becomes significantly stronger. Collision efficiency is increased by more than one order of magnitude compared to no charge condition when r_2 < 5 μm. Even if r_2 is large, the collision efficiency could still be increased by about 2 times.~~

5.2. Evolution of ~~cloud spectrum~~ droplet size distribution

This part shows the ~~electric~~ electrostatic effects on ~~spectrum evolution with different initial~~ the evolution of different droplet size distribution. As discussed in Section 4, this study uses three initial size distributions, ~~i.e.,~~ where $\bar{r}$ = 15 μm, 9 μm and 6.5 μm, respectively. For each initial size distribution, comparisons are made among four different electric conditions, ~~including~~ namely ~~no charge, charged without field~~ uncharged droplets, charged droplets without electric field, charged droplets with a 200 V cm^{-1} electric field, and charged droplets with a 400 V cm^{-1} electric field. Note that "charged droplets" here refers to the initial charge distribution shown in ~~Fig. 4~~ Fig. 5. ~~The magnitude of 400 V cm-1 corresponds to the early stage of a thunderstorm.~~ We also compare the results of the uncharged clouds with $\bar{r}$ = 15 μm, 9 μm and 6.5 μm, which represents the aerosol effects, and then investigate whether the electrostatic effects can mitigate the aerosol effects during the collision-coalescence process.

Figure ~~7~~ 9 shows the evolution of ~~the spectrum~~ droplet size distribution with initial $\bar{r}$ = 15 μm, ~~which has an initial droplet number concentration of 71 cm^{-3}.~~ The 4 rows show different times (t = 7.5, 15, 22.5, and 30 min) during ~~spectrum~~ the simulated evolution. The left ~~side denotes the spectrum mass density~~ column shows the size distribution of droplet mass concentration $M(\ln r)$, and the right ~~side shows the droplet number concentration~~ column shows the size distribution of droplet number concentration $n(\ln r)$. They are related as $M(\ln r) = 4\pi r^3 \rho/3 \cdot n(\ln r)$. A second mode in size distribution gradually form as droplets undergo the collision-coalescence process from t = 7.5 to 30 min. Although the second mode can be clearly seen in the plots of $n(\ln r)$, we show $M(\ln r)$ here so that the second mode can be seen as a peak. In each panel, the dotted line denotes the initial ~~spectrum~~ size distribution (t = 0 min) for reference. It is seen that droplet ~~spectra~~ size distributions under 4 electric conditions have similar behavior for initial $\bar{r}$ = 15 μm: ~~All the spectra~~ they all evolve to a double-peak form, regardless of electric charge or field. At 30 min, the 4 cases all have a modal radius of about 200 μm (Fig. 9d). The ~~electric~~ electrostatic effect is not notable for large droplets in the $\bar{r}$ = 15 μm cases, because the initial radius is large enough to start gravitational collision-coalescence quickly. ~~Consequently, the electric effect is negligible in this case.~~

The evolution of droplet total number concentration and total positive charge concentration (also equal to the total negative charge concentration) is shown in Fig. 10. It is evident that droplet total number concentration decreases from 71 cm^{-3} to less than 5 cm^{-3} in 30 minutes, and is nearly not affected by the 4 different electric conditions. Both of the positive charge and negative charge concentration decrease from 9384 to about 1000 e cm^{-3}, as droplets with opposite-sign charges go through collision-coalescence and charge neutrality occurs.

Figure ~~8~~ 11 shows the evolution of ~~the spectrum~~ droplet size distribution with initial $\bar{r}$ = 9 μm. For the uncharged ~~spectrum~~ cloud, it takes 60 min to have the second peak grow to about 200 μm. Therefore, the 4 panels of Fig. 11 show the ~~spectrum~~ simulated evolution for t = 15, 30, 45, and 60 min. The charges and the electric fields have more significant effect in the $\bar{r}$ = 9 μm case than in the $\bar{r}$ = 15 μm case. It is seen that, at 15 and 30 min, the ~~spectra~~

clouds with different electric conditions evidently differ from each other, but the second mode is not obvious. At 45 min, the electrostatic effects ~~of charge and electric field~~ on the second peak is evident. ~~The small droplet peak on the left is lower, and the second peak on the right is higher, indicating that~~ The charged cloud (red line) evolves more quickly than the uncharged cloud, as can been from the lower first peak and the growing second peak. Moreover, ~~external~~ the downward electric fields further boost the collision-coalescence process of charged droplets (green and purple lines). ~~Under the electric field of 200 V cm^{-1}, the second peak is two times higher than the no-field case (red line) at 45 min. Under the electric field of 400 V cm^{-1}, the second peak is even higher.~~ At 60 min, the modal radius of the second peak is about 200 μm for ~~no-charge situation~~ the uncharged cloud, 300 μm for ~~charged without field situation~~ the charged cloud but without an electric field, 500 μm for ~~charged with 200 V cm^{-1} situation~~ the charged cloud with a field of 200 V cm^{-1}, and 700 μm for ~~charged with 400 V cm^{-1} situation~~ the charged cloud with a field of 400 V cm^{-1}, respectively.

As for the evolution of droplet total number concentration and charge concentration, Fig. 12 shows that they are distinctly affected by the 4 different electric conditions. The charged cloud with a field of 400 V cm^{-1} has very low droplet number concentration and charge concentration at 60 min. the electrostatic effects play an important role in converting smaller droplets to larger droplets. The 2-dimensional ~~spectrum~~ distribution of droplet mass concentration for $\bar{r}$ = 9 μm at 60 min is shown in Fig. 13. Figure 13a is for the ~~no-charge~~ uncharged situation. Figs. 13b, 13c, and 13d are for the situations with charges and with electric fields of 0, 200, 400 V cm^{-1}, respectively. After 60 min of evolution, ~~these charge distributions are~~ the distribution of mass over the charge bins is still symmetric. ~~These clearly show the process that charge transports to large droplets during coalescence growth.~~ It is also shown that both mass and charges are transported from smaller droplets to larger droplets during collision-coalescence. Note that the integration of this 2-dimensional ~~spectrum~~ distribution along the charge ~~axis~~ bins gives the 1-dimentional ~~size~~ distribution over droplet size at 60 min as shown in Fig. 11d.

Figure ~~10~~ 14 shows the evolution of ~~the spectrum~~ droplet size distribution with initial $\bar{r}$ = 6.5 μm. For the uncharged cloud, it takes 120 min to have the second peak grow to about 200 μm. Therefore, the 4 panels of Fig. 14 show the ~~spectrum~~ simulated evolution for t = 30, 60, 90 and 120 min. The enhancement ~~of~~ by the electric field on collision-coalescence process is much more obvious than $\bar{r}$ = 9 μm. After 90 min of evolution, ~~the spectra for the situations with no charge and with charge but no electric field~~ the uncharged cloud (blue line) and charged cloud without field (red line) are almost the same as the initial ~~spectrum~~ distribution. This is because the droplets are too small to initiate gravitational collision. At 120 min, a second peak has formed for the situations with no charge and with charge but no field. In ~~comparison~~ contrast, under the external ~~electric~~ field of 200 and 400 V cm^{-1} (green and purple lines), the cloud droplets grow much more quickly than the no-field ~~conditions~~ situations. ~~At 120 min, the modal radius of the second peak is at about 200 μm for the no-charge situation (blue line) and 300 μm for the charged-without-field situation (red line). The droplets in two charged-with-field situations~~ Some droplets even have evolved to larger than 1024 μm, which ~~have precipitated out~~ are supposed to precipitate out from the clouds. The evolution of droplet total number concentration and charge concentration is shown in Fig. 15, which indicates that droplet total number concentrations and charge concentration are strongly affected by the electrostatic effects. These results show that, the electric field would remarkably trigger the collision-coalescence process for the small droplets.

As for the initial mean droplet radius $\bar{r}$ < 6 μm (figure not shown), similar to Fig ~~10~~ 14, the ~~spectra~~ droplet size distribution of uncharged and charged cloud without electric field would nearly have no difference, while the effect of electric fields is much stronger. This means that charge effect is relatively small compared to electric fields when the initial droplet radius of the cloud is small enough.

Now we compare the electrostatic effects shown above with the aerosol effects. Let us take the cases with $\bar{r}$ = 15 μm and $\bar{r}$ = 9 μm as examples. When there is no electrostatic effects, the case with $\bar{r}$ = 15 μm can develop a significant second peak in the size distribution in less than 30 min, while it takes about 60 min for the $\bar{r}$ = 9 μm case to develop a similar

second peak, as can be seen in Figs. 9 and 11. This can be regarded as an aerosol effect. When considering the electrostatic effects, it only takes about 45 min for the $\bar{r}$ = 9 μm case to develop a similar second peak, as can be seen in Fig. 9. Therefore, the aerosol-induced precipitation suppression effect is mitigated by the electrostatic effects.

6 Discussion

According to Eq. (2), collection kernel K is composed of the collision efficiency E, relative terminal velocity, and coalescence efficiency ε. It is found that the total electrostatic effect on K is mainly contributed by E. ~~The electric enhancement of collision efficiency E is particularly significant for small droplets, as shown in Sect. 6.1.~~ The relative terminal velocity term also contributes to the collection kernel K~~, and the electric field can affect terminal velocity of small charged droplets significantly.~~. As mentioned in Section 3.4, terminal velocities $\boldsymbol{V_1}$ or $\boldsymbol{V_2}$ are derived by simulating just single one charged droplet in air with a certain electric field, and letting it fall until its velocity converges to the terminal velocity. Therefore, the electric field can affect terminal velocities of charged droplets, thus to affect the collection kernels. Terminal velocities of droplets in an external electric field is illustrated in Fig. 16. ~~As shown in Fig. 11,~~ In a downward electric field of 400 V cm^{-1}, the terminal velocity of a large droplet is ~~nearly not~~ hardly affected. The difference of velocity caused by the electric field ~~of~~ for r = 1000 μm does not exceed 1%, and ~~difference at the one for~~ 100 μm does not exceed 5%. On the contrary, electric fields strongly affect the ~~sedimentation~~ terminal velocities of charged small droplets. For r < 5 μm, the terminal velocity of a negatively-charged droplet even turns "upwards". ~~This is due to the fact that~~ Electric fields mainly affect terminal velocities of small charged droplets because droplet mass $m \propto r^3$, while droplet charge $q \propto r^2$ according to observation. ~~So~~ Therefore, $q \propto m^{2/3}$ means that the acceleration ~~of~~ contributed by the electric force decreases with increasing droplet mass. ~~which indicates that small droplets are more sensitive to electric charge and field.~~

This study still neglects some possible electrostatic effects in collision-coalescence process. Electrostatic effect on coalescence efficiency ε is neglected. Rebound (collide but not coalesce) happens because of an air film temporally trapped between the two surfaces, which is a barrier to coalescence. This barrier may be overcome by strong electric attraction occurring at small distance. Many experiments show that electric charges and fields would enhance coalescence efficiency, such as Jayaratne and Mason (1964) and Beard et. al. (2002). The latter experiment indicates that even minimal electric charge incapable of enhancing collision can significantly increase ε, while the marginal utility of larger electric charges on ε is very small. ~~But~~ However, there is no proper numerical model to evaluate the effect. ~~So~~ Therefore, this study may underestimate the electrostatic effect on droplet collision-coalescence process.

Induced charge redistribution is also neglected when rebound happens. For instance, let us consider a rebound event in a positive (downward) electric field. The larger droplet is often above the smaller droplet, and the smaller one will carry positive charge instantaneously according to electrostatic induction, then move apart. The rebound would cause charge redistribution between the pair. This may lead to some change in the ~~spectrum~~ evolution of clouds.

7 Conclusion

The effect of electric charges and atmospheric electric fields on cloud droplet collision-coalescence and on ~~spectrum~~ the evolution of cloud droplet size distribution is studied numerically. The equations of motion ~~equation~~ for cloud droplets ~~in the atmosphere is~~ are solved to get the trajectories of droplet pair of any radii (2 to 1024 μm) and charges (-32 to +32r^2, in unit of elementary charge, droplet radius r in unit of μm) in different strength of downward electric fields (0, 200 and 400 V cm^{-1}). Based on trajectories, we determine whether a droplet pair collide or not. Thus, collision efficiencies for the droplet pairs are derived. It is seen that collision efficiency is increased by electric charges and fields, especially when the droplet pair are oppositely charged or both negatively charged in a downward

electric field. We consider these effects as the electrostatic effects. The increase of collision efficiency is particularly significant for a pair of small droplets.

With collision efficiencies derived in this study, the SCE is solved to simulate the evolution of cloud droplet ~~spectrum~~ size distribution under the influence of electrostatic effects. The initial droplet size ~~conditions~~ distributions include $\bar{r}$ = 15 μm, 9 μm, and 6.5 μm, and the initial electric conditions include ~~no charge~~ uncharged and charged droplets (with charge amount proportional to droplet surface area) in different strength of electric fields (0, 200 and 400 V cm^{-1}). The ~~conditions~~ magnitudes of electric charges and fields used in this study represent the the ~~real conditions in the atmosphere~~ observed atmospheric conditions. In the natural precipitation process, the charge amount, the strength of electric fields, and the time scale of the ~~droplet spectrum~~ evolution are similar to those in this study. It is seen that the electrostatic effects ~~of both the electric charge and field~~ are not notable for clouds with initial $\bar{r}$ =15μm, since the initial radius is large enough to start gravitational collision quickly. For clouds with initial $\bar{r}$ = 9 μm, electric charges could enhance ~~spectrum~~ droplet collision evidently compared to the ~~no charge~~ uncharged condition when there is no electric field, and the existence of electric fields further accelerates collision-coalescence and the ~~large drop~~ formation of large drops. For clouds with initial $\bar{r}$ = 6.5 μm, it is difficult for gravitational collision to occur. The enhancement of droplet collision merely by electric charge without field is still not significant, but electric fields could remarkably enhance the collision process. These results indicate that ~~the~~ clouds with ~~small~~ droplet sizes smaller than 10 μm are more sensitive to ~~electric charge and field~~ electrostatic effects, which can significantly enhance the collision-coalescence process and trigger the raindrop formation.

It is known that the increase of aerosol number and therefore the decrease of cloud droplet size lead to suppressed precipitation and longer cloud lifetime. ~~as observed in the polluted clouds (Albrecht, 1989).~~ But with the electrostatic effect ~~of electric charge and field~~, ~~this Albrecht effect~~ the aerosol effect can be mitigated to a certain extent. The three initial droplet size distributions used in this study, with $\bar{r}$ = 15, 9, and 6.5 μm, have an initial droplet number concentration of 71, 325, and 851 cm^{-3}, respectively. The three cases can represent different aerosol conditions. Smaller droplets size and higher droplet number concentration represents a more polluted condition. It is seen that collision-coalescence process is significantly slowed down as $\bar{r}$ changes from 15 μm to 9 μm, and to 6.5 μm. It takes about 30 min, 60 min, and 120 min, respectively, for the three cases to form a mode of 200 μm in droplet size distribution. We consider this as an aerosol effect. When the electrostatic effect is considered, the case with $\bar{r}$ = 9 μm now only takes about 45 min to form the mode of 200 μm. Therefore, the enhancement of raindrop formation due to electrostatic effects can mitigate the suppression of rain due to aerosols.

Code and data availability

Data and programs are available from Shian Guo (guoshian@pku.edu.cn) upon request.

Author contribution

Shian Guo developed the model, wrote the codes of program, and performed the simulation. Huiwen Xue advised on the case settings of the numerical simulation. Huiwen Xue and Shian Guo worked together to prepare the manuscript.

Competing interests

The authors declare that they have no conflict of interest.

Acknowledgements

This study is supported by the National Innovative Training Program and the Chines NSF grant 41675134. We are grateful to Jost Heintzenberg and Shizuo Fu for constructive discussions on this study.

References

Albrecht, B. A.: Aerosols, cloud microphysics, and fractional cloudiness., Science, 245, 1227–1230, doi:10.1126/science.245.4923.1227., 1989.

Baumgaertner, A. J. G., Lucas, G. M., Thayer, J. P., Mallios, S. A.: On the role of clouds in the fair weather part of the global electric circuit, Atmos. Chem. Phys., 14, 8599–8610, doi:10.5194/acp-14-8599-2014, 2014.

Beard, K. V., Durkee, R. I., Ochs, H. T.: Coalescence efficiency measurements for minimally charged cloud drops, J. Atmos. Sci., 59, 233–243., doi: 10.1175/1520-0469(2002)059<0233:CEMFMC>2.0.CO;2, 2002.

Beard, K. V.: Terminal velocity and shape of cloud and precipitation drops aloft, J. Atmos. Sci, 33, 851-864, doi: 10.1175/1520-0469(1976)033<0851:TVASOC>2.0.CO;2, 1976.

Beard, K.V. and Ochs III, H.T.: Collection and coalescence efficiencies for accretion, J. Geophys. R., 41, 863-867, doi:10.1029/JD089iD05p07165, 1984.

Bott, A.: A flux method for the numerical solution of the stochastic collection equation, J. Atmos. Sci, 55, 2284-2293, doi: 10.1175/1520-0469(1998)055<2284:AFMFTN>2.0.CO;2, 1998.

Bott, A.: A flux method for the numerical solution of the stochastic collection equation: extension to two-dimensional particle distributions, J. Atmos. Sci, 57, 284-294, doi: 10.1175/1520-0469(2000)057<0284:AFMFTN>2.0.CO;2, 2000.

Davis, M. H.: Two charged spherical conductors in a uniform electric field: Forces and field strength, Q. J. Mech. Appl. Math., 17, 499– 511., doi:10.1093/qjmam/17.4.499, 1964.

Eow, J.S., Ghadiri, M., Sharif, A. O., Williams, TJ.: Electrostatic enhancement of coalescence of water droplets in oil: a review of the current understanding, Chem. Eng. J., 84, 173–192, doi:10.1016/S1385-8947(00)00386-7, 2001.

Hamielec, A. E. and Johnson, A. I.: Viscous flow around fluid spheres at intermediate Reynolds numbers, Can. J. Chem. Eng., 40, 41-45, doi:10.1002/cjce. 5450400202, 1962.

Hamielec, A. E. and Johnson, A. I.: Viscous flow around fluid spheres at intermediate Reynolds numbers (II), Can. J. Chem. Eng., 41, 246-251, doi:10.1002/cjce.5450410604, 1963.

Harrison, R. G., Carslaw, K. S.: Ion-Aerosol-Cloud Processes in the Lower Atmosphere, Rev. Geophys., 41(3), doi:10.1029/2002RG000114, 2003.

Harrison, R. G., Nicoll, K. A., Ambaum, M. H. P.: On the microphysical effects of observed cloud edge charging, Q. J. R. Meteorol. Soc., 141, 2690–2699, doi:10.1002/qj.2554, 2015.

Jayaratne, O. W. and Mason, B. J.: The coalescence and bouncing of water drops at an air/water interface, P. R. Soc. London, 280, 545-565, doi:10.1098/rspa.1964.0161, 1964.

Khain, A., Arkhipov, V., Pinsky, M., Feldman, Y. and Ryabov., Ya.: Rain enhancement and fog elimination by seeding with charged droplets. part I: theory and numerical simulations. J. Appl. Meteorol., 43:1513–1529, doi:10.1175/JAM2131.1, 2004.

Klimin, N. N., Rivkind, V. Ya., Pachin, V. A.: Collision efficiency calculation model as a software tool for microphysics of electrified clouds, Meteorol. Atmos. Phys, 53, 111-120, doi:10.1007/BF01031908, 1994.

Lamb, D. and Verlinde, J.: Physics and Chemistry of Clouds, Cambridge University Press, 2011.

Miles, N. L., Verlinde, J., Clothiaux, E. E.: 2000 Cloud droplet size distributions in low-level stratiform clouds, J. Atmos. Sci., 57 (2), 295–311, doi: 10.1175/1520-0469(2000)057<0295:CDSDIL>2.0.CO;2,2000.

Pinsky, M., and Khain, A.: Collision efficiency of drops in a wide range of Reynolds numbers: effects of pressure on spectrum evolution, J. Atmos. Sci, 58, 742-763, doi: 10.1175/1520-0469(2001)058<0742:CEODIA>2.0.CO;2, 2000.

Pruppacher, H. R. and Klett, J. D.: Microphysics of Clouds and Precipitation, Kluwer Academic Publishers, 1997.

Schlamp, R. J., Grover, S. N., Pruppacher, H. R., and Hamielec, A. E.: A numerical investigation of the effect of electric charges and vertical external electric fields on the collision efficiency of cloud drops, J. Atmos. Sci., 33. 1747-1755, doi:10.1175/1520-0469(1976)033<1747:ANIOTE>2.0.CO;2, 1976.

Takahashi, T.: Measurement of electric charge of cloud droplets, drizzle, and raindrops, Rev. Geophys. Space. Ge., 11, 903-924, doi:10.1029/RG011i004p00903, 1973.

Telford, J. W.: A new aspect of coalescence theory, J. Meteorol, 12, 436-444, 1955.

Tinsley, B. A., Zhou, L., Plemmons, A.: Changes in scavenging of particles by droplets due to weak electrification in clouds, Atmos. Res., 79, 266 – 295, doi:10.1016/j.atmosres.2005.06.004, 2006.

Twomey, S.: Pollution and the planetary albedo, Atmos. Environ., 8, 1251-1256. doi:10.1016/0004-6981(74)90004-3, 1974.

Wallace, J. M., Hobbs, P. V.: Atmospheric Science, Second Edition, Academic Press, 2006.

Wang, L. P., Ayala, O., Grabowski, W. W.: Improved Formulations of the Superposition Method, J. Atmos. Sci, 62(4):1255-1266, doi: 10.1175/JAS3397.1, 2005.

Warner, J.: The water content of cumuliform cloud, Tellus, 7:4, 449-457, doi: 10.3402/tellusa.v7i4.8917, 1955.

Zhou, L., Tinsley, B. A., Plemmons, A.: Scavenging in weakly electrified saturated and subsaturated clouds, treating aerosol particles and droplets as conducting spheres, J. Geophys. R., 114, D18201, doi:10.1029/2008JD011527, 2009.

Table 1. Meaning of the 6 different curves in Fig. 6.

$r_1 = 30$ μm curve settings	q_1 (e)	q_2 (e)	electric field E_0 (V cm^{-1})
(1)	0	0	0
(2)	$+32\ r_1^2$	$+32\ r_2^2$	0
(3)	$+32\ r_1^2$	$+32\ r_2^2$	+400
(4)	$-32\ r_1^2$	$-32\ r_2^2$	+400
(5)	$+32\ r_1^2$	$-32\ r_2^2$	0
(6)	$+32\ r_1^2$	$-32\ r_2^2$	+400

Table 2. Total number concentration and charge content for all initial droplet distributions

mean radius $\bar{r}$ (μm)	total number concentration (cm^{-3})	total positive charge concentration (e cm^{-3})	total negative charge concentration (e cm^{-3})
15	70.6	+9384	-9384
9	324.8	+15638	-15638
6.5	850.5	+21634	-21634

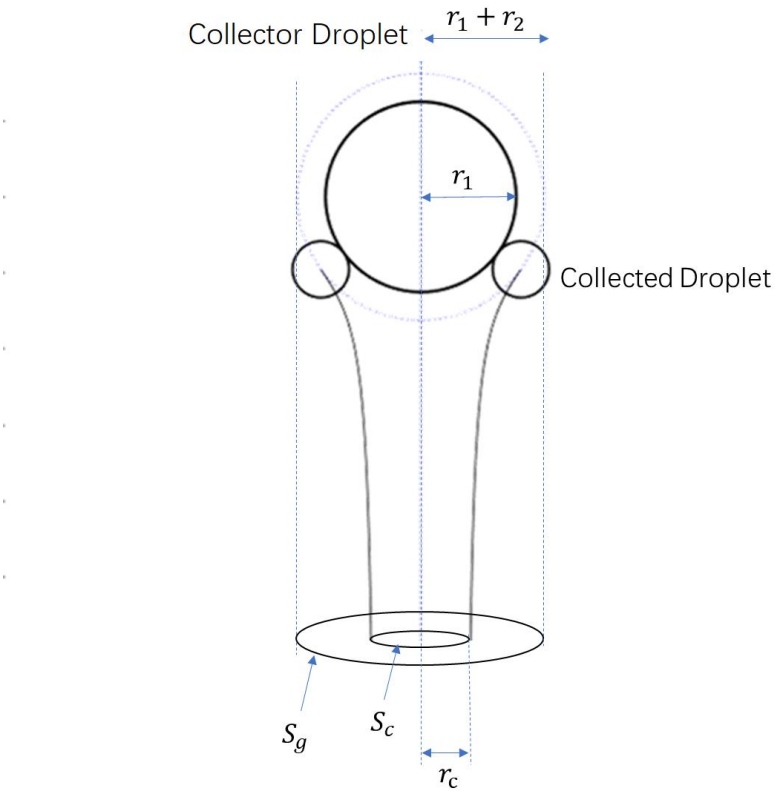

FIG. 1. A geometry sketch map of collision. ~~Original~~ The initial vertical distance between the center of the two droplets is set to be $30(r_1 + r_2)$, which ~~approximates to coming from~~ can approximately represent that the droplets initially has a distance of infinity. To calculate the collection cross section $S_c = \pi r_c^2$, ~~we need to adjust~~ the initial horizontal distance needs to be changed with the bisection method, until it converges to r_c. Collision happens only when the initial horizontal distance is smaller than r_c.

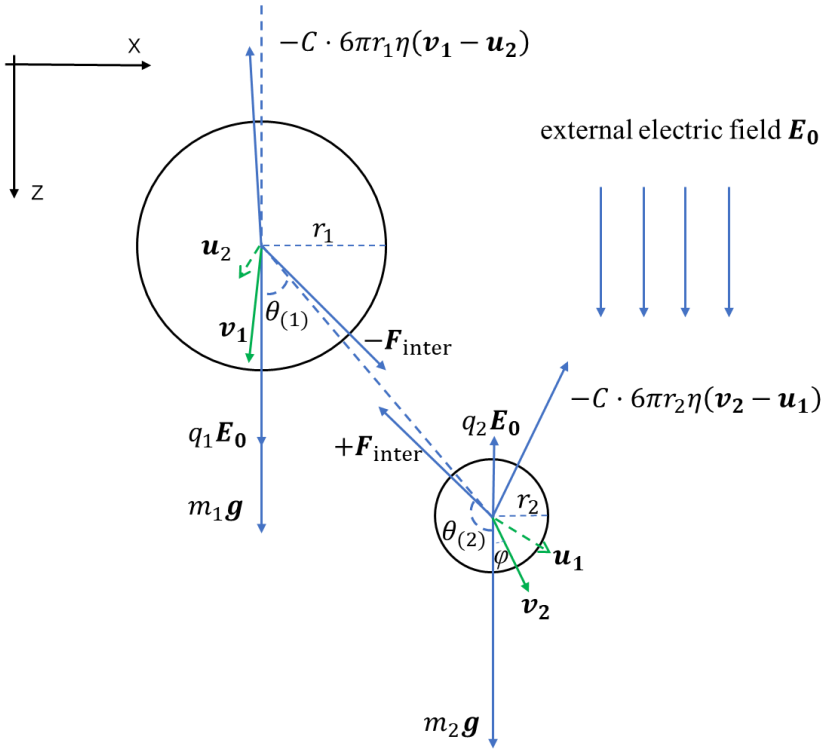

FIG. 2. A schematic diagram of all the forces acting on the two droplets, as well as droplet velocities and the induced flow velocities. The electric field $\boldsymbol{E_0}$ is vertically downward, and electric charges $q_1 > 0$, $q_2 < 0$. Note that the electrostatic force $\boldsymbol{F}_{e1}$, $\boldsymbol{F}_{e2}$ include two parts: the electric force from the other droplet ($\boldsymbol{F}_{\text{inter}}$, in the figure), and the force purely from the external electric field ($q_1\boldsymbol{E_0}$, $q_2\boldsymbol{E_0}$ in the figure).

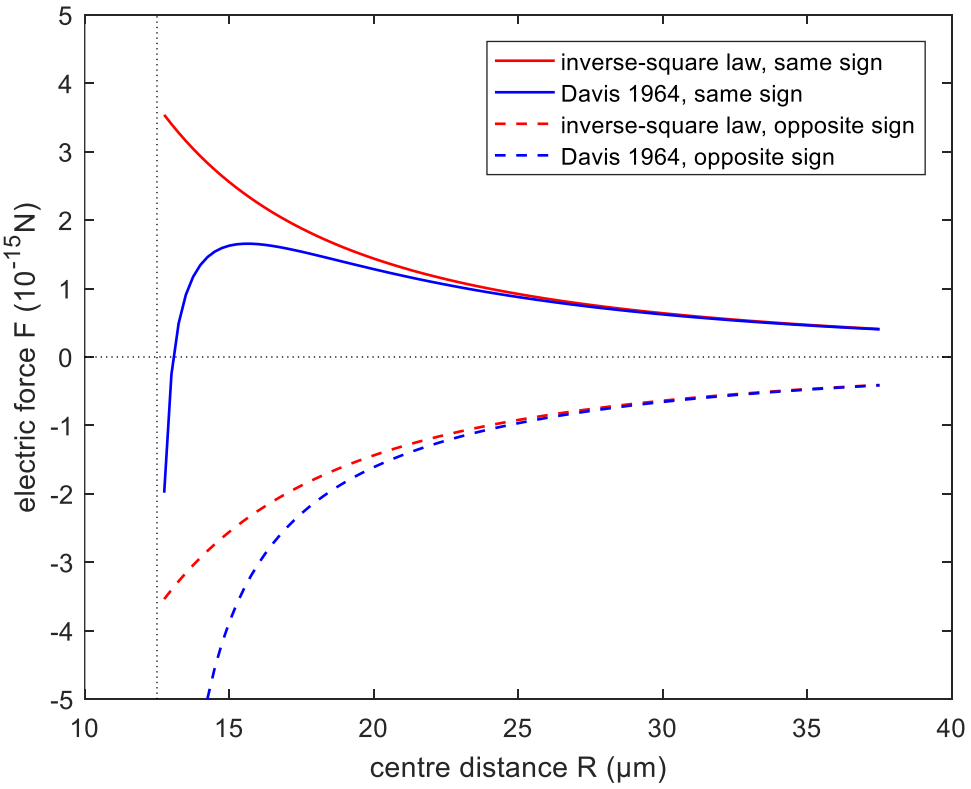

~~FIG. 2~~ **FIG. 3.** Comparison of the electric force from the conductor model (Davis 1964, Eq. 15 in this study) and the inverse-square law (Eq. 12 in this study) ~~where,~~. Positive force represents repulsion and negative force represents attraction. Radius of the pair is set to $r_1 =$ 10 μm and $r_2 =$ 2.5 μm respectively. Solid lines ~~denote~~ are for the droplet pair with the same sign of electric charges, with $q_1 = +100$ e, and $q_2 =$ +25 e. Dashed lines ~~denote~~ are for the droplet pair with the opposite sign of electric charges, with $q_1 = +100$ e, and $q_2 =$ -25 e.

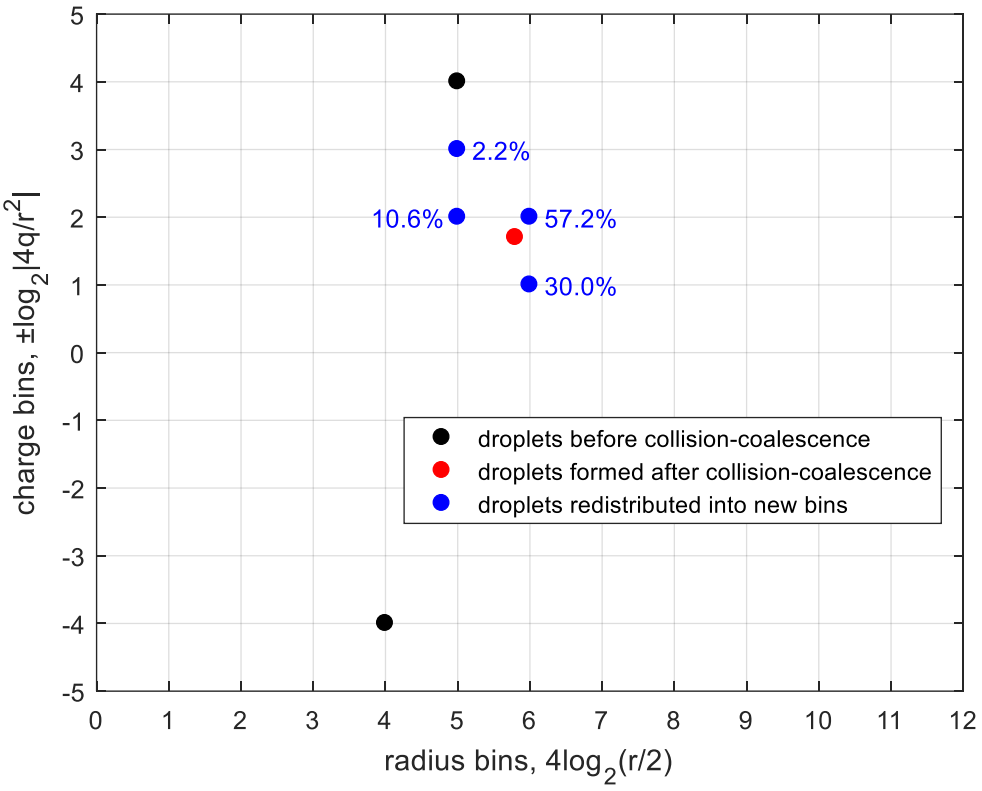

~~FIG. 3~~ **FIG. 4.** An example of droplet redistribution ~~of coalescence between two bins~~ to the new size and charge bins after collision-coalescence. Black dots denote the two bins of droplets before collision-coalescence. The red dot ~~refers to the droplet after coalescence but not on the bin grids~~ denotes the droplets after collision-coalescence but not on the bin grids. Blue dots ~~show the redistribution method and proportion of each redistributed bin~~ denote the droplets that are redistributed to the new bins. Numbers close to the blue dots are the percentage of droplets that are redistributed into that bin. ~~which is~~ The redistribution method is constrained by particle number conservation, mass conservation, and charge conservation.

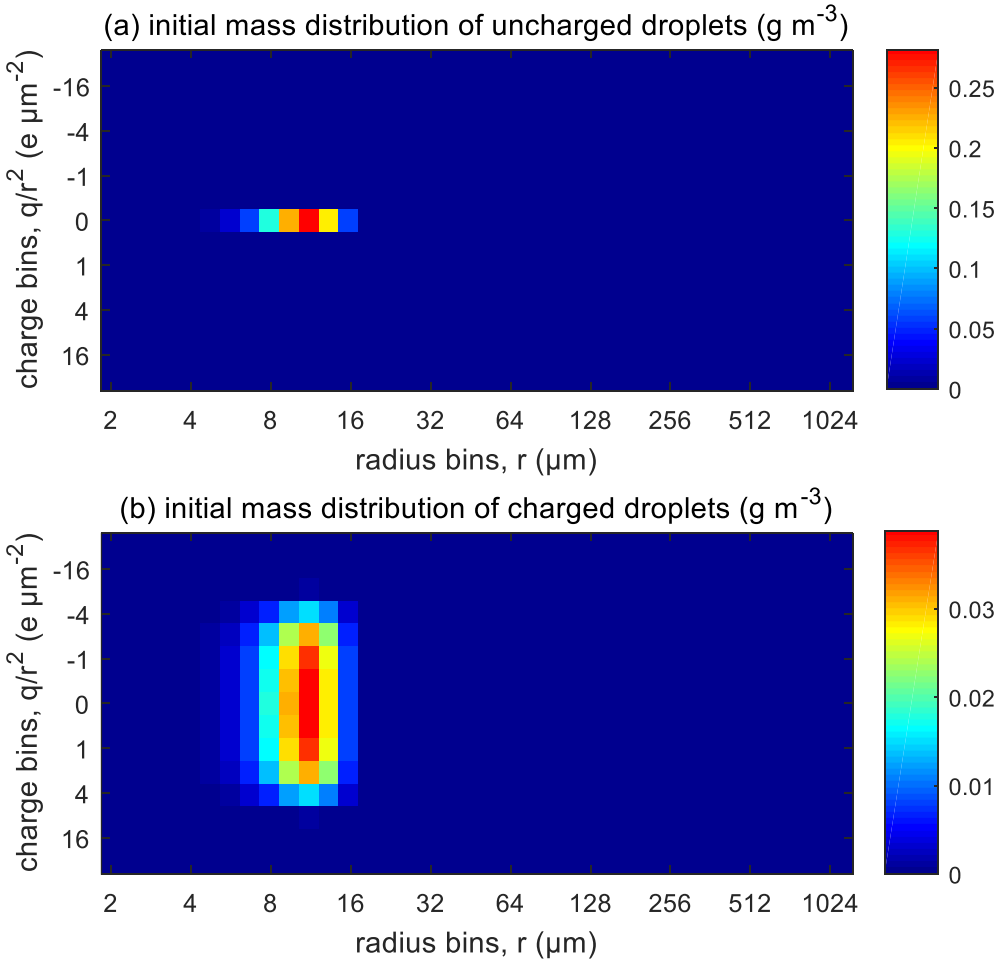

~~FIG. 4~~ **FIG. 5.** ~~Initial spectrum mass distribution shown in 2-dimensional grids of bins~~ The initial spectrum droplet mass distributed over the size and charge bins. ~~Different~~ Colours stand for water mass content in the bins (in unit of g m^{-3}). (a) Uncharged ~~spectrum mass distribution~~ droplets (b) charged ~~spectrum mass distribution~~ droplets.

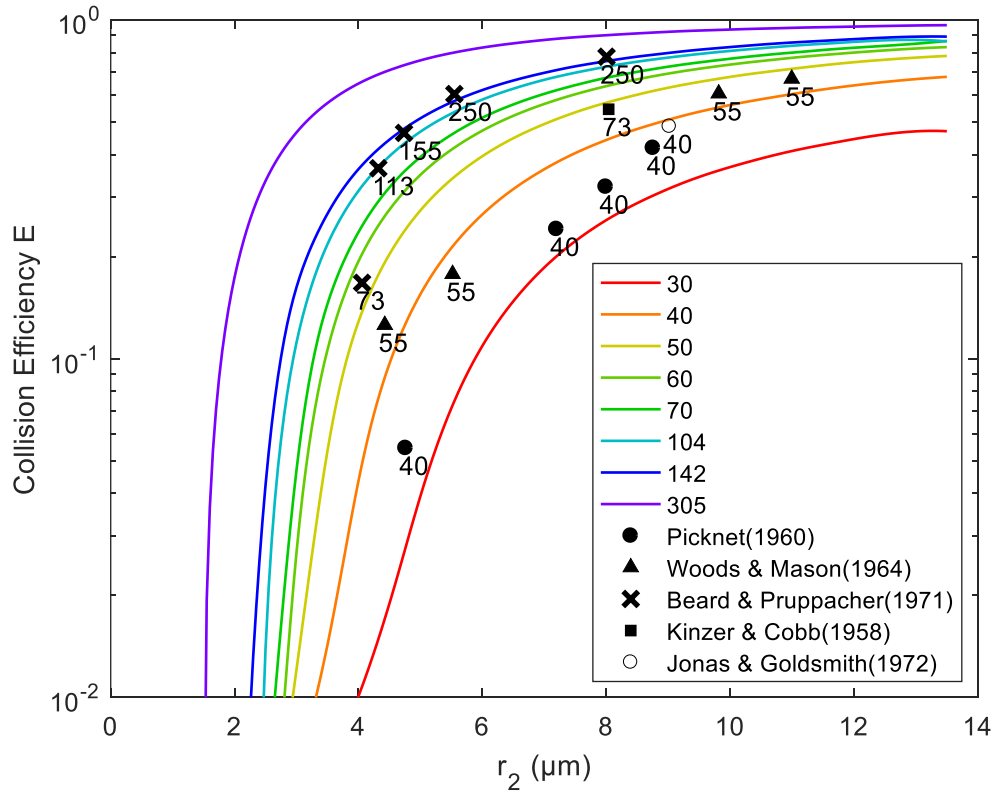

~~FIG. 5~~ **FIG. 6.** Collision efficiency ~~between~~ for droplets with no electric charge or field. ~~Colour~~ Lines are results computed in this study. Different lines ~~show~~ represent different ~~large~~ collector radius r_1, from 30 to 305 μm. X-axis denotes the ~~smaller~~ collected droplet radius r_2. Scatter points are collision efficiencies from previous experimental studies.

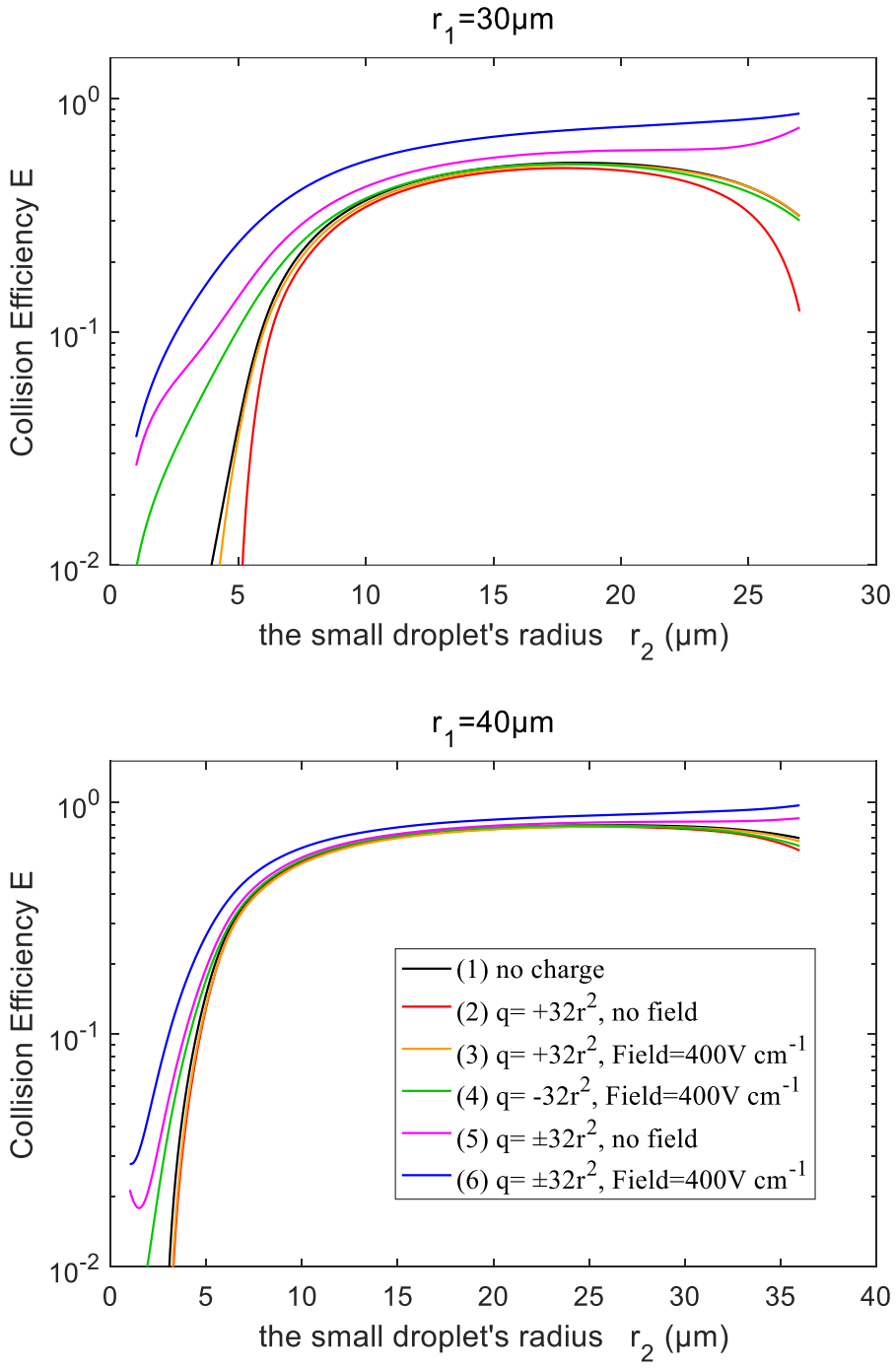

FIG. 7. Collision efficiency for droplets with electric charge and field. The radius of the collector droplet r_1 is：(a) 30.0 μm, (b) 40.0 μm. X-axis denotes the collected droplet radius r_2. The two droplets carry electric charges proportional to r^2. The lines for droplet pairs with no charge (line 1 in Fig. 7a and 7b) are the same as the 30 μm and 40 μm lines in Fig. 6.

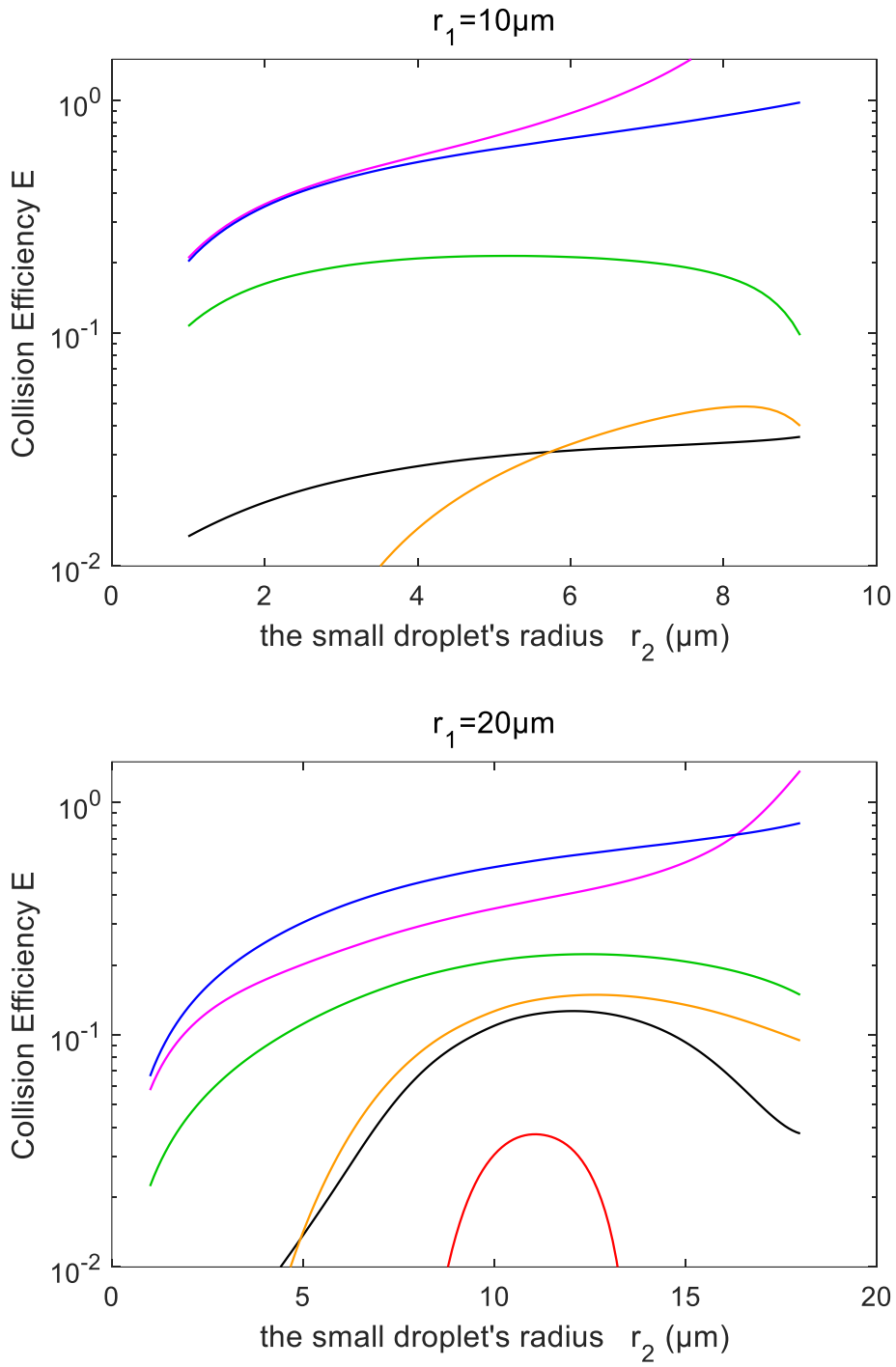

FIG. 8. Collision efficiency for droplets with electric charge and field. The radius of the collector droplet r_1 is：(a) 10.0 μm, (b) 20.0 μm. The other characteristics of the droplet pairs are similar to those in Fig. 7.

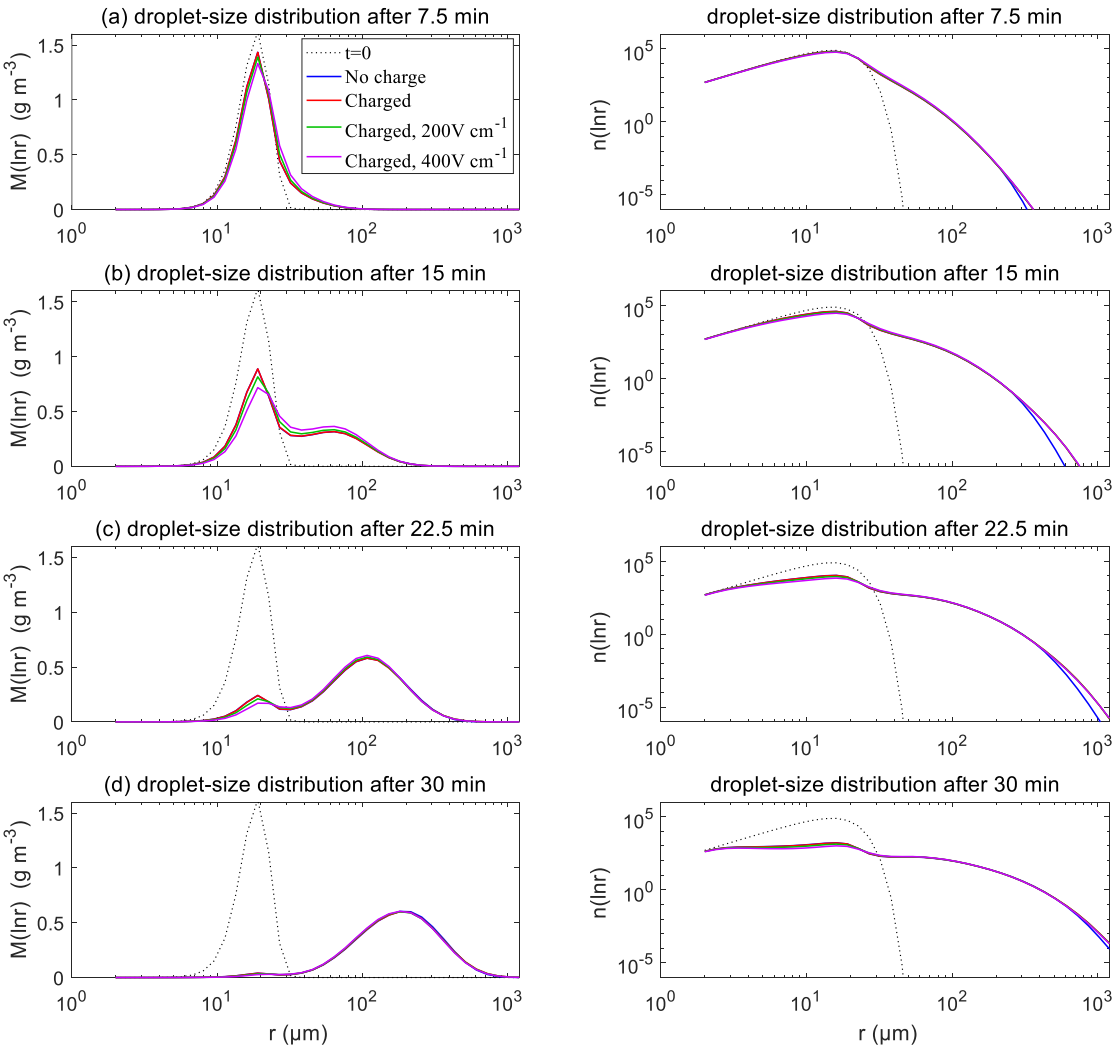

~~FIG. 7~~ **FIG. 9.** The evolution of ~~spectrum~~ droplet size distribution with initial $\bar{r}$ = 15 μm. These panels show different stages of the evolution from top to bottom. The left ~~side shows the mass density of cloud spectra~~ column shows the size distribution of droplet mass concentration, and the right ~~side show the number concentration of droplets under logarithmic coordinates~~ column shows the size distribution of droplet number concentration, on logarithmic scales. In each panel, comparisons are made for 4 different electric conditions. Blue lines denote the uncharged cloud ~~spectrum~~. Red lines denote charged cloud without electric field. Green and purple lines denote charged cloud with a field of 200 V cm^{-1} and 400 V cm^{-1}, respectively. Dotted lines show the initial ~~mass~~ size distribution.

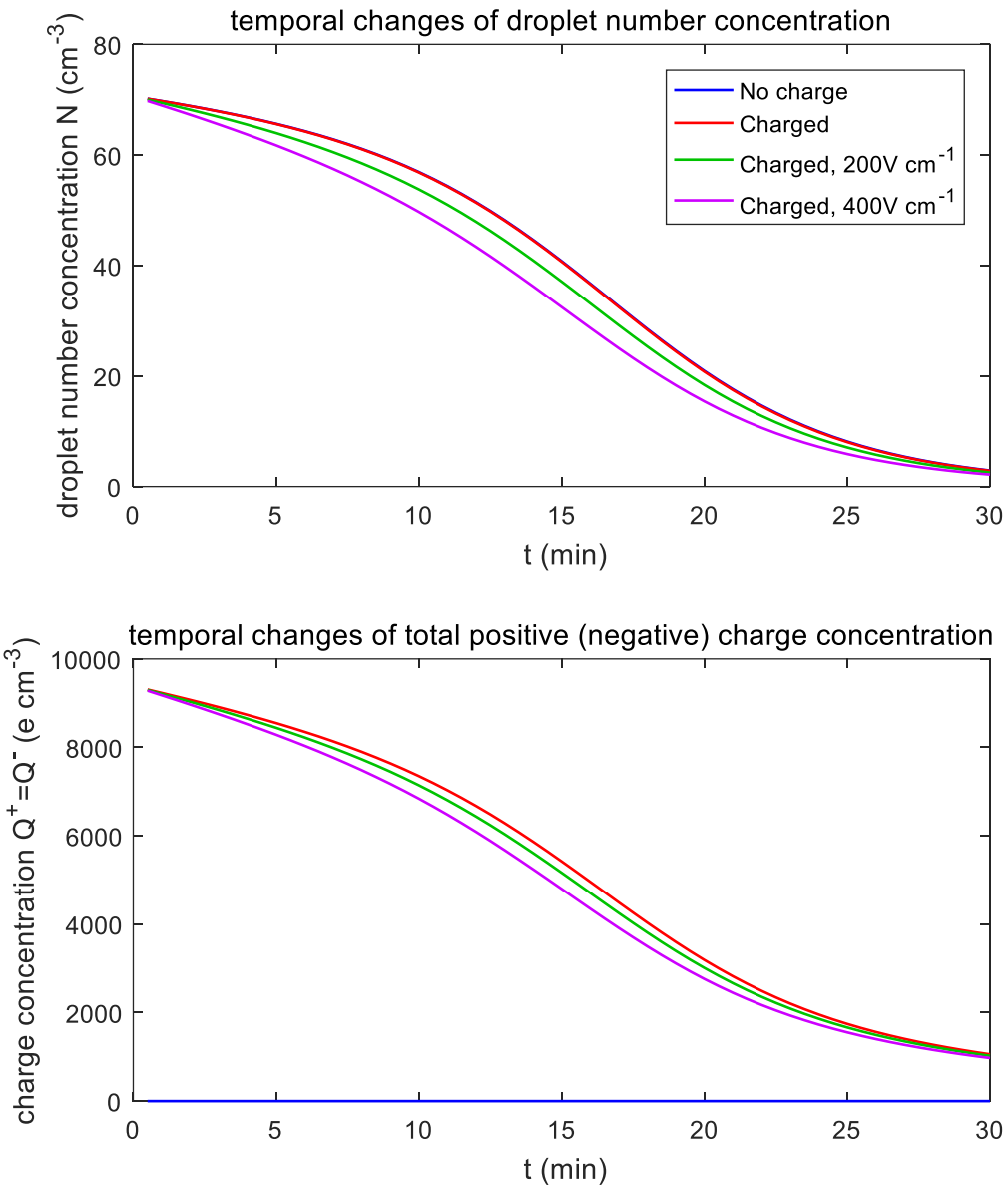

FIG. 10. Temporal changes of droplet total number concentration and total charge content for $\bar{r}$ =15 μm

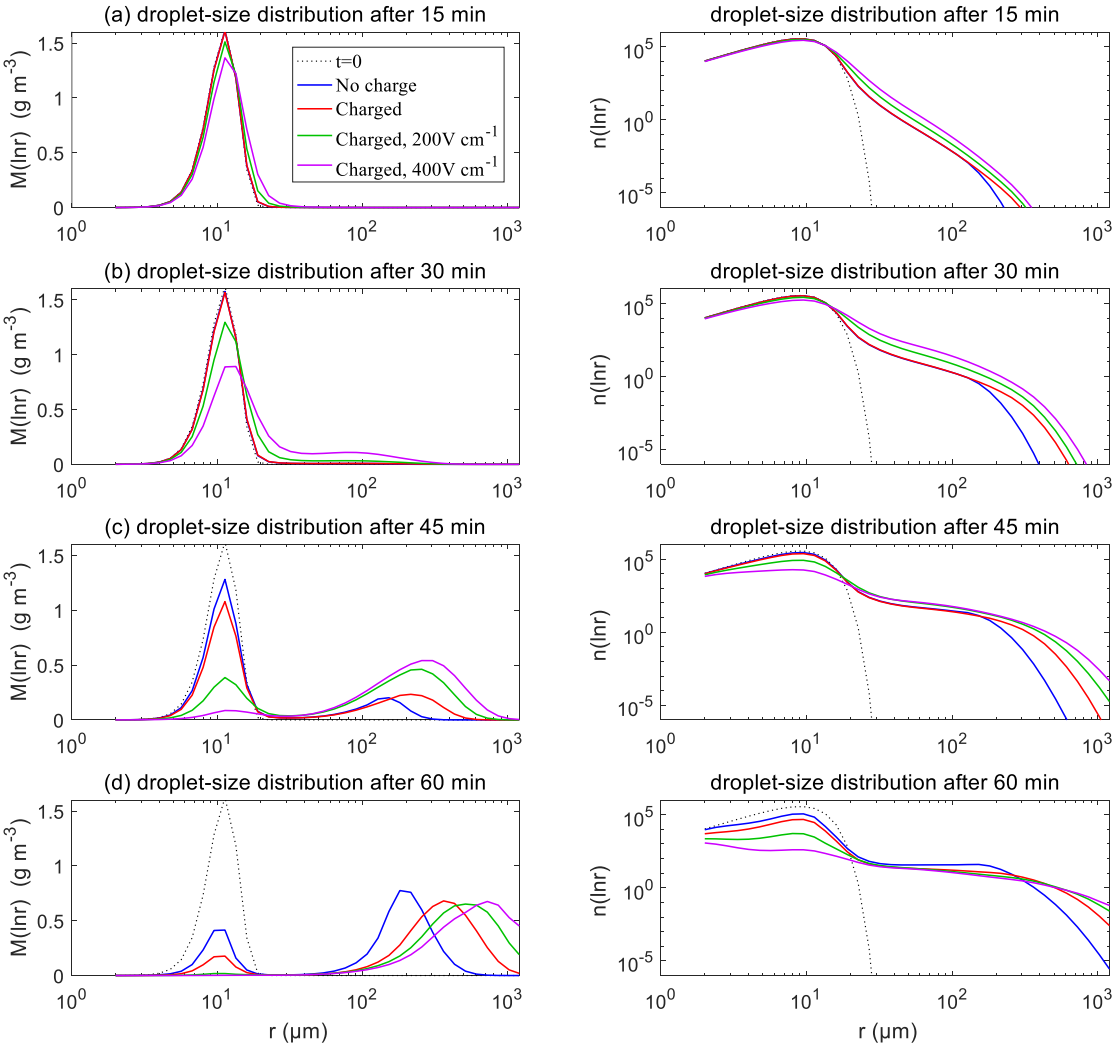

~~FIG. 8.~~ **FIG. 11.** The evolution of ~~spectrum~~ droplet size distribution with initial $\bar{r} = 9$ μm.

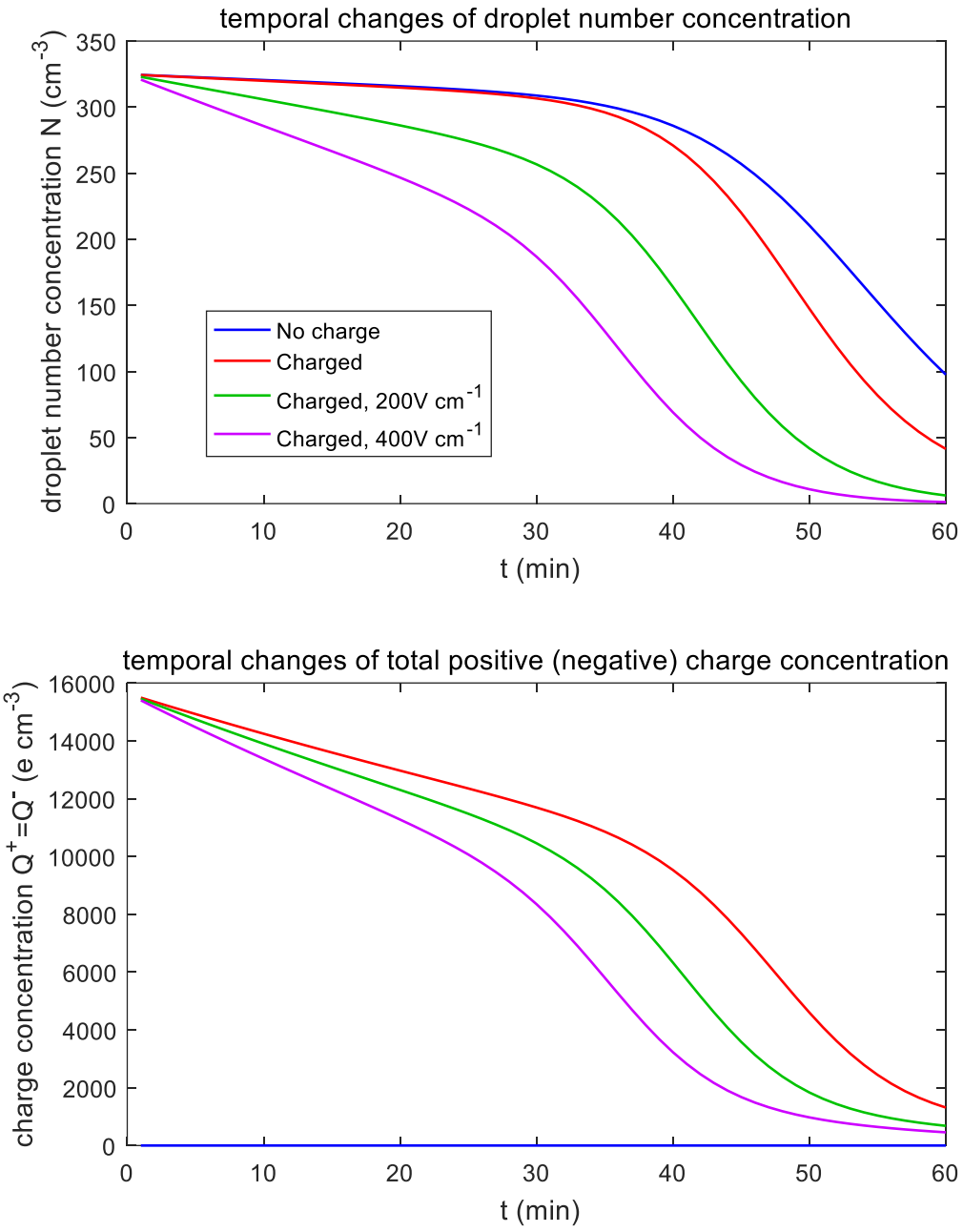

FIG. 12. Temporal changes of droplet total number concentration and total charge content for $\bar{r}$ =9 μm

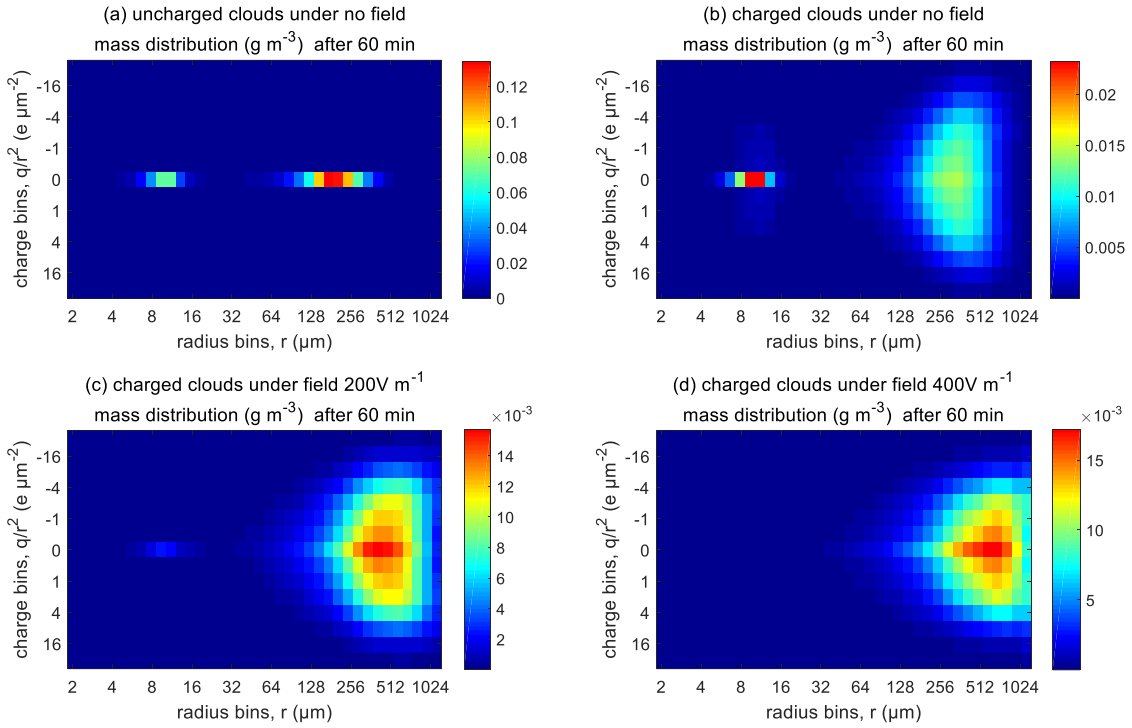

~~FIG. 9.~~ **FIG. 13.** Comparison of evolutions of 2-dimensional ~~spectrum evolution~~ distribution of droplet mass concentration with different electric conditions at 60 min (initial $\bar{r}$ = 9 μm).

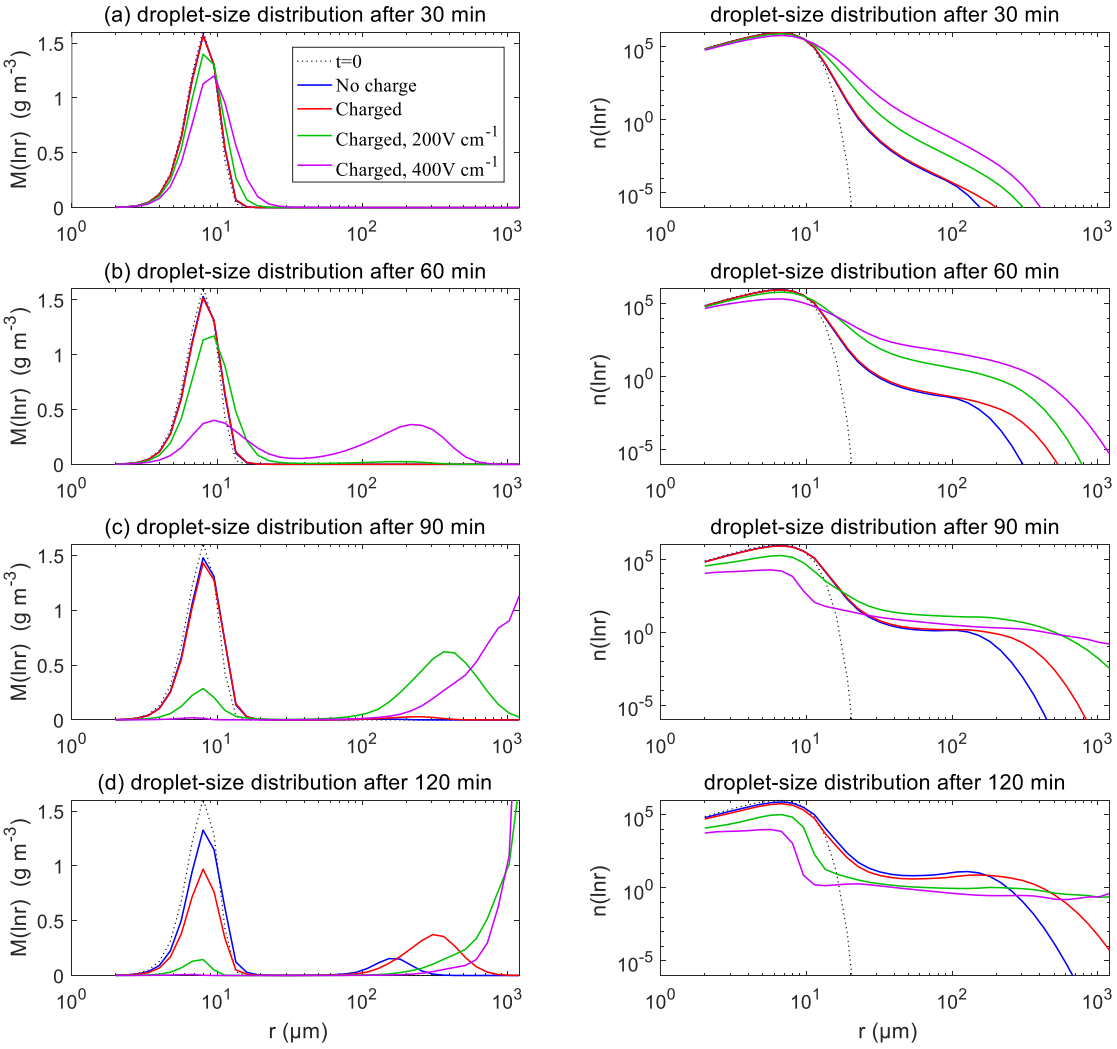

~~FIG. 10.~~ **FIG. 14.** The evolution of ~~spectrum~~ droplet size distribution with initial $\bar{r}$ = 6.5 μm.

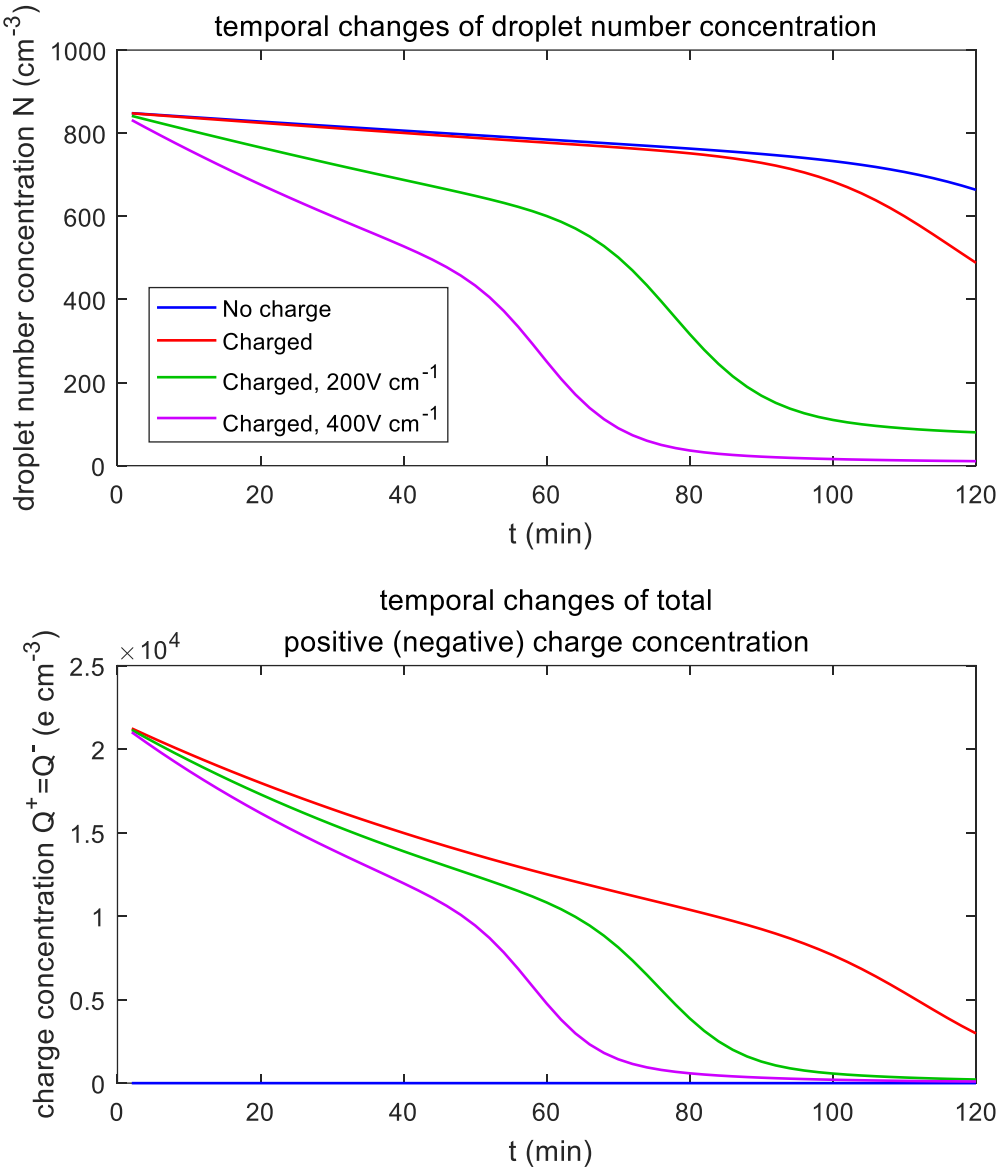

FIG. 15. Temporal changes of droplet total number concentration and total charge content for $\bar{r}$ =6.5 μm.

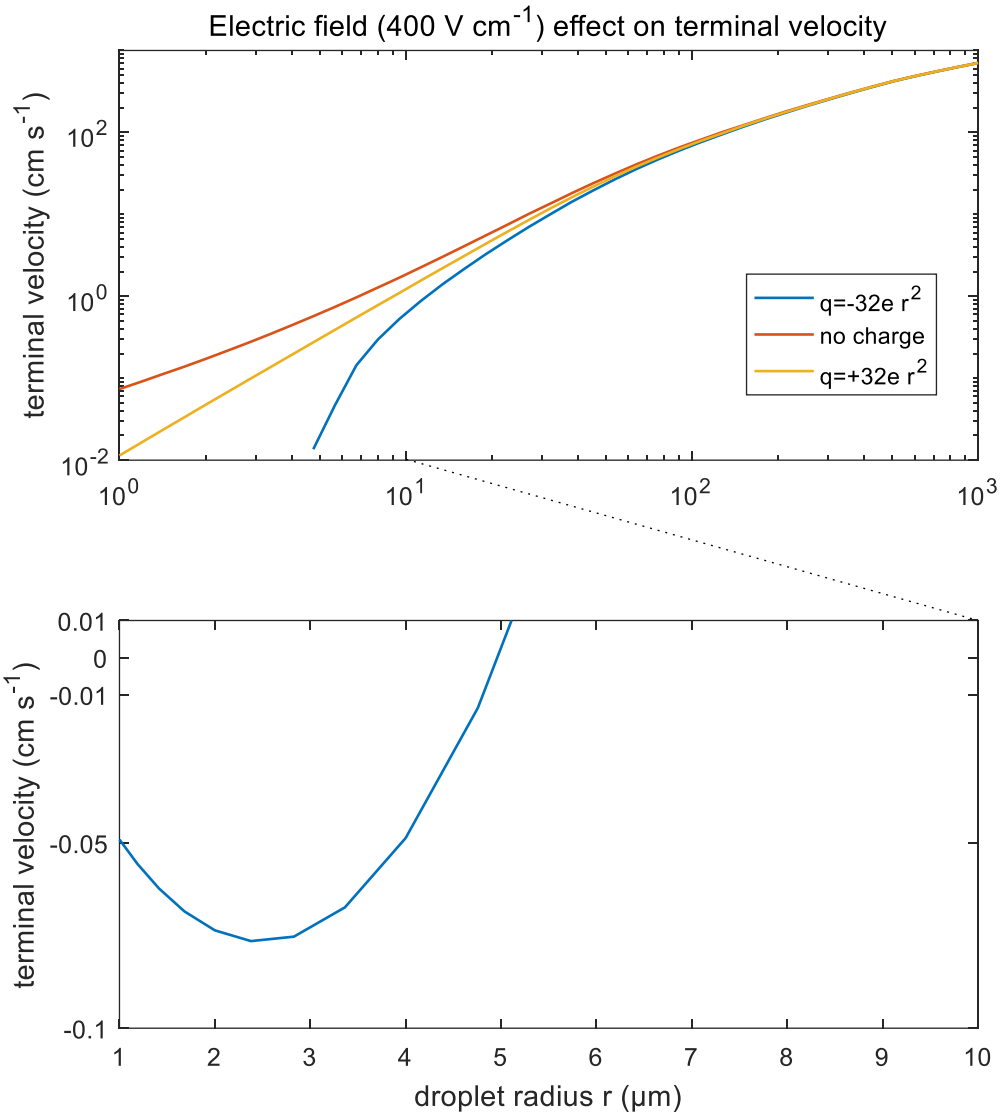

~~FIG. 11.~~ **FIG. 16.** Terminal velocities of droplets in an external electric field 400 V cm^{-1}. Different lines denote different droplet charge conditions. It is significant that terminal velocity of negatively charged droplets smaller than 5 μm would turn upwards, which leads to the discontinuity of the lower curve in the figure.